

Sketched Ridge Regression: Optimization Perspective, Statistical Perspective, and Model Averaging

Shusen Wang

shusen@berkeley.edu

*International Computer Science Institute and Department of Statistics
University of California at Berkeley
Berkeley, CA 94720, USA*

Alex Gittens

gittea@rpi.edu

*Computer Science Department
Rensselaer Polytechnic Institute
Troy, NY 12180, USA*

Michael W. Mahoney

mmahoney@stat.berkeley.edu

*International Computer Science Institute and Department of Statistics
University of California at Berkeley
Berkeley, CA 94720, USA*

Abstract

We address the statistical and optimization impacts of using classical sketch versus Hessian sketch to solve approximately the Matrix Ridge Regression (MRR) problem. Prior research has considered the effects of classical sketch on least squares regression (LSR), a strictly simpler problem. We establish that classical sketch has a similar effect upon the optimization properties of MRR as it does on those of LSR—namely, it recovers nearly optimal solutions. In contrast, Hessian sketch does not have this guarantee; instead, the approximation error is governed by a subtle interplay between the “mass” in the responses and the optimal objective value.

For both types of approximations, the regularization in the sketched MRR problem gives it significantly different statistical properties from the sketched LSR problem. In particular, there is a bias-variance trade-off in sketched MRR that is not present in sketched LSR. We provide upper and lower bounds on the biases and variances of sketched MRR; these establish that the variance is significantly increased when classical sketches are used, while the bias is significantly increased when using Hessian sketches. Empirically, sketched MRR solutions can have risks that are higher by an order-of-magnitude than those of the optimal MRR solutions.

We establish theoretically and empirically that model averaging greatly decreases this gap. Thus, in the distributed setting, sketching combined with model averaging is a powerful technique that quickly obtains near-optimal solutions to the MRR problem while greatly mitigating the statistical risks incurred by sketching.

Keywords: randomized linear algebra, matrix sketching, ridge regression

1. Introduction

Regression is one of the most fundamental problems in machine learning. The simplest and most thoroughly studied regression model is least squares regression (LSR). Given features $\mathbf{X} = [\mathbf{x}_1^T; \dots, \mathbf{x}_n^T] \in \mathbb{R}^{n \times d}$ and responses $\mathbf{y} = [y_1, \dots, y_n]^T \in \mathbb{R}^n$, the LSR problem $\min_{\mathbf{w}} \|\mathbf{X}\mathbf{w} - \mathbf{y}\|_2^2$ can be solved in $\mathcal{O}(nd^2)$ time using the QR decomposition or in $\mathcal{O}(ndt)$ time using accelerated gradient descent algorithms. Here, t is the number of iterations, which depends on the initialization, the condition number of \mathbf{X} , and the stopping criterion.

This paper considers the $n \gg d$ problem, where there is much redundancy in \mathbf{X} . Matrix sketching, as used within Randomized Linear Algebra (RLA) (Mahoney, 2011, Woodruff, 2014), works by reducing the size of \mathbf{X} without losing too much information; this operation can be modeled as taking actual rows or linear combinations of the rows of \mathbf{X} with a sketching matrix \mathbf{S} to form the sketch $\mathbf{S}^T \mathbf{X}$. Here $\mathbf{S} \in \mathbb{R}^{n \times s}$ satisfies $d < s \ll n$ so that $\mathbf{S}^T \mathbf{X}$ generically has the same rank but much fewer rows as \mathbf{X} . Sketching has been used to speed up LSR (Drineas et al., 2006b, 2011, Clarkson and Woodruff, 2013, Meng and Mahoney, 2013, Nelson and Nguyn, 2013) by solving the sketched LSR problem $\min_{\mathbf{w}} \|\mathbf{S}^T \mathbf{X}\mathbf{w} - \mathbf{S}^T \mathbf{y}\|_2^2$ instead of the original LSR problem. Solving sketched LSR costs either $\mathcal{O}(sd^2 + T_s)$ time using the QR decomposition or $\mathcal{O}(sdt + T_s)$ time using accelerated gradient descent algorithms, where t is as defined previously¹ and T_s is the time cost of sketching. For example, $T_s = \mathcal{O}(nd \log s)$ when \mathbf{S} is the subsampled randomized Hadamard transform Drineas et al. (2011), and $T_s = \mathcal{O}(nd)$ when \mathbf{S} is a CountSketch matrix Clarkson and Woodruff (2013).

There has been much work in RLA on analyzing the quality of sketched LSR with different sketching methods and different objectives; see the reviews Mahoney (2011), Woodruff (2014) and the references therein.

The concept of sketched LSR originated in the theoretical computer science literature, e.g., Drineas et al. (2006b, 2011), where the behavior of sketched LSR was studied from an optimization perspective. Let \mathbf{w}^* be the optimal LSR solution and $\tilde{\mathbf{w}}$ be the solution to sketched LSR. This line of work established that if $s = \mathcal{O}(d/\epsilon + \text{poly}(d))$, then the objective function value $\|\mathbf{X}\tilde{\mathbf{w}} - \mathbf{y}\|_2^2$ is at most ϵ times worse than $\|\mathbf{X}\mathbf{w}^* - \mathbf{y}\|_2^2$. These works also bounded $\|\tilde{\mathbf{w}} - \mathbf{w}^*\|_2^2$ in terms of the difference in the objective function values and the condition number of $\mathbf{X}^T \mathbf{X}$.

A more recent line of work has studied sketched LSR from a statistical perspective: Ma et al. (2015), Raskutti and Mahoney (2016), Pilanci and Wainwright (2015), Wang et al. (2016d) considered statistical properties of sketched LSR like the bias and variance. In particular, Pilanci and Wainwright (2015) showed that sketched LSR has much higher variance than the optimal solution.

Both of these perspectives are important and of practical interest. The optimization perspective is relevant when the data can be taken as deterministic values. The statistical perspective is relevant in machine learning and statistics applications where the data are random, and the regression coefficients are therefore themselves random variables.

In practice, regularized regression, e.g., ridge regression and LASSO, exhibit more attractive bias-variance trade-offs and generalization errors than vanilla LSR. Furthermore,

1. The condition number of $\mathbf{X}^T \mathbf{S} \mathbf{S}^T \mathbf{X}$ is very close to that of $\mathbf{X}^T \mathbf{X}$, and thus the number of iterations t is almost unchanged.

the matrix generalization of LSR, where multiple responses are to be predicted, is often more useful than LSR. However, the properties of sketched regularized matrix regression are largely unknown. Hence, the question: *how, if at all, does our understanding of the optimization and statistical properties of sketched LSR generalize to sketched regularized regression?* We answer this question for sketched matrix ridge regression (MRR).

Recall that \mathbf{X} is $n \times d$. Let $\mathbf{Y} \in \mathbb{R}^{n \times m}$ denote the matrix of corresponding responses. We study the MRR problem

$$\min_{\mathbf{W}} \left\{ f(\mathbf{W}) \triangleq \frac{1}{n} \|\mathbf{X}\mathbf{W} - \mathbf{Y}\|_F^2 + \gamma \|\mathbf{W}\|_F^2 \right\}, \quad (1)$$

which has optimal solution

$$\mathbf{W}^* = (\mathbf{X}^T \mathbf{X} + n\gamma \mathbf{I}_d)^{\dagger} \mathbf{X}^T \mathbf{Y}. \quad (2)$$

Here, $(\cdot)^{\dagger}$ denotes the Moore-Penrose inversion operation. LSR is a special case of MRR, with $m = 1$ and $\gamma = 0$. The optimal solution \mathbf{W}^* can be obtained in $\mathcal{O}(nd^2 + nmd)$ time using a QR decomposition of \mathbf{X} . Sketching can be applied to MRR in two ways:

$$\mathbf{W}^c = (\mathbf{X}^T \mathbf{S} \mathbf{S}^T \mathbf{X} + n\gamma \mathbf{I}_d)^{\dagger} (\mathbf{X}^T \mathbf{S} \mathbf{S}^T \mathbf{Y}), \quad (3)$$

$$\mathbf{W}^h = (\mathbf{X}^T \mathbf{S} \mathbf{S}^T \mathbf{X} + n\gamma \mathbf{I}_d)^{\dagger} \mathbf{X}^T \mathbf{Y}. \quad (4)$$

Following the convention of [Pilanci and Wainwright \(2015\)](#), [Wang et al. \(2016a\)](#), we call \mathbf{W}^c **classical sketch** and \mathbf{W}^h **Hessian sketch**. Table 1 lists the time costs of the three solutions to MRR.

Table 1: The time cost of the solutions to MRR. Here $T_s(\mathbf{X})$ and $T_s(\mathbf{Y})$ denote the time cost of forming the sketches $\mathbf{S}^T \mathbf{X} \in \mathbb{R}^{s \times d}$ and $\mathbf{S}^T \mathbf{Y} \in \mathbb{R}^{s \times m}$.

Solution	Definition	Time Complexity
Optimal Solution	(2)	$\mathcal{O}(nd^2 + nmd)$
Classical Sketch	(3)	$\mathcal{O}(sd^2 + smd) + T_s(\mathbf{X}) + T_s(\mathbf{Y})$
Hessian Sketch	(4)	$\mathcal{O}(sd^2 + nmd) + T_s(\mathbf{X})$

1.1 Main Results and Contributions

We summarize all of our upper bounds in Table 2. Our optimization analysis bounds the objective function values, while our statistical analysis guarantees the bias and variance.

We first study classical and Hessian sketches from the **optimization perspective**. Theorems 1 and 2 show that

- Classical sketch achieves relative error in the objective value. With sketch size $s = \tilde{\mathcal{O}}(d/\epsilon)$, the objective satisfies $f(\mathbf{W}^c) \leq (1 + \epsilon)f(\mathbf{W}^*)$.
- Hessian sketch does not achieve relative error in the objective value. In particular, if $\frac{1}{n}\|\mathbf{Y}\|_F^2$ is much larger than $f(\mathbf{W}^*)$, then $f(\mathbf{W}^h)$ can be far larger than $f(\mathbf{W}^*)$.

Table 2: In the table, \mathbf{W} can be the solution of classical/Hessian sketch with/without model averaging (mod. avg.); \mathbf{W}^* is the optimal solution; g is the number of repeat of model averaging; $\beta = \frac{\|\mathbf{X}\|_2^2}{\|\mathbf{X}\|_2^2 + n\gamma} \leq 1$, where γ is the regularization parameter. For this summary table, we assume the sketching matrix $\mathbf{S} \in \mathbb{R}^{n \times s}$ is Gaussian projection, SRHT, or shrinkage leverage score sampling. Similar but more complex expressions hold for uniform sampling (with/without mod. avg.) and CountSketch (only for without mod. avg.) All the bounds hold with constant probabilities.

	Classical Sketch		Hessian Sketch	
	w/o mod. avg.	w/ mod. avg.	w/o mod. avg.	w/ mod. avg.
$s =$	$\tilde{\mathcal{O}}(\beta d/\epsilon)$			$\tilde{\mathcal{O}}(\beta^2 d/\epsilon)$
$f(\mathbf{W}) - f(\mathbf{W}^*) \leq$ Theorems	$\epsilon f(\mathbf{W}^*)$ Theorem 1	$(\frac{\epsilon}{g} + \beta^2 \epsilon^2) f(\mathbf{W}^*)$ Theorem 8	$\epsilon \left[\frac{\ \mathbf{Y}\ _F^2}{n} - f(\mathbf{W}^*) \right]$ Theorem 2	$(\frac{\epsilon}{g^2} + \frac{\epsilon^2}{\beta^2}) \left[\frac{\ \mathbf{Y}\ _F^2}{n} - f(\mathbf{W}^*) \right]$ Theorem 9
$s =$ $\frac{\text{bias}(\mathbf{W})}{\text{bias}(\mathbf{W}^*)} \leq$ $\frac{\text{var}(\mathbf{W})}{\text{var}(\mathbf{W}^*)} \leq$ Theorems	$\tilde{\mathcal{O}}(d/\epsilon^2)$ 1 + ϵ $(1 + \epsilon) \frac{n}{s}$ Theorem 5	1 + ϵ $\frac{n}{s} \left(\sqrt{\frac{1 + \epsilon/g}{g}} + \epsilon \right)^2$ Theorem 11	$\tilde{\mathcal{O}}(d/\epsilon^2)$ $(1 + \epsilon) \left(1 + \frac{\epsilon \ \mathbf{X}\ _2^2}{n\gamma} \right)$ 1 + ϵ Theorem 7	$1 + \epsilon + (\frac{\epsilon}{g} + \epsilon^2) \frac{\ \mathbf{X}\ _2^2}{n\gamma}$ 1 + ϵ Theorem 13

- For both classical and Hessian sketch, the relative quality of approximation improves as the regularization parameter γ increases.

We then study classical sketch and Hessian sketch from the **statistical perspective**, by modeling $\mathbf{Y} = \mathbf{X}\mathbf{W}_0 + \mathbf{\Xi}$ as the sum of a true linear model and random noise, decomposing the risk $R(\mathbf{W}) = \mathbb{E}\|\mathbf{X}\mathbf{W} - \mathbf{X}\mathbf{W}_0\|_F^2$ into bias and variance terms, and bounding these terms. The risk $R(\mathbf{W})$ determines how well the trained model \mathbf{W} generalizes to the test samples; see the discussions in Appendix A. We draw the following conclusions (see Theorems 4, 5, 7 for the details):

- The bias of classical sketch can be nearly as small as that of the optimal solution. The variance is $\Theta(\frac{n}{s})$ times that of the optimal solution; this bound is optimal. Therefore over-regularization² should be used to suppress the variance. (As γ increases, the bias increases, and the variance decreases.)
- Since \mathbf{Y} is not sketched with Hessian sketch, the variance of Hessian sketch can be close to the optimal solution. However, Hessian sketch has high bias, especially when $n\gamma$ is small compared to $\|\mathbf{X}\|_2^2$. This indicates that over-regularization is necessary for Hessian sketch to have low bias.

Our empirical evaluations bear out these theoretical results. In particular, in Section 4, we show in Figure 3 that even when the regularization parameter γ is fine-tuned, the risks of classical sketch and Hessian sketch are worse than that of the optimal solution by an order of magnitude. This is an empirical demonstration of the fact that the near-optimal properties

2. By over-regularization, we mean choosing a larger value of the regularization parameter γ than what we would optimally choose for the unsketched problem.”

of sketching from the optimization perspective are much less relevant in a statistical setting than its sub-optimal statistical properties.

We propose to use **model averaging**, which averages the solutions of g sketched MRR problems, to attain lower optimization and statistical errors. Without ambiguity, we denote classical and Hessian sketches with model averaging by \mathbf{W}^c and \mathbf{W}^h , respectively. Theorems 8, 9, 11, 13 establish the following results:

- Classical Sketch. Model averaging improves the objective function value and the variance and does not increase the bias. Specifically, with the same sketch size s , model averaging makes $\frac{f(\mathbf{W}^c) - f(\mathbf{W}^*)}{f(\mathbf{W}^*)}$ and $\frac{\text{var}(\mathbf{W}^c)}{\text{var}(\mathbf{W}^*)}$ respectively decrease to almost $\frac{1}{g}$ of those of classical sketch without model averaging, provided that $s \gg d$. See Table 2 for the details.
- Hessian Sketch. Model averaging decreases the objective function value and the bias and does not increase the variance.

Note that classical sketch with uniform sampling and model averaging is essentially bagging (synonym bootstrap aggregating) (Breiman, 1996) (or a variant called pasting (Breiman, 1999)) for ridge regression. Our work lends strong guarantees to bagging for ridge regression. Different from bagging, our approach is not limited to uniform sampling.

Classical sketch with model averaging has three immediate applications. In the single-machine setting,

- Classical sketch with model averaging offers a way to improve the statistical performance in the presence of heavy noise. Assume the sketch size is $s = \tilde{\mathcal{O}}(\sqrt{nd})$. As g grows larger than $\frac{n}{s}$, the variance of the averaged solution can be even lower than the optimal solution. See Corollary 12 for further discussions. Using sketching methods other than uniform sampling, the performance is independent of matrix coherence, which is an improvement over the traditional bagging (Breiman, 1996).

In the distributed setting, the feature-response pairs $(\mathbf{x}_1, \mathbf{y}_1), \dots, (\mathbf{x}_n, \mathbf{y}_n) \in \mathbb{R}^d \times \mathbb{R}^m$ are divided among g machines. Assuming that the data have been shuffled randomly, each machine contains a sketch constructed by uniformly sampled rows from the dataset without replacement. We illustrate this procedure in Figure 1. In this setting, the model averaging procedure will communicate the g local models only once to return the final estimate; this process has very low communication and latency costs, and it suggests two further applications of classical sketch with model averaging:

- Model Averaging for Machine Learning. If a low-precision solution is acceptable, the averaged solution can be used in lieu of distributed numerical optimization algorithms requiring multiple rounds of communication. If $\frac{n}{g}$ is big enough compared to d and the row coherence of \mathbf{X} is small, then “one-shot” model averaging has bias and variance comparable to the optimal solution.
- Model Averaging for Optimization. If a high-precision solution to MRR is required, then an iterative numerical optimization algorithm must be used. The cost of such

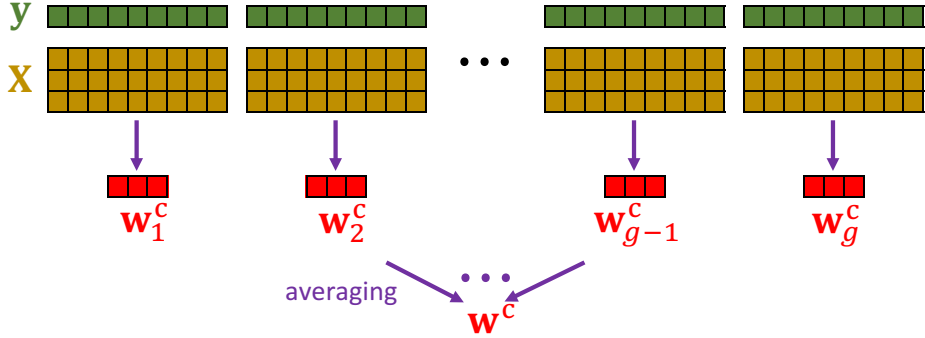


Figure 1: Illustration of classical sketch with model averaging in the distributed setting.

numerical optimization algorithms heavily depends on the quality of the initialization.³ A good initialization saves lots of iterations. The averaged model is provably close to the optimal solution, so model averaging provides a high-quality initialization for more expensive algorithms.

1.2 Prior Work

The body of work on sketched LSR mentioned earlier (Drineas et al., 2006b, 2011, Clarkson and Woodruff, 2013, Meng and Mahoney, 2013, Nelson and Nguyn, 2013) shares many similarities with our results. However, the theories of sketched LSR developed from the optimization perspective do not obviously extend to MRR, and the statistical analysis of LSR and MRR differ: among other differences, LSR is unbiased while MRR has a nontrivial bias and therefore has a bias-variance tradeoff that must be considered.

Lu et al. (2013) has considered a different application of sketching to ridge regression: they assume $d \gg n$, reduce the number of features in \mathbf{X} using sketching, and conduct statistical analysis. Our setting differs in that we consider $n \gg d$, reduce the number of samples by sketching, and allow for multiple responses.

The model averaging analyzed in this paper is similar in spirit to the AVGM algorithm of (Zhang et al., 2013). When classical sketch is used with uniform row sampling without replacement, our model averaging procedure is a special case of AVGM. However, our results do not follow from those of (Zhang et al., 2013). First, we make no assumption on the data, whereas they assumed $\mathbf{x}_1, \dots, \mathbf{x}_n$ are i.i.d. from an unknown distribution. Second, the objectives are different: we study the distances $\|\mathbf{X}\mathbf{W}^c - \mathbf{X}\mathbf{W}^*\|_F^2$ and $\mathbb{E}\|\mathbf{X}\mathbf{W}^c - \mathbf{X}\mathbf{W}_0\|_F^2$, where \mathbf{W}^c is the averaged classical sketches, \mathbf{W}_0 is the unknown ground truth, and \mathbf{W}^* is the optimal solution based on the observed data; they essentially studied $\mathbb{E}\|\mathbf{W}^c - \mathbf{W}^*\|_F^2$; our expectation is taken w.r.t. the random noise in the responses, while their expectation is w.r.t. the distribution of $\mathbf{x}_1, \dots, \mathbf{x}_n$. Third, our results apply to many other sketching

3. For example, the conjugate gradient method satisfies $\frac{\|\mathbf{W}^{(t)} - \mathbf{W}^*\|_F^2}{\|\mathbf{W}^{(0)} - \mathbf{W}^*\|_F^2} \leq \theta_1^t$; the stochastic block coordinate descent (Tu et al., 2016) satisfies $\frac{\mathbb{E}f(\mathbf{W}^{(t)}) - f(\mathbf{W}^*)}{f(\mathbf{W}^{(0)}) - f(\mathbf{W}^*)} \leq \theta_2^t$. Here $\mathbf{W}^{(t)}$ is the output of the t -th iteration; $\theta_1, \theta_2 \in (0, 1)$ depend on the condition number of $\mathbf{X}^T \mathbf{X} + n\gamma \mathbf{I}_d$ and some other factors.

ensembles than uniform sampling without replacement. Our results clearly indicate that the performance critically depends on the row coherence of \mathbf{X} ; this dependence is not captured in (Zhang et al., 2013). For similar reasons, our work is different from the divide-and-conquer kernel ridge regression algorithm of (Zhang et al., 2015).

Iterative Hessian sketch has been studied by Pilanci and Wainwright (2015), Wang et al. (2016a). By way of comparison, all the algorithms in this paper are “one-shot” rather than iterative. Upon completion of this paper, we noticed the contemporary works (Avron et al., 2016, Thanei et al., 2017). Avron et al. (2016) studied classical sketch from the optimization perspective, and Thanei et al. (2017) studied LSR with model averaging.

1.3 Paper Organization

Section 2 defines our notation and introduces the sketching schemes we consider. Section 3 presents our theoretical results. Sections 4 and 5 conduct experiments to verify our theories and demonstrates the usefulness of model averaging. Section 6 shows the sketch of proof. The proofs of the theorems are in the appendix.

2. Preliminaries

Throughout, we take \mathbf{I}_n to be the $n \times n$ identity matrix and $\mathbf{0}$ to be a vector or matrix of all zeroes of the appropriate size. Given a matrix $\mathbf{A} = [a_{ij}]$, the i -th row is denoted by $\mathbf{a}_{i:}$, and the j -th column is by $\mathbf{a}_{:j}$. The Frobenius and spectral norms of \mathbf{A} are written as, respectively, $\|\mathbf{A}\|_F$ and $\|\mathbf{A}\|_2$. The set $\{1, 2, \dots, n\}$ is written $[n]$. Let \mathcal{O} , Ω , and Θ be the standard asymptotic notation. Let $\tilde{\mathcal{O}}$ conceal logarithm factors.

Throughout, we fix $\mathbf{X} \in \mathbb{R}^{n \times d}$ as our matrix of features. We set $\rho = \text{rank}(\mathbf{X})$ and write the SVD of \mathbf{X} as $\mathbf{X} = \mathbf{U}\Sigma\mathbf{V}^T$, where \mathbf{U} , Σ , \mathbf{V} are respectively $n \times \rho$, $\rho \times \rho$, and $d \times \rho$ matrices. We let $\sigma_1 \geq \dots \geq \sigma_\rho > 0$ be the singular values of \mathbf{X} . The Moore-Penrose inverse of \mathbf{X} is defined by $\mathbf{X}^\dagger = \mathbf{V}\Sigma^{-1}\mathbf{U}^T$. The row leverage scores of \mathbf{X} are $l_i = \|\mathbf{u}_{:i}\|_2^2$ for $i \in [n]$. The row coherence of \mathbf{X} is $\mu(\mathbf{X}) = \frac{n}{\rho} \max_i \|\mathbf{u}_{:i}\|_2^2$. Throughout, we let μ be shorthand for $\mu(\mathbf{X})$. The notation defined in Table 3 are used throughout this paper.

Matrix sketching turns big matrices into smaller ones without losing too much information useful in tasks like linear regression. We denote the process of sketching a matrix $\mathbf{X} \in \mathbb{R}^{n \times d}$ by $\mathbf{X}' = \mathbf{S}^T\mathbf{X}$. Here, $\mathbf{S} \in \mathbb{R}^{n \times s}$ is called a sketching matrix and $\mathbf{X}' \in \mathbb{R}^{s \times d}$ is called a sketch of \mathbf{X} . In practice, except for Gaussian projection (where the entries of \mathbf{S} are i.i.d. sampled from $\mathcal{N}(0, 1/s)$), the sketching matrix \mathbf{S} is not formed explicitly.

Matrix sketching can be accomplished by random selection or random projection. **Random sampling** corresponds to sampling rows of \mathbf{X} i.i.d. with replacement according to given row sampling probabilities $p_1, \dots, p_m \in (0, 1)$. The corresponding (random) sketching matrix $\mathbf{S} \in \mathbb{R}^{n \times s}$ has exactly one non-zero entry, whose position indicates the index of the selected row; in practice, this \mathbf{S} is not explicitly formed. **Uniform sampling** fixes $p_1 = \dots = p_n = \frac{1}{n}$. **Leverage score sampling** sets p_i proportional to the (exact or approximate (Drineas et al., 2012)) row leverage scores l_i of \mathbf{X} . In practice **shrinked leverage score sampling** can be a better choice than leverage score sampling (Ma et al.,

Table 3: The commonly used notation.

Notation	Definition
$\mathbf{X} \in \mathbb{R}^{n \times d}$	each row is a data sample (feature vector)
$\mathbf{Y} \in \mathbb{R}^{n \times m}$	each row contains the corresponding responses
$\mathbf{U}\Sigma\mathbf{V}^T$	the SVD of \mathbf{X}
ρ	the rank of \mathbf{X}
μ	the row coherence of \mathbf{X}
σ_i	the i -th largest singular value of \mathbf{X}
γ	the regularization parameter
β	$\beta = \frac{\ \mathbf{X}\ _2^2}{\ \mathbf{X}\ _2^2 + n\gamma} \leq 1$
$\mathbf{S} \in \mathbb{R}^{n \times s}$	the sketching matrix
$\mathbf{W}^* \in \mathbb{R}^{d \times m}$	the optimal solution (2)
$\mathbf{W}^c \in \mathbb{R}^{d \times m}$	classical sketch (3)
$\mathbf{W}^h \in \mathbb{R}^{d \times m}$	Hessian sketch (4)

2015). The sampling probabilities of shrinked leverage score sampling are defined by $p_i = \frac{1}{2} \left(\frac{l_i}{\sum_{j=1}^n l_j} + \frac{1}{n} \right)$.⁴

The exact leverage scores are unnecessary in practice; constant-factor approximation to the leverage scores is sufficient. Leverage scores can be efficiently approximated by the algorithms of (Drineas et al., 2012). Let l_1, \dots, l_n be the true leverage scores. We denote the approximate leverages by $\tilde{l}_1, \dots, \tilde{l}_n$ such that

$$\tilde{l}_q \in [l_q, \tau l_q] \quad \text{for all } q \in [n], \quad (5)$$

where $\tau \geq 1$ indicates the quality of approximation. We can use $p_q = \tilde{l}_q / \sum_j \tilde{l}_j$ as the sampling probability. For the shrinked leverage score sampling, we define the sampling probabilities

$$p_i = \frac{1}{2} \left(\frac{\tilde{l}_i}{\sum_{j=1}^n \tilde{l}_j} + \frac{1}{n} \right) \quad \text{for } i = 1, \dots, n. \quad (6)$$

Using the approximate leverage scores to replace the exact ones, we only need to make the sketch size τ times larger. As long as τ is a small constant, the orders of the sketch sizes of the exact and approximate leverage score sampling are the same. Thus we do not distinguish the exact and approximate leverage scores in this paper.

Gaussian projection is also well-known as the prototypical Johnson-Lindenstrauss transform (Johnson and Lindenstrauss, 1984). Let $\mathbf{G} \in \mathbb{R}^{m \times s}$ be a standard Gaussian matrix, i.e., each entry is sampled independently from $\mathcal{N}(0, 1)$. The matrix $\mathbf{S} = \frac{1}{\sqrt{s}} \mathbf{G}$ is a Gaussian projection matrix. It takes $\mathcal{O}(nds)$ time to apply $\mathbf{S} \in \mathbb{R}^{n \times s}$ to any $n \times d$ dense matrix, which makes Gaussian projection inefficient relative to other forms of sketching.

Subsampled randomized Hadamard transform (SRHT) (Drineas et al., 2011, Lu et al., 2013, Tropp, 2011) is a more efficient alternative to Gaussian projection. Let

4. In fact, p_i can be any convex combination of $\frac{l_i}{\sum_{j=1}^n l_j}$ and $\frac{1}{n}$ (Ma et al., 2015). We use the weight $\frac{1}{2}$ for convenience; our conclusions extend in a straightforward manner to other weightings.

$\mathbf{H}_n \in \mathbb{R}^{n \times n}$ be the Walsh-Hadamard matrix with $+1$ and -1 entries, $\mathbf{D} \in \mathbb{R}^{n \times n}$ be a diagonal matrix with diagonal entries sampled uniformly from $\{+1, -1\}$, and $\mathbf{P} \in \mathbb{R}^{n \times s}$ be the uniform row sampling matrix defined above. The matrix $\mathbf{S} = \frac{1}{\sqrt{n}} \mathbf{D} \mathbf{H}_n \mathbf{P} \in \mathbb{R}^{n \times s}$ is an SRHT matrix, and can be applied to any $n \times d$ matrix in $\mathcal{O}(nd \log s)$ time. In practice, the subsampled randomized Fourier transform (SRFT) (Woolfe et al., 2008) is often used in lieu of the SRHT, because the SRFT exists for all values of n , whereas \mathbf{H}_n exists only for some values of n . Their performance and theoretical analyses are very similar.

CountSketch can be applied to any $\mathbf{X} \in \mathbb{R}^{n \times d}$ in $\mathcal{O}(nd)$ time (Charikar et al., 2004, Clarkson and Woodruff, 2013, Meng and Mahoney, 2013, Nelson and Nguyn, 2013, Pham and Pagh, 2013, Weinberger et al., 2009). Though more efficient to apply, CountSketch requires a bigger sketch size than Gaussian projections, SRHT, and leverage score sampling to attain the same theoretical guarantees. The readers can refer to (Woodruff, 2014) for a detailed description of CountSketch. CountSketch may not be applicable to model averaging as a theoretically sound approach like the other sketching methods. See Remark 20 for the reasons.

3. Main Results

Sections 3.1 and 3.2 analyze sketched MRR from, respectively, optimization and statistical perspectives. Sections 3.3 and 3.4 capture the impacts of model averaging on, respectively, the optimization and statistical properties of sketched MRR.

We described six sketching methods in Section 2. For simplicity, in this section, we refer to leverage score sampling, shranked leverage score sampling, Gaussian projection, and SRHT as **the four sketching methods**; and we will mention explicitly uniform sampling and CountSketch. Throughout, let μ be the row coherence of \mathbf{X} and $\beta = \frac{\|\mathbf{X}\|_2^2}{\|\mathbf{X}\|_2^2 + n\gamma} \leq 1$.

3.1 Sketched MRR: Optimization Perspective

Theorem 1 shows that $f(\mathbf{W}^c)$, the objective value of classical sketch, is very close to the optimal objective value $f(\mathbf{W}^*)$. The approximation quality improves as γ increases.

Theorem 1 (Classical Sketch) *Let $\beta = \frac{\|\mathbf{X}\|_2^2}{\|\mathbf{X}\|_2^2 + n\gamma} \leq 1$. For the four sketching methods with $s = \tilde{\mathcal{O}}\left(\frac{\beta d}{\epsilon}\right)$, uniform sampling with $s = \mathcal{O}\left(\mu \frac{\beta d \log d}{\epsilon}\right)$, and CountSketch with $s = \mathcal{O}\left(\frac{\beta d^2}{\epsilon}\right)$, the inequality*

$$f(\mathbf{W}^c) - f(\mathbf{W}^*) \leq \epsilon f(\mathbf{W}^*)$$

holds with probability at least 0.9.

The corresponding guarantee for the performance of Hessian sketch is given in Theorem 2. It is weaker than the guarantee for classical sketch, especially when $\frac{1}{n} \|\mathbf{Y}\|_F^2$ is far larger than $f(\mathbf{W}^*)$. If \mathbf{Y} is nearly noiseless— \mathbf{Y} is well-explained by a linear combination of the columns of \mathbf{X} —and γ is small, then $f(\mathbf{W}^*)$ is close to zero, and consequently $f(\mathbf{W}^*)$ can be far smaller than $\frac{1}{n} \|\mathbf{Y}\|_F^2$. Therefore, in this case which is ideal for MRR, $f(\mathbf{W}^h)$ is not close to $f(\mathbf{W}^*)$ and our theory suggests Hessian sketch does not perform as well as classical sketch. This is verified by our experiments (see Figure 2), which show that unless

γ is big or a large portion of \mathbf{Y} is outside the column space of \mathbf{X} , the ratio $\frac{f(\mathbf{W}^h)}{f(\mathbf{W}^*)}$ can be large.

Theorem 2 (Hessian Sketch) *Let $\beta = \frac{\|\mathbf{X}\|_2^2}{\|\mathbf{X}\|_2^2 + n\gamma} \leq 1$. For the four sketching methods with $s = \tilde{\mathcal{O}}(\frac{\beta^2 d}{\epsilon})$, uniform sampling with $s = \mathcal{O}(\frac{\mu\beta^2 d \log d}{\epsilon})$, and CountSketch with $s = \mathcal{O}(\frac{\beta^2 d^2}{\epsilon})$, the inequality*

$$f(\mathbf{W}^h) - f(\mathbf{W}^*) \leq \epsilon \left(\frac{\|\mathbf{Y}\|_F^2}{n} - f(\mathbf{W}^*) \right).$$

holds with probability at least 0.9.

These two results imply that $f(\mathbf{W}^c)$ and $f(\mathbf{W}^h)$ can be close to $f(\mathbf{W}^*)$. When this is the case, curvature of the objective function ensures that the sketched solutions \mathbf{W}^c and \mathbf{W}^h are close to the optimal solution \mathbf{W}^* . Lemma 3 studies the Mahalanobis distance $\|\mathbf{M}(\mathbf{W} - \mathbf{W}^*)\|_F^2$. Here \mathbf{M} is any non-singular matrix; in particular, it can be the identity matrix or $(\mathbf{X}^T \mathbf{X})^{1/2}$. Lemma 3 is a consequence of Lemma 31.

Lemma 3 *Let f be the objective function of MRR defined in (1), $\mathbf{W} \in \mathbb{R}^{d \times m}$ be arbitrary, and \mathbf{W}^* be the optimal solution defined in (2). For any non-singular matrix \mathbf{M} , the Mahalanobis distance satisfies*

$$\frac{1}{n} \|\mathbf{M}(\mathbf{W} - \mathbf{W}^*)\|_F^2 \leq \frac{f(\mathbf{W}) - f(\mathbf{W}^*)}{\sigma_{\min}^2[(\mathbf{X}^T \mathbf{S} \mathbf{S}^T \mathbf{X} + n\gamma \mathbf{I}_d)^{1/2} \mathbf{M}^{-1}]}.$$

By choosing $\mathbf{M} = (\mathbf{X}^T \mathbf{X})^{1/2}$, we can bound $\frac{1}{n} \|\mathbf{XW} - \mathbf{XW}^*\|_F^2$ in terms of the difference in the objective values:

$$\frac{1}{n} \|\mathbf{XW} - \mathbf{XW}^*\|_F^2 \leq \beta [f(\mathbf{W}) - f(\mathbf{W}^*)],$$

where $\beta = \frac{\|\mathbf{X}\|_2^2}{\|\mathbf{X}\|_2^2 + n\gamma} \leq 1$. With Lemma 3, we can directly apply Theorems 1 or 2 to bound $\frac{1}{n} \|\mathbf{XW}^c - \mathbf{XW}^*\|_F^2$ or $\frac{1}{n} \|\mathbf{XW}^h - \mathbf{XW}^*\|_F^2$.

3.2 Sketched MRR: Statistical Perspective

We consider the following fixed design model. Let $\mathbf{X} \in \mathbb{R}^{n \times d}$ be the observed feature matrix, $\mathbf{W}_0 \in \mathbb{R}^{d \times m}$ be the true and unknown model, $\boldsymbol{\Xi} \in \mathbb{R}^{n \times m}$ contain unknown random noise, and

$$\mathbf{Y} = \mathbf{XW}_0 + \boldsymbol{\Xi} \tag{7}$$

be the observed responses. We make the following standard weak assumptions on the noise:

$$\mathbb{E}[\boldsymbol{\Xi}] = \mathbf{0} \quad \text{and} \quad \mathbb{E}[\boldsymbol{\Xi} \boldsymbol{\Xi}^T] = \xi^2 \mathbf{I}_n.$$

We observe \mathbf{X} and \mathbf{Y} and seek to estimate \mathbf{W}_0 .

We can evaluate the quality of the estimate by the risk:

$$R(\mathbf{W}) = \frac{1}{n} \mathbb{E} \|\mathbf{XW} - \mathbf{XW}_0\|_F^2, \tag{8}$$

where the expectation is taken w.r.t. the noise $\boldsymbol{\Xi}$. In Appendix A we explain that $R(\mathbf{W})$ determines how well \mathbf{W} generalize to test data. We study the risk functions $R(\mathbf{W}^*), R(\mathbf{W}^c)$, and $R(\mathbf{W}^h)$ in the following.

Theorem 4 (Bias-Variance Decomposition) *We consider the data model described in this subsection. Let \mathbf{W} be \mathbf{W}^* , \mathbf{W}^c , or \mathbf{W}^h , as defined in (2), (3), (4), respectively; then the risk function can be decomposed as*

$$R(\mathbf{W}) = \text{bias}^2(\mathbf{W}) + \text{var}(\mathbf{W}).$$

Recall the SVD of \mathbf{X} defined in Section 2: $\mathbf{X} = \mathbf{U}\Sigma\mathbf{V}^T$. The bias and variance terms can be written as

$$\begin{aligned} \text{bias}(\mathbf{W}^*) &= \gamma\sqrt{n}\left\|(\Sigma^2 + n\gamma\mathbf{I}_\rho)^{-1}\Sigma\mathbf{V}^T\mathbf{W}_0\right\|_F, \\ \text{var}(\mathbf{W}^*) &= \frac{\xi^2}{n}\left\|(\mathbf{I}_\rho + n\gamma\Sigma^{-2})^{-1}\right\|_F^2, \\ \text{bias}(\mathbf{W}^c) &= \gamma\sqrt{n}\left\|(\mathbf{U}^T\mathbf{S}\mathbf{S}^T\mathbf{U} + n\gamma\Sigma^{-2})^\dagger\Sigma^{-1}\mathbf{V}^T\mathbf{W}_0\right\|_F, \\ \text{var}(\mathbf{W}^c) &= \frac{\xi^2}{n}\left\|(\mathbf{U}^T\mathbf{S}\mathbf{S}^T\mathbf{U} + n\gamma\Sigma^{-2})^\dagger\mathbf{U}^T\mathbf{S}\mathbf{S}^T\right\|_F^2, \\ \text{bias}(\mathbf{W}^h) &= \gamma\sqrt{n}\left\|\left(\Sigma^{-2} + \frac{\mathbf{U}^T\mathbf{S}\mathbf{S}^T\mathbf{U} - \mathbf{I}_\rho}{n\gamma}\right)(\mathbf{U}^T\mathbf{S}\mathbf{S}^T\mathbf{U} + n\gamma\Sigma^{-2})^\dagger\Sigma\mathbf{V}^T\mathbf{W}_0\right\|_F, \\ \text{var}(\mathbf{W}^h) &= \frac{\xi^2}{n}\left\|(\mathbf{U}^T\mathbf{S}\mathbf{S}^T\mathbf{U} + n\gamma\Sigma^{-2})^\dagger\right\|_F^2. \end{aligned}$$

Throughout this paper, we compare the bias and variance of classical sketch and Hessian sketch to those of the optimal solution \mathbf{W}^* . We first study the bias, variance, and risk of \mathbf{W}^* , which will help us understand the subsequent comparisons. Here we can assume that $\Sigma^2 = \mathbf{V}^T\mathbf{X}^T\mathbf{X}\mathbf{V}$ is linear with n , which is reasonable because $\mathbf{X}^T\mathbf{X} = \sum_{i=1}^n \mathbf{x}_i\mathbf{x}_i^T$ and \mathbf{V} is orthogonal matrix.

- **Bias.** The bias of \mathbf{W}^* is independent of n and is increasing with γ . The bias is a price paid for suppressing the variance; for least squares regression, γ is zero, and the bias equals to zero.
- **Variance.** The variance of \mathbf{W}^* is inversely proportional to n . As n grows, the variance decreases to zero. Thus it is highly interesting to compare the variance of approximate solutions to $\text{var}(\mathbf{W}^*)$.
- **Risk.** Note that \mathbf{W}^* is not the minimizer of $R(\cdot)$; \mathbf{W}_0 is the minimizer because $R(\mathbf{W}_0) = 0$. Nevertheless, because \mathbf{W}_0 is unknown, \mathbf{W}^* with fine-tuned γ is a standard choice in practice. It is thus highly interesting to find solutions with risks comparable to or even better than $R(\mathbf{W}^*)$.

Theorem 5 provides upper and lower bounds on the bias and variance of classical sketch. In particular, we see that that $\text{bias}(\mathbf{W}^c)$ is within a factor of $(1 \pm \epsilon)$ of $\text{bias}(\mathbf{W}^*)$. However, $\text{var}(\mathbf{W}^c)$ can be $\Theta(\frac{n}{s})$ times worse than $\text{var}(\mathbf{W}^*)$.

Theorem 5 (Classical Sketch) *For Gaussian projection and SRHT sketching with $s = \tilde{\mathcal{O}}(\frac{d}{\epsilon^2})$, uniform sampling with $s = \mathcal{O}(\mu \frac{d \log d}{\epsilon^2})$, or CountSketch with $s = \mathcal{O}(\frac{d^2}{\epsilon^2})$, the inequalities*

$$\begin{aligned} 1 - \epsilon &\leq \frac{\text{bias}(\mathbf{W}^c)}{\text{bias}(\mathbf{W}^*)} \leq 1 + \epsilon, \\ (1 - \epsilon)\frac{n}{s} &\leq \frac{\text{var}(\mathbf{W}^c)}{\text{var}(\mathbf{W}^*)} \leq (1 + \epsilon)\frac{n}{s} \end{aligned}$$

hold with probability at least 0.9.

For shrinked leverage score sampling with $s = \mathcal{O}(\frac{d \log d}{\epsilon^2})$, theses inequalities, except for the lower bound on the variance, hold with probability at least 0.9.

Remark 6 To establish upper (lower) bound on the variance, we need the upper (lower) bound on $\|\mathbf{S}\|_2^2$. For leverage score sampling, there is neither nontrivial upper nor lower bound on $\|\mathbf{S}\|_2^2$, which is why the variance of leverage score sampling cannot be bounded. For shrinked leverage score sampling, we only have the upper bound $\|\mathbf{S}\|_2^2 \leq \frac{2n}{s}$; but $\|\mathbf{S}\|_2^2$ does not have a nontrivial lower bound, which is why shrinked leverage score sampling lacks lower bound on variance. In Remark 18, we explain why for (shrinked) leverage score sampling, $\|\mathbf{S}\|_2^2$ does not have upper and (or) lower bound.

Theorem 7 establishes similar upper and lower bounds on the bias and variance of Hessian sketch. The situation is the reverse of that with classical sketch: the variance of \mathbf{W}^h is close to that of \mathbf{W}^* if s is large enough, but as the regularization parameter γ goes to zero, $\text{bias}(\mathbf{W}^h)$ becomes much larger than $\text{bias}(\mathbf{W}^*)$.

Theorem 7 (Hessian Sketch) For the four sketching methods with $s = \tilde{\mathcal{O}}(\frac{d}{\epsilon^2})$, uniform sampling with $s = \mathcal{O}(\mu \frac{d \log d}{\epsilon^2})$, and CountSketch with $s = \mathcal{O}(\frac{d^2}{\epsilon^2})$, the inequalities

$$\begin{aligned} \frac{\text{bias}(\mathbf{W}^h)}{\text{bias}(\mathbf{W}^*)} &\leq (1 + \epsilon) \left(1 + \frac{\epsilon \|\mathbf{X}\|_2^2}{n\gamma}\right), \\ 1 - \epsilon &\leq \frac{\text{var}(\mathbf{W}^h)}{\text{var}(\mathbf{W}^*)} \leq 1 + \epsilon \end{aligned}$$

hold with probability at least 0.9. Further assume that $\sigma_\rho^2 \geq \frac{n\gamma}{\epsilon}$. Then

$$\frac{\text{bias}(\mathbf{W}^h)}{\text{bias}(\mathbf{W}^*)} \geq \frac{1}{1 + \epsilon} \left(\frac{\epsilon \sigma_\rho^2}{n\gamma} - 1 \right)$$

holds with probability at least 0.9.

The lower bound on the bias shows that Hessian sketch can suffer from a much higher bias than the optimal solution. The gap between $\text{bias}(\mathbf{W}^h)$ and $\text{bias}(\mathbf{W}^*)$ can be lessened by increasing the regularization parameter γ , but such over-regularization increases the baseline $\text{bias}(\mathbf{W}^*)$ itself. It is also worth mentioning that unlike $\text{bias}(\mathbf{W}^*)$ and $\text{bias}(\mathbf{W}^c)$, $\text{bias}(\mathbf{W}^h)$ is not monotonically increasing with γ , as is empirically verified in Figure 3.

In sum, our theories show that the classical and Hessian sketches are not statistically comparable to the optimal solutions: classical sketch has too high a variance, and Hessian sketch has too high a bias for reasonable amounts of regularization. In practice, the regularization parameter γ should be tuned to optimize the prediction accuracy. Our experiments in Figure 3 show that even with fine-tuned γ , the risks of classical and Hessian sketches can be higher than the risk of the optimal solution by an order of magnitude. Formally speaking, $\min_\gamma R(\mathbf{W}^c) \gg \min_\gamma R(\mathbf{W}^*)$ and $\min_\gamma R(\mathbf{W}^h) \gg \min_\gamma R(\mathbf{W}^*)$ hold in practice.

Our empirical study in Figure 3 suggests classical and Hessian sketches both require over-regularization, i.e., setting γ larger than what is best for the optimal solution \mathbf{W}^* . Formally

speaking, $\text{argmin}_\gamma R(\mathbf{W}^c) > \text{argmin}_\gamma R(\mathbf{W}^*)$ and $\text{argmin}_\gamma R(\mathbf{W}^h) > \text{argmin}_\gamma R(\mathbf{W}^*)$. Although this is the case for both types of sketches, the underlying explanations are different. Classical sketch has a high variance, so a large γ is required to suppress the variance (its variance is non-increasing with γ). Hessian sketch has very high bias when γ is small, so a reasonably large γ is necessary to lower its bias.

3.3 Model Averaging: Optimization Perspective

We consider model averaging as an approach to increasing the accuracy of sketched MRR solutions. The model averaging procedure is straightforward: one independently draws g sketching matrices $\mathbf{S}_1, \dots, \mathbf{S}_g \in \mathbb{R}^{n \times s}$, uses these to form g sketched MRR solutions, denoted by $\{\mathbf{W}_i^c\}_{i=1}^g$ or $\{\mathbf{W}_i^h\}_{i=1}^g$, and averages these solutions to obtain the final estimate $\mathbf{W}^c = \frac{1}{g} \sum_{i=1}^g \mathbf{W}_i^c$ or $\mathbf{W}^h = \frac{1}{g} \sum_{i=1}^g \mathbf{W}_i^h$. Practical applications of model averaging are enumerated in Section 1.1.

Theorems 8 and 9 present guarantees on the optimization accuracy of using model averaging to combine the classical/Hessian sketch solutions. We can contrast these with the guarantees provided for sketched MRR in Theorems 1 and 2. For classical sketch with model averaging, we see that when $\epsilon \leq \frac{1}{g}$, the bound on $f(\mathbf{W}^h) - f(\mathbf{W}^*)$ is proportional to ϵ/g . From Lemma 3 we can see that the distances from \mathbf{W}^c to \mathbf{W}^* also decreases accordingly.

Theorem 8 (Classical Sketch with Model Averaging) *Let $\beta = \frac{\|\mathbf{X}\|_2^2}{\|\mathbf{X}\|_2^2 + n\gamma} \leq 1$. For the four methods, let $s = \tilde{\mathcal{O}}\left(\frac{\beta d}{\epsilon}\right)$; for uniform sampling, let $s = \mathcal{O}\left(\frac{\mu\beta d \log d}{\epsilon}\right)$. Then the inequality*

$$f(\mathbf{W}^c) - f(\mathbf{W}^*) \leq \left(\frac{\epsilon}{g} + \beta^2 \epsilon^2\right) f(\mathbf{W}^*)$$

holds with probability at least 0.8.

For Hessian sketch with model averaging, if $\frac{\epsilon}{\beta^2} \leq \frac{1}{g^2}$, then the bound on $f(\mathbf{W}^h) - f(\mathbf{W}^*)$ is proportional to $\frac{\epsilon}{g^2}$.

Theorem 9 (Hessian Sketch with Model Averaging) *Let $\beta = \frac{\|\mathbf{X}\|_2^2}{\|\mathbf{X}\|_2^2 + n\gamma} \leq 1$. For the four methods let $s = \tilde{\mathcal{O}}\left(\frac{\beta^2 d}{\epsilon}\right)$, and for uniform sampling let $s = \mathcal{O}\left(\frac{\mu\beta^2 d \log d}{\epsilon}\right)$, then the inequality*

$$f(\mathbf{W}^h) - f(\mathbf{W}^*) \leq \left(\frac{\epsilon}{g^2} + \frac{\epsilon^2}{\beta^2}\right) \left(\frac{\|\mathbf{Y}\|_F^2}{n} - f(\mathbf{W}^*)\right).$$

holds with probability at least 0.8.

3.4 Model Averaging: Statistical Perspective

Model averaging also has the salutatory property of reducing the risks of the classical and Hessian sketches. Our first result conducts a bias-variance decomposition for the averaged solution of sketched MRR.

Theorem 10 (Bias-Variance Decomposition) *We consider the fixed design model (7). The risk function defined in (8) can be decomposed as*

$$R(\mathbf{W}) = \text{bias}^2(\mathbf{W}) + \text{var}(\mathbf{W}).$$

The bias and variance terms are

$$\begin{aligned} \text{bias}(\mathbf{W}^c) &= \gamma\sqrt{n}\left\|\frac{1}{g}\sum_{i=1}^g (\mathbf{U}^T \mathbf{S}_i \mathbf{S}_i^T \mathbf{U} + n\gamma \boldsymbol{\Sigma}^{-2})^\dagger \boldsymbol{\Sigma}^{-1} \mathbf{V}^T \mathbf{W}_0\right\|_F, \\ \text{var}(\mathbf{W}^c) &= \frac{\xi^2}{n}\left\|\frac{1}{g}\sum_{i=1}^g (\mathbf{U}^T \mathbf{S}_i \mathbf{S}_i^T \mathbf{U} + n\gamma \boldsymbol{\Sigma}^{-2})^\dagger \mathbf{U}^T \mathbf{S}_i \mathbf{S}_i^T\right\|_F^2, \\ \text{bias}(\mathbf{W}^h) &= \gamma\sqrt{n}\left\|\frac{1}{g}\sum_{i=1}^g (\boldsymbol{\Sigma}^{-2} + \frac{\mathbf{U}^T \mathbf{S}_i \mathbf{S}_i^T \mathbf{U} - \mathbf{I}_p}{n\gamma})(\mathbf{U}^T \mathbf{S}_i \mathbf{S}_i^T \mathbf{U} + n\gamma \boldsymbol{\Sigma}^{-2})^\dagger \boldsymbol{\Sigma} \mathbf{V}^T \mathbf{W}_0\right\|_F, \\ \text{var}(\mathbf{W}^h) &= \frac{\xi^2}{n}\left\|\frac{1}{g}\sum_{i=1}^g (\mathbf{U}^T \mathbf{S}_i \mathbf{S}_i^T \mathbf{U} + n\gamma \boldsymbol{\Sigma}^{-2})^\dagger\right\|_F^2. \end{aligned}$$

Theorems 11 and 13 provide upper bounds on the bias and variance of model-averaged sketched MRR for, respectively, classical sketch and Hessian sketch. We can contrast them with Theorems 5 and 7 to see the statistical benefits of model averaging.

Theorem 11 (Classical Sketch with Model Averaging) *For shrinked leverage score sampling, Gaussian projection, and SRHT with $s = \tilde{\mathcal{O}}(\frac{d}{\epsilon^2})$, or uniform sampling with $s = \mathcal{O}(\frac{\mu d \log d}{\epsilon^2})$, the inequalities*

$$\begin{aligned} \frac{\text{bias}(\mathbf{W}^c)}{\text{bias}(\mathbf{W}^*)} &\leq 1 + \epsilon, \\ \frac{\text{var}(\mathbf{W}^c)}{\text{var}(\mathbf{W}^*)} &\leq \frac{n}{s} \left(\sqrt{\frac{1+\epsilon/g}{g}} + \epsilon \right)^2 \end{aligned}$$

hold with probability at least 0.8.

Bagging (Breiman, 1996) works in the following way: first, randomly generates g datasets by uniform sampling with or without replacement; second, solves the matrix regression/classification problem independently on each generated dataset; last, aggregates the solutions in some way, e.g., model averaging. We show in Corollary 12 to show bagging indeed achieves better variance than the optimal solution \mathbf{W}^* . Note that our approaches are more general than the traditional bagging: the g datasets can be formed by any sketching and not limited to uniform sampling.

Corollary 12 (Bagging) *Let $g = \mathcal{O}(\frac{n}{s})$; for shrinked leverage score sampling, Gaussian projection, and SRHT with $s = \tilde{\mathcal{O}}(\sqrt{nd})$, or uniform sampling with $s = \mathcal{O}(\sqrt{\mu nd \log d})$, it holds with probability 0.8 that*

$$\text{var}(\mathbf{W}^c) \leq \text{var}(\mathbf{W}^*).$$

Furthermore, for shrinked leverage score sampling, Gaussian projection, and SRHT with $s = \tilde{\mathcal{O}}(dg) \leq n$, or uniform sampling with $s = \mathcal{O}(\mu gd \log d)$, it holds with probability 0.8 that

$$\text{var}(\mathbf{W}^c) = \mathcal{O}\left(\frac{1}{g} \text{var}(\mathbf{W}^*)\right).$$

Theorem 13 shows that model averaging decreases the bias of Hessian sketch without increasing the variance. For Hessian sketch without model averaging, recall that $\text{bias}(\mathbf{W}^h)$ is larger than $\text{bias}(\mathbf{W}^*)$ by a factor of $\mathcal{O}(\|\mathbf{X}\|_2^2/(n\gamma))$. Theorem 13 shows that model averaging reduces this ratio by a factor of $\frac{\epsilon}{g}$ when $\epsilon \leq \frac{1}{g}$.

Theorem 13 (Hessian Sketch with Model Averaging) *For the four methods with $s = \tilde{\mathcal{O}}\left(\frac{d}{\epsilon^2}\right)$, or uniform sampling with $s = \mathcal{O}\left(\frac{\mu d \log d}{\epsilon^2}\right)$, the inequalities*

$$\begin{aligned}\frac{\text{bias}(\mathbf{W}^h)}{\text{bias}(\mathbf{W}^*)} &\leq 1 + \epsilon + \left(\frac{\epsilon}{g} + \epsilon^2\right) \frac{\|\mathbf{X}\|_2^2}{n\gamma}, \\ \frac{\text{var}(\mathbf{W}^h)}{\text{var}(\mathbf{W}^*)} &\leq 1 + \epsilon\end{aligned}$$

hold with probability at least 0.8.

4. Experiments on Synthetic Data

We conduct experiments on synthetic data to verify our main Theorems. Section 4.1 describes the data model and experiment settings. Sections 4.2 and 4.3 study classical and Hessian sketches from the optimization and statistical perspectives, respectively, to verify Theorems 1, 2, 5, 7. Sections 4.4 and 4.5 study the model averaging from the optimization and statistical perspectives, respectively, to corroborate Theorems 8, 9, 11, 13.

4.1 Settings

Following (Ma et al., 2015, Yang et al., 2016), we construct $\mathbf{X} = \mathbf{U}\text{diag}(\boldsymbol{\sigma})\mathbf{V}^T \in \mathbb{R}^{n \times d}$ and $\mathbf{y} = \mathbf{X}\mathbf{w}_0 + \boldsymbol{\varepsilon} \in \mathbb{R}^n$ in the following way.

- Let the rows of $\mathbf{A} \in \mathbb{R}^{n \times d}$ be i.i.d. sampled from multivariate t -distribution with covariance matrix \mathbf{C} and $v = 2$ degree of freedom, where the (i, j) -th entry of $\mathbf{C} \in \mathbb{R}^{m \times n}$ is $2 \times 0.5^{|i-j|}$. \mathbf{A} has high row coherence. Let \mathbf{U} be the orthonormal bases of \mathbf{A} .
- Let the entries of $\mathbf{b} \in \mathbb{R}^d$ be equally paced between 0 and -6 . Let $\sigma_i = 10^{b_i}$ for all $i \in [d]$.
- Let $\mathbf{V} \in \mathbb{R}^{d \times d}$ be the orthonormal bases of a $d \times d$ standard Gaussian matrix.
- Let $\mathbf{w}_0 = [\mathbf{1}_{0.2d}; 0.1\mathbf{1}_{0.6d}; \mathbf{1}_{0.2d}]$.
- The entries of $\boldsymbol{\varepsilon} \in \mathbb{R}^n$ are i.i.d. sampled from $\mathcal{N}(0, \xi^2)$.

In this way, \mathbf{X} has high row coherence; its condition number is $\kappa(\mathbf{X}^T \mathbf{X}) = 10^{12}$. Let $\mathbf{S} \in \mathbb{R}^{n \times s}$ be any of the six sketching methods considered in this paper. We fix $n = 10^5$, $d = 500$, and $s = 5,000$. Since the sketching methods are randomized, we always repeat sketching 10 times and report the averaged results.

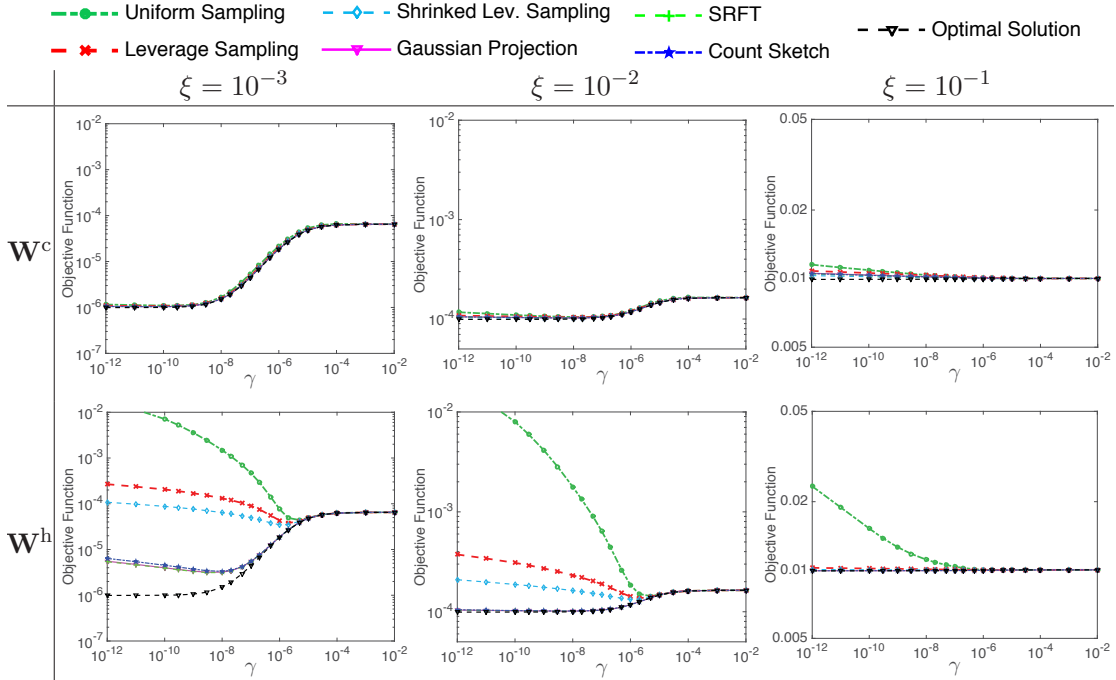


Figure 2: Empirical study of classical sketch and Hessian sketch from optimization perspective. The x -axis is the regularization parameter γ (log-scale); the y -axis is the objective function values (log-scale).

4.2 Sketched MRR: Optimization Perspective

We seek to verify Theorems 1 and 2 which study classical and Hessian sketches, respectively, from the optimization perspective. In Figure 2, we plot the objective function value $f(\mathbf{w}) = \frac{1}{n} \|\mathbf{X}\mathbf{w} - \mathbf{y}\|_2^2 + \gamma \|\mathbf{w}\|_2^2$ against γ , under different settings of noise intensity ξ . The black curves correspond to the optimal solution \mathbf{w}^* ; the color curves are classical or Hessian sketch with different sketching methods. The results verify our theory: classical sketch \mathbf{w}^c is always close to optimal; Hessian sketch \mathbf{w}^h is much worse than the optimal when γ is small and \mathbf{y} is mostly in the column space of \mathbf{X} .

4.3 Sketched MRR: Statistical Perspective

In Figure 3, we plot the analytical expressions for the squared bias, variance, and risk stated in Theorem 4 against the regularization parameter γ . Because the analytical expressions involve the random sketching matrix \mathbf{S} , we randomly generate \mathbf{S} , repeat this procedure 10 times, and report the average of the computed squared biases, variances, and risks. We fix $\xi = 0.1$. The results of this experiment match our theory: classical sketch magnified the variance, and Hessian sketch increased the bias. Even when γ is fine-tuned, the risks of classical and Hessian sketches can be much higher than those of the optimal solution. Our experiment also indicates that classical and Hessian sketches require setting γ larger than the best regularization parameter for the optimal solution \mathbf{W}^* .

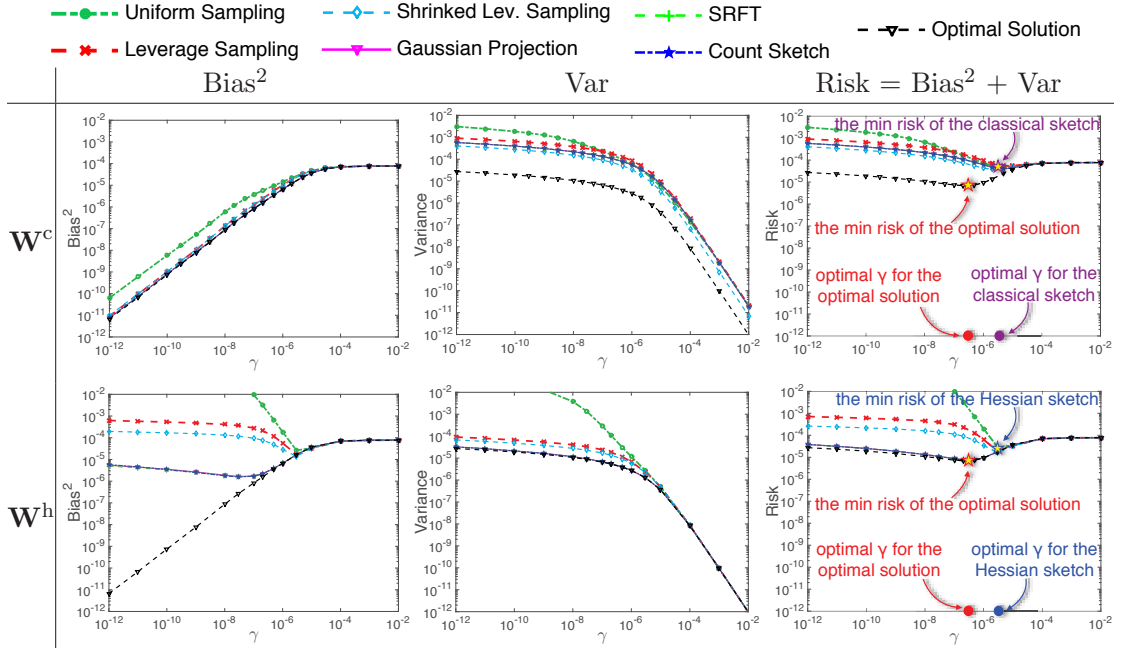


Figure 3: Empirical study of classical sketch and Hessian sketch from statistical perspective. The x -axis is the regularization parameter γ (log-scale); the y -axes are respectively bias², variance, and risk (log-scale). We annotate the minimum risks and optimal γ in the plots

Classical sketch and Hessian sketch do not outperform each other in terms of the risk. When variance dominates bias, Hessian sketch is better in terms of the risk; when bias dominates variance, classical sketch is better. In the experiment yielding Figure 3, Hessian sketch had lower risk than classical sketch. This is not generally true: if we used a smaller ξ , so that the variance is dominated by bias, then classical sketch results in lower risks than Hessian sketch.

4.4 Model Averaging: Optimization Objective

We use different intensity of noise—we set $\xi = 10^{-2}$ or 10^{-1} , where ξ defined in Section 4.1 indicates the intensity of the noise in the response vector \mathbf{y} . We calculate the objective function values $f(\mathbf{w}_{[g]}^c)$ and $f(\mathbf{w}_{[g]}^h)$ under different settings of g, γ . We use different matrix sketching but fix the sketch size $s = 5,000$.

Theorem 8 shows that for large s , e.g., Gaussian projection with $s = \tilde{\mathcal{O}}\left(\frac{\beta d}{\epsilon}\right)$, then

$$f(\mathbf{w}_{[g]}^c) - f(\mathbf{w}^*) \leq \left(\frac{\epsilon}{g} + \beta^2 \epsilon^2\right) f(\mathbf{w}^*), \quad (9)$$

where $\beta = \frac{\|\mathbf{X}\|_2^2}{\|\mathbf{X}\|_2^2 + n\gamma} \leq 1$. In Figure 4(a) we plot g against the ratio

$$\frac{f(\mathbf{w}_{[1]}^c) - f(\mathbf{w}^*)}{f(\mathbf{w}_{[g]}^c) - f(\mathbf{w}^*)}. \quad (10)$$

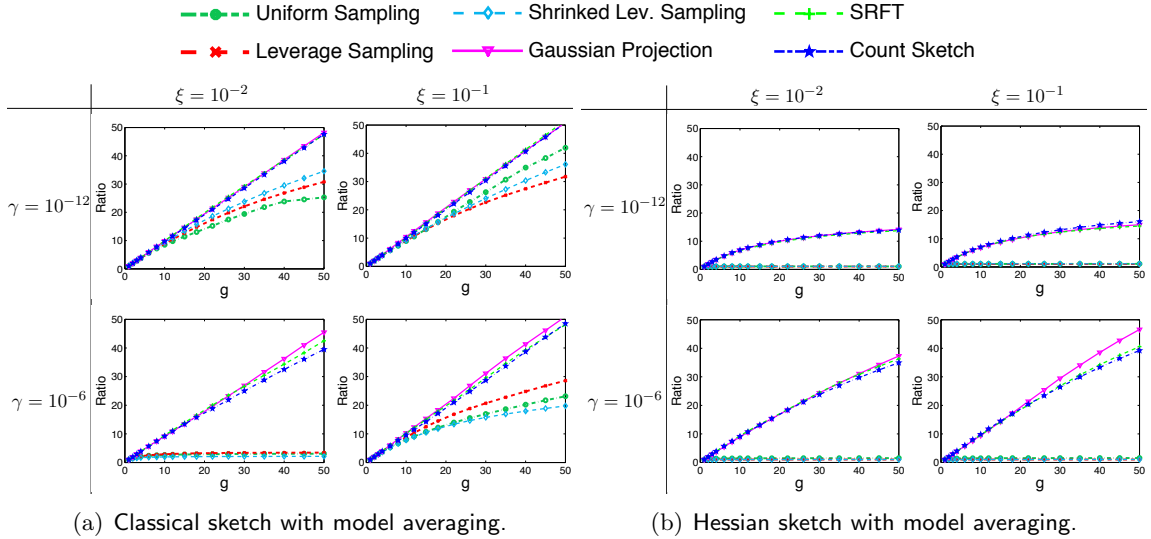


Figure 4: Empirical study of model averaging from optimization perspective. The x -axis is g , i.e. the number of samples over which model averaging averages. In 4(a), the y -axis is the ratio (log-scale) defined in (10). In 4(b), the y -axis is the ratio (log-scale) defined in (11).

Rapid growth of the ratio indicates high effectiveness of the model averaging. The results in Figure 4(a) indicate model averaging significantly improves the accuracy in terms of the objective function value. For the three random projection methods, the growth rate is almost linear in g . In Figure 4(a), we observe that the regularization parameter γ affects the ratio (10). The ratio grows faster when $\gamma = 10^{-12}$ than when $\gamma = 10^{-6}$. However, this phenomenon cannot be explained by our theory.

Theorem 9 shows that for large sketch size s , e.g., Gaussian projection with $s = \tilde{\mathcal{O}}\left(\frac{\beta^2 d}{\epsilon}\right)$, then

$$f(\mathbf{w}^h) - f(\mathbf{w}^*) \leq \left(\frac{\epsilon}{g^2} + \frac{\epsilon^2}{\beta^2}\right) \left(\frac{\|\mathbf{y}\|_2^2}{n} - f(\mathbf{w}^*)\right),$$

where $\beta = \frac{\|\mathbf{X}\|_2^2}{\|\mathbf{X}\|_2^2 + n\gamma} \leq 1$. In Figure 4(b), we plot g against the ratio

$$\frac{f(\mathbf{w}_{[1]}^h) - f(\mathbf{w}^*)}{f(\mathbf{w}_{[g]}^h) - f(\mathbf{w}^*)}. \quad (11)$$

Rapid growth of the ratio indicates high effectiveness of the model averaging. If $\frac{\epsilon}{\beta^2} \leq \frac{1}{g^2}$, equivalently s is at least $\tilde{\mathcal{O}}(dg^2)$, the ratio (11) should grow nearly quadratically with g . However, the requirement on the sketch size s can be hardly satisfied, unless s is big and g is small. The empirical results reflects that the growth rate is moderately rapid for very small g and very slow for large g . This is in accordance with the theory.

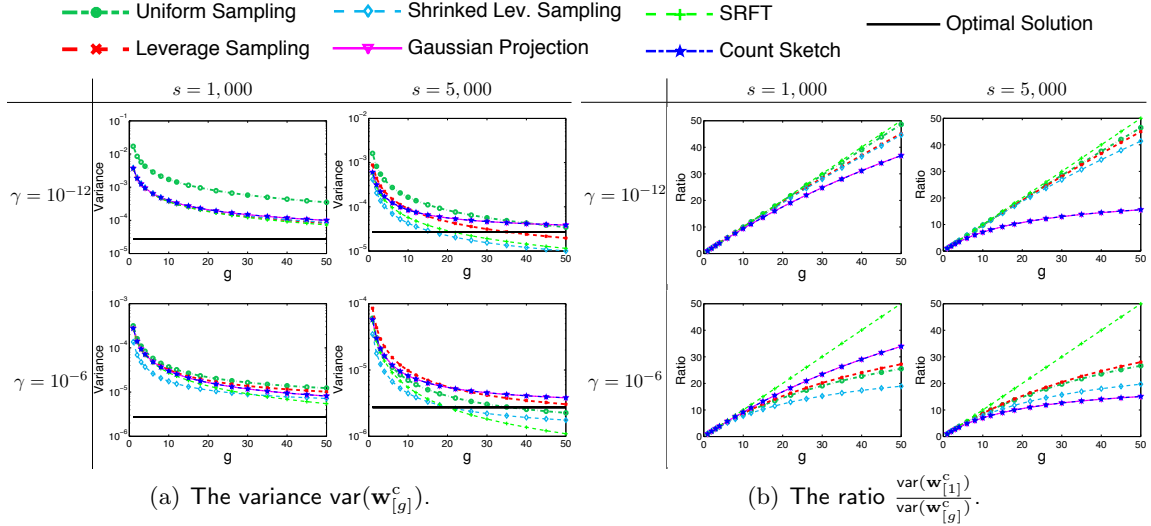


Figure 5: Empirical study of the variance of classical sketch with model averaging. The x -axis is g , i.e. the number of samples over which model averaging averages. In 5(a), the y -axis is the variance $\text{var}(\mathbf{w}_{[g]}^c)$ (log-scale) defined in Theorem 10. In 5(b), the y -axis is the ratio $\frac{\text{var}(\mathbf{w}_{[1]}^c)}{\text{var}(\mathbf{w}_{[g]}^c)}$.

4.5 Model Averaging: Statistical Perspective

We study the model averaging from the statistical perspective. We calculate $\text{bias}(\mathbf{w}^*)$, $\text{var}(\mathbf{w}^*)$ (optimal solution) according to Theorem 4 and $\text{bias}(\mathbf{w}_{[g]}^c)$, $\text{var}(\mathbf{w}_{[g]}^c)$ (classical sketch) and $\text{bias}(\mathbf{w}_{[g]}^h)$, $\text{var}(\mathbf{w}_{[g]}^h)$ (Hessian sketch) according to Theorem 10.

4.5.1 CLASSICAL SKETCH

Theorem 11 shows that for large enough s , e.g., Gaussian projection with $s = \tilde{\mathcal{O}}\left(\frac{d}{\epsilon^2}\right)$, then

$$\frac{\text{bias}(\mathbf{w}_{[g]}^c)}{\text{bias}(\mathbf{w}^*)} \leq 1 + \epsilon \quad \text{and} \quad \frac{\text{var}(\mathbf{w}_{[g]}^c)}{\text{var}(\mathbf{w}^*)} \leq \frac{n}{s} \left(\sqrt{\frac{1+\epsilon/g}{g}} + \epsilon \right)^2$$

hold with high probability. The theorem indicates that model averaging does not make the bias worse and that it improves the variance. We conduct experiments to verify this point.

In Figure 5(a) we plot g against the variance $\text{var}(\mathbf{w}_{[g]}^c)$; the variance of the optimal solution \mathbf{w}^* is employed for comparison. Clearly, the variance drops as g grows. In particular, when s is big ($s = 5,000$) and g exceeds $\frac{n}{s}$ ($= \frac{100,000}{5,000} = 20$), $\text{var}(\mathbf{w}_{[g]}^c)$ can be even lower than $\text{var}(\mathbf{w}^*)$. This verifies Corollary 12. This has an important implication: if \mathbf{y} is corrupted by intense noise, we can use the classical sketch with model averaging to obtain a solution which has lower variance than the optimal solution \mathbf{w}^* .

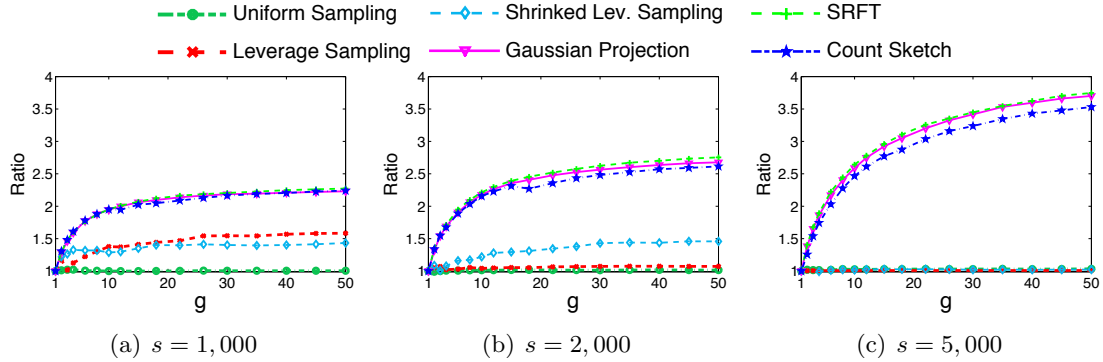


Figure 6: Empirical study of the bias of Hessian sketch with model averaging. The x -axis is g (number of samples over which model averaging averages); the y -axis is the ratio (12).

To make the decrease of $\text{var}(\mathbf{w}_{[g]}^c)$ more clear, in Figure 5(b) we plot g against the ratio $\frac{\text{var}(\mathbf{w}_{[1]}^c)}{\text{var}(\mathbf{w}_{[g]}^c)}$. According to Theorem 11, this ratio grows linearly with g if s is at least $\tilde{\mathcal{O}}(dg)$. Otherwise, the ratio is sublinear with g . The theory is verified by the empirical results in Figure 5(b).

We plotted g against $\text{bias}(\mathbf{w}_{[g]}^c)$ in the same way as Figures 5(a) and 5(b). All the curves of g against the bias are almost horizontal, indicating that *the increase of g does make the bias better or worse*. We do not show the plots in the paper because these nearly horizontal curves are not interesting.

4.5.2 HESSIAN SKETCH

Theorem 13 shows that for large enough s , e.g., Gaussian projection with $s = \tilde{\mathcal{O}}(\frac{d}{\epsilon^2})$, the inequalities

$$\frac{\text{bias}(\mathbf{w}_{[g]}^h)}{\text{bias}(\mathbf{w}^*)} \leq 1 + \epsilon + \left(\frac{\epsilon}{g} + \epsilon^2\right) \frac{\|\mathbf{X}\|_2^2}{n\gamma} \quad \text{and} \quad \frac{\text{var}(\mathbf{w}_{[g]}^h)}{\text{var}(\mathbf{w}^*)} \leq 1 + \epsilon$$

hold with high probability. Theoretically speaking, model averaging improves the bias without making the variance worse. The bound

$$\frac{\text{bias}(\mathbf{w}_{[g]}^h) - \text{bias}(\mathbf{w}^*)}{\text{bias}(\mathbf{w}^*)} \leq \epsilon + \left(\frac{\epsilon}{g} + \epsilon^2\right) \frac{\|\mathbf{X}\|_2^2}{n\gamma}$$

indicates that if (1) $n\gamma$ is much smaller than $\|\mathbf{X}\|_2^2$ and (2) $\epsilon \leq \frac{1}{g}$, equivalently s is at least $\tilde{\mathcal{O}}(dg^2)$, then the ratio is proportional to $\frac{\epsilon}{g}$.

To verify Theorem 13, we set γ very small— $\gamma = 10^{-12}$ —and vary s and g . In Figure 6 we plot the ratio

$$\frac{\text{bias}(\mathbf{w}_{[1]}^h) - \text{bias}(\mathbf{w}^*)}{\text{bias}(\mathbf{w}_{[g]}^h) - \text{bias}(\mathbf{w}^*)}, \quad (12)$$

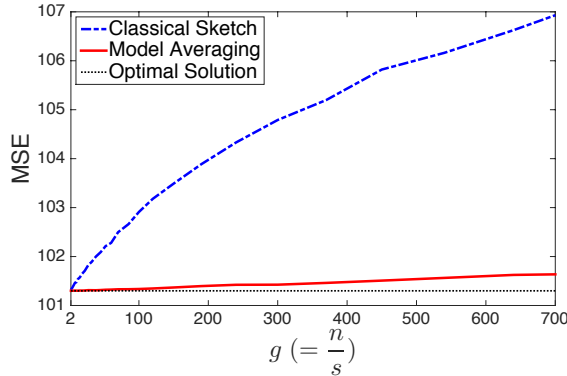


Figure 7: Prediction performance of classical sketch with/without model averaging on the Year Prediction dataset. The x -axis is g (the number of data partitions); the y -axis is the mean squared error (MSE) on the test set.

by fixing $\gamma = 10^{-12}$ and vary s and g . Ideally, for large sketch size $s = \tilde{\mathcal{O}}(dg^2)$, the ratio should grow nearly linearly with g . Figure 6 shows only for large s and very small g , the growth can be near linear with g ; this verifies our theory.

We have also plotted g against $\text{var}(\mathbf{w}_{[g]}^h)$. We observe that $\text{var}(\mathbf{w}_{[g]}^h)$ remains nearly unaffected as g grows from 1 to 50. Since the curves of g against $\text{var}(\mathbf{w}_{[g]}^h)$ are almost horizontal lines, we do not show the plot in the paper.

5. Model Averaging Experiments on Real-World Data

In Section 1 we mentioned that in the distributed setting where the feature-response pairs $(\mathbf{x}_1, \mathbf{y}_1), \dots, (\mathbf{x}_n, \mathbf{y}_n) \in \mathbb{R}^{d \times m}$ are stored across g machines, classical sketch with model averaging requires only one round of communication, and is therefore a communication-efficient algorithm that can be used to: (1) obtain an approximate solution of the MRR problem with risk comparable to a batch solution, and (2) obtain a low-precision solution of the MRR optimization problem that can be used as an initializer for more communication-intensive optimization algorithms. In this section, we demonstrate both applications.

We use the Million Song Year Prediction Dataset, which has 463,715 training samples and 51,630 test samples with 90 features and one response. We normalize the data by shifting the responses to have zero mean and scaling the range of each feature to $[-1, 1]$. We randomly partition the training data into g parts, which amounts to uniform row selection with sketch size $s = \frac{n}{g}$.

5.1 Prediction Error

We tested the prediction performance of sketched ridge regression by implementing classical sketch with model averaging in PySpark (Zaharia et al., 2010).⁵ We ran our experiments using PySpark in local mode; the experiments had three steps: (1) use five-fold cross-validation to determine the regularization parameter γ ; (2) learn the model \mathbf{w} using

5. The code is available at <https://github.com/wangshusen/SketchedRidgeRegression.git>

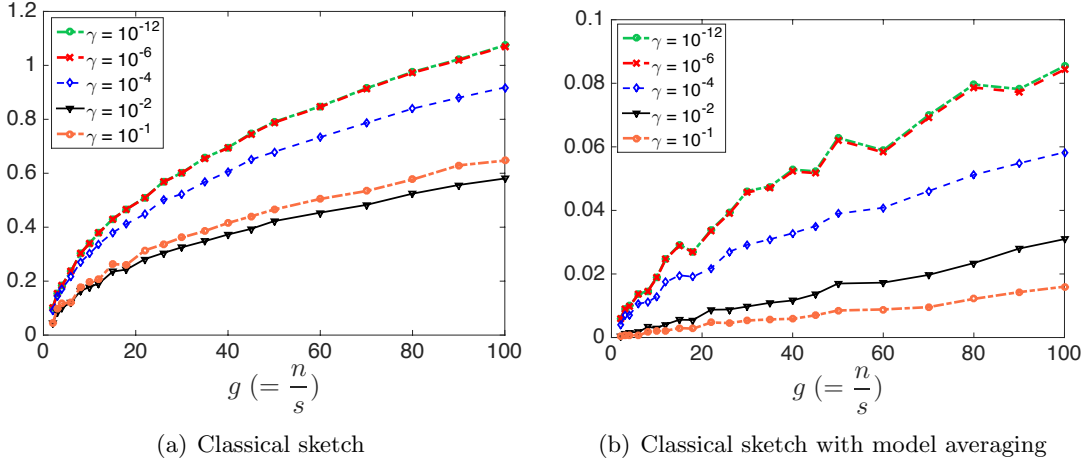


Figure 8: Optimization performance of classical sketch with/without model averaging. The x -axis is g (the number of data partitions); the y -axis is the ratio $\frac{\|\mathbf{w} - \mathbf{w}^*\|_2}{\|\mathbf{w}^*\|_2}$.

the selected γ ; and (3) use \mathbf{w} to predict on the test set and record the mean squared errors (MSEs). These steps map nicely onto the Map-Reduce programming model used by PySpark.

We plot $g = \frac{n}{s}$ against the MSE in Figure 7. As g grows, the sketch size $s = \frac{n}{g}$ decreases, so the performance of classical sketching deteriorates. However classical sketch with model averaging always has MSE comparable to the optimal solution.

5.2 Optimization Error

We mentioned earlier that classical sketch with or without model averaging can be used to initialize optimization algorithms for solving MRR. If \mathbf{w} is initialized with zero-mean random variables or deterministically with zeros, then $\mathbb{E}\|\mathbf{w} - \mathbf{w}^*\|_2/\|\mathbf{w}^*\|_2 \geq 1$. Any \mathbf{w} with the above ratio substantially smaller than 1 provides a better initialization. We implemented classical sketch with and without model averaging in Python and calculated the above ratio on the training set of the Year Prediction dataset; to estimate the expectation, we repeated the procedure 100 times and report the average of the ratios.

In Figure 8 we plot g against the average of the ratio $\frac{\|\mathbf{w} - \mathbf{w}^*\|_2}{\|\mathbf{w}^*\|_2}$ at different settings of the regularization parameter γ . Clearly, classical sketch does not give a very good initialization unless g is small (equivalently, the sketch size $s = \frac{n}{g}$ is large). In contrast, the averaged solution is always close to \mathbf{w}^* .

6. Sketch of Proof

In this section, we provide an outline of the proofs of our main results. Detailed proofs can be found in the Appendix. Section 6.1 shows some key properties of matrix sketching. Section 6.2 considers taking average of sketched matrices; the results will be applied to analyze sketched MRR with model averaging. Sections 6.3 to 6.6 establish the structural results of sketched MRR with or without model averaging.

Our main results in Section 3 (Theorems 1, 2, 5, 7, 8, 9, 11, 13) directly follow from the key properties of matrix sketching and the structural results of sketched MRR. Table 4 summarizes the dependency relationship among the theorems. For example, Theorem 1, which studies classical sketch from optimization perspective, is one of our main theorems and can be proved using Theorems 16 and 21.

Table 4: The summary and dependency relationship of the theorems.

Main Theorems	Solution	Perspective	Dependency
Theorem 1	classical	optimization	Theorems 16 and 21
Theorem 2	Hessian	optimization	Theorems 16 and 22
Theorem 5	classical	statistical	Theorems 16, 17, 23, 24
Theorem 7	Hessian	statistical	Theorems 16 and 25
Theorem 8	classical, averaging	optimization	Theorems 19 and 26
Theorem 9	Hessian, averaging	optimization	Theorems 19 and 27
Theorem 11	classical, averaging	statistical	Theorems 19 and 28
Theorem 13	Hessian, averaging	statistical	Theorems 19 and 29

6.1 Properties of Matrix Sketching

Our analysis of the sketched MRR uses some of the three key properties defined in Assumption 1. Theorem 16 establishes that the six sketching methods consider in this paper under different settings enjoy the three key properties. Finally, we show in Theorem 17 the lower bounds of $\|\mathbf{S}\|_2^2$; the theorem will be used to prove the lower bounds of variance in Theorem 5.

In Assumption 1, the subspace embedding property is that sketching preserves the product of a row orthogonal matrix and its transpose. Equivalently, it ensures that all the singular values of any sketched column orthogonal matrix are around one. The matrix multiplication property states that sketching preserves the multiplication of a row orthogonal matrix and an arbitrary matrix. The bounded spectral norm property is that the spectral norm of $\mathbf{S} \in \mathbb{R}^{n \times s}$ is around $\frac{n}{s}$.

Assumption 1 Let $\eta, \epsilon \in (0, 1)$ be any fixed parameters. Let \mathbf{B} be any matrix of proper size, $\rho = \text{rank}(\mathbf{X})$, and $\mathbf{U} \in \mathbb{R}^{n \times \rho}$ be the orthogonal bases of \mathbf{X} . Let $\mathbf{S} \in \mathbb{R}^{n \times s}$ be a sketching matrix where s depends on η and/or ϵ . Assume \mathbf{S} satisfies

- 1.1 $\|\mathbf{U}^T \mathbf{S} \mathbf{S}^T \mathbf{U} - \mathbf{I}_\rho\|_2 \leq \eta$ (Subspace Embedding Property);
- 1.2 $\|\mathbf{U}^T \mathbf{S} \mathbf{S}^T \mathbf{B} - \mathbf{U}^T \mathbf{B}\|_F^2 \leq \epsilon \|\mathbf{B}\|_F^2$ (Matrix Multiplication Property);
- 1.3 $\|\mathbf{S}\|_2^2 \leq \frac{\theta n}{s}$ for some constant θ (Bounded Spectral Norm Property).

Remark 14 Note that the first two assumptions were identified in (Mahoney, 2011) and are the relevant structural conditions needed to be satisfied to obtain strong results from the optimization perspective. The third condition is new, but Ma et al. (2015), Raskutti and Mahoney (2016) demonstrated that some sort of additional condition is needed to obtain strong results from the statistical perspective.

Remark 15 We note that $\mathbf{U}^T \mathbf{U} = \mathbf{I}_p$, and thus Assumption 1.1 can actually be expressed in the form of an approximate matrix multiplication bound (Drineas et al., 2006a). We call it the Subspace Embedding Property since, as first highlighted in Drineas et al. (2006b), this subspace embedding property is the key result to obtain high-quality sketching algorithms for regression and related problems.

Theorem 16 shows that the six sketching methods with sufficiently large s satisfy the three properties. We prove Theorem 16 in Appendix B. Theorem 16 shows that for all the sketching methods except leverage score sampling,⁶ $\|\mathbf{S}\|_2^2$ has nontrivial upper bound. That is why Theorems 5 and 11 are not applicable to leverage score sampling. That is also the motivation of using the shrunked leverage score sampling.

Theorem 16 Fix failure probability δ and error parameters η and ϵ ; set the sketch size s as Table 5. Assumption 1.1 is satisfied with probability at least $1 - \delta_1$. Assumption 1.2 is satisfied with probability at least $1 - \delta_2$. Assumption 1.3 is satisfied either surely or with probability close to one; the parameter θ is shown in Table 5.

Table 5: The two middle columns list the sketch size s for satisfying the subspace embedding property and the matrix multiplication property, respectively; the right column lists the parameter θ . Here τ is defined in (5) and reflects the quality of approximation to the leverage scores of \mathbf{U} ; μ is the row coherence of \mathbf{U} . For Gaussian projection and CountSketch, the small- o notation is a consequence of $s = o(n)$.

Sketching	Subspace Embedding	Matrix Multiplication	Spectral Norm
Leverage	$s = \mathcal{O}\left(\frac{\tau\rho}{\eta^2} \log \frac{\rho}{\delta_1}\right)$	$s = \mathcal{O}\left(\frac{\tau\rho}{\epsilon\delta_2}\right)$	$\theta = \infty$
Uniform	$s = \mathcal{O}\left(\frac{\mu\rho}{\eta^2} \log \frac{\rho}{\delta_1}\right)$	$s = \mathcal{O}\left(\frac{\mu\rho}{\epsilon\delta_2}\right)$	$\theta = 1$
Shrunked Leverage	$s = \mathcal{O}\left(\frac{\tau\rho}{\eta^2} \log \frac{\rho}{\delta_1}\right)$	$s = \mathcal{O}\left(\frac{\tau\rho}{\epsilon\delta_2}\right)$	$\theta = 2$
SRHT	$s = \mathcal{O}\left(\frac{\rho + \log n}{\eta^2} \log \frac{\rho}{\delta_1}\right)$	$s = \mathcal{O}\left(\frac{\rho + \log n}{\epsilon\delta_2}\right)$	$\theta = 1$
Gaussian Projection	$s = \mathcal{O}\left(\frac{\rho + \log(1/\delta_1)}{\eta^2}\right)$	$s = \mathcal{O}\left(\frac{\rho}{\epsilon\delta_2}\right)$	$\theta = 1 + o(1)$ w.h.p.
CountSketch	$s = \mathcal{O}\left(\frac{\rho^2}{\delta_1\eta^2}\right)$	$s = \mathcal{O}\left(\frac{\rho}{\epsilon\delta_2}\right)$	$\theta = 1 + o(1)$ w.h.p.

Theorem 17 establishes lower bound on $\|\mathbf{S}\|_2^2$. The results will be applied to prove the lower bound of the variance of classical sketch. From Table 6 we can see that the bound of (shrunked) leverage score sampling is not interesting, because μ can be very large. That is why in Theorems 5, the shrunked leverage score sampling lacks nontrivial lower bound. We prove Theorem 17 in Appendix B.

Theorem 17 (Lower Bound on the Spectral Norm of Sketching Matrix) The sketching methods and ϑ are described in Table 6. Then $\mathbf{S}^T \mathbf{S} \succeq \frac{\vartheta n}{s} \mathbf{I}_s$ holds either surely or with probability close to one.

6. If one leverage score approaches zero, then the corresponding sampling probability p_i goes to zero. By the definition of \mathbf{S} , the scaling $\frac{1}{\sqrt{sp_i}}$ goes to infinity, which makes $\|\mathbf{S}\|_2^2$ unbounded.

Table 6: The lower bound on ϑ (defined in Theorem 17). The (shrinked) leverage score sampling are according to the row leverage scores of any matrix $\mathbf{X} \in \mathbb{R}^{n \times d}$; μ is the row coherence of \mathbf{X} .

Uniform	$\vartheta = 1$
Leverage	$\vartheta \geq \frac{1}{\mu}$
Shrinked Leverage	$\vartheta \geq \frac{\mu}{1+\mu}$
SRHT	$\vartheta = 1$
Gaussian Projection	$\vartheta \geq 1 - o(1)$ w.h.p.
CountSketch	$\vartheta \geq 1 - o(1)$ w.h.p.

Remark 18 Let p_1, \dots, p_n be the sampling probabilities. By the definition of \mathbf{S} , the non-zero entries of \mathbf{S} can be any of $\frac{1}{\sqrt{sp_i}}$, for $i \in [n]$.

For leverage score sampling, $\|\mathbf{S}\|_2^2$ has neither nontrivial upper nor lower bound.⁷ It is because $\min_i p_i$ can be close to zero and $\max_i p_i$ can be large (close to one).

For shrinked leverage score sampling, because $\min_i p_i$ is at least $\frac{1}{2n}$, $\|\mathbf{S}\|_2^2$ has nontrivial upper bound; unfortunately, similar to leverage score sampling, $\max_i p_i$ can be large, and thereby $\|\mathbf{S}\|_2^2$ does not have nontrivial lower bound.

6.2 Matrix Sketching with Averaging

We have shown that sketching can be applied to approximate matrix multiplication; see Assumptions 1.1 and 1.2. What will happen if we independently draw g sketches, approximately compute the multiplications, and average the g products? Intuitively, the averaged product should better approximate the true product.

Let us justify the intuition formally. Let $\mathbf{S}_1, \dots, \mathbf{S}_g \in \mathbb{R}^{n \times s}$ be some sketching matrices and \mathbf{A} and \mathbf{B} are arbitrary fixed matrices with proper size. It is not hard to show that

$$\frac{1}{g} \sum_{i=1}^g \mathbf{A}^T \mathbf{S}_i \mathbf{S}_i^T \mathbf{B} = \mathbf{A}^T \mathbf{S} \mathbf{S}^T \mathbf{B},$$

where $\mathbf{S} = \frac{1}{\sqrt{g}} [\mathbf{S}_1, \dots, \mathbf{S}_g] \in \mathbb{R}^{n \times gs}$. Clearly \mathbf{S} is a sketching matrix larger than any of $\mathbf{S}_1, \dots, \mathbf{S}_g$. If $\mathbf{S}_1, \dots, \mathbf{S}_g$ are column selection, SRHT, or Gaussian projection matrices, then \mathbf{S} is the same type of sketching matrix.⁸

To analyze the sketched MRR with model averaging, we make the following assumptions. Here Assumption 2.1 is the subspace embedding property; Assumption 2.2 is the matrix multiplication property; Assumption 2.3 is the bounded spectral norm property.

Assumption 2 Let $\eta, \epsilon \in (0, 1)$ be any fixed parameters. Let \mathbf{B} be any matrix of proper size, $\rho = \text{rank}(\mathbf{X})$, and $\mathbf{U} \in \mathbb{R}^{n \times \rho}$ be the orthogonal bases of \mathbf{X} . Let $\mathbf{S}_1, \dots, \mathbf{S}_g \in \mathbb{R}^{n \times s}$ be

7. In our application, nontrivial bound means $\|\mathbf{S}\|_2^2$ is of order $\frac{n}{s}$.

8. The CountSketch does not enjoy such property. If $\mathbf{S}_i \in \mathbb{R}^{n \times s}$ is CountSketch matrix, then it has only one non-zero entry in each row. In contrast, $\mathbf{S} \in \mathbb{R}^{n \times gs}$ has g non-zero entries in each row; thus \mathbf{S} is not CountSketch matrix.

certain sketching matrices and $\mathbf{S} = \frac{1}{\sqrt{g}}[\mathbf{S}_1, \dots, \mathbf{S}_g] \in \mathbb{R}^{n \times gs}$; here s depends on η and/or ϵ . Assume \mathbf{S}_i and \mathbf{S} satisfy

- 2.1 $\|\mathbf{U}^T \mathbf{S}_i \mathbf{S}_i^T - \mathbf{I}_\rho\|_2 \leq \eta$ for all $i \in [g]$ and $\|\mathbf{U}^T \mathbf{S} \mathbf{S}^T \mathbf{U} - \mathbf{I}_\rho\|_2 \leq \frac{\eta}{g}$;
- 2.2 $(\frac{1}{g} \sum_{i=1}^g \|\mathbf{U}^T \mathbf{S}_i \mathbf{S}_i^T \mathbf{B} - \mathbf{U}^T \mathbf{B}\|_F)^2 \leq \epsilon \|\mathbf{B}\|_F^2$ and $\|\mathbf{U}^T \mathbf{S} \mathbf{S}^T \mathbf{B} - \mathbf{U}^T \mathbf{B}\|_F^2 \leq \frac{\epsilon}{g} \|\mathbf{B}\|_F^2$;
- 2.3 For some constant θ , $\|\mathbf{S}_i\|_2^2 \leq \frac{\theta n}{s}$ for all $i \in [g]$, and $\|\mathbf{S}\|_2^2 \leq \frac{\theta n}{gs}$.

Theorem 19 shows that random column selection, SRHT, and Gaussian projection matrices satisfy Assumptions 2.1, 2.2, 2.3. We prove Theorem 19 in Appendix B.

Theorem 19 *Let $\mathbf{S}_1, \dots, \mathbf{S}_g \in \mathbb{R}^{n \times s}$ be the same type of random sketching matrices, which can be independently drawn random column selection, SRHT, or Gaussian projection matrices. Fix failure probability δ and error parameters η and ϵ ; set the sketch size s as Table 5.*

Then Assumption 2.1 holds with probability at least $1 - g\delta_1 - \delta_1$. Assumption 2.2 holds with probability at least $1 - 2\delta_2$. Assumption 2.3 satisfied either surely or with probability close to one; the parameter θ is defined in Table 5.

In Theorem 16, Assumption 1.1 fails with probability at most δ_1 . In contrast, in Theorem 19, the counterpart assumption fails with probability at most $(g+1)\delta_1$. However, this makes little different, because δ_1 is in the logarithm and can be set very small (recall Table 5).

Remark 20 *We do not know whether CountSketch enjoys the properties in Assumption 2. This problem is difficult for two reasons. First, as aforementioned, the concatenation of multiple CountSketch matrices is not a CountSketch matrix. Second, the failure probability of the subspace embedding property of CountSketch is constant, rather than exponentially small.*

6.3 Sketched MRR: Optimization Perspective

Theorem 21 holds under the subspace embedding property and the matrix multiplication property (Assumptions 1.1 and 1.2). We prove Theorems 21 in Appendix C.

Theorem 21 (Classical Sketch) *Let Assumptions 1.1 and 1.2 hold for the sketching matrix $\mathbf{S} \in \mathbb{R}^{n \times s}$. Let η and ϵ be defined in Assumption 1. Let $\alpha = \frac{2 \max\{\epsilon, \eta^2\}}{1-\eta}$ and $\beta = \frac{\|\mathbf{X}\|_2^2}{\|\mathbf{X}\|_2^2 + n\gamma}$. Then*

$$f(\mathbf{W}^c) - f(\mathbf{W}^*) \leq \alpha \beta f(\mathbf{W}^*).$$

Theorem 22 holds under the subspace embedding property (Assumption 1.1). We prove Theorems 22 in Appendix C.

Theorem 22 (Hessian Sketch) *Let Assumption 1.1 hold for the sketching matrix $\mathbf{S} \in \mathbb{R}^{n \times s}$. Let η be defined in Assumption 1 and $\beta = \frac{\|\mathbf{X}\|_2^2}{\|\mathbf{X}\|_2^2 + n\gamma}$. Then*

$$f(\mathbf{W}^h) - f(\mathbf{W}^*) \leq \frac{\eta^2 \beta^2}{(1-\eta)^2} \left(\frac{\|\mathbf{Y}\|_F^2}{n} - f(\mathbf{W}^*) \right).$$

6.4 Sketched MRR: Statistical Perspective

Theorem 23 holds under the subspace embedding property (Assumption 1.1) and the bounded spectral norm property (Assumption 1.3). The theorem shows that for classical sketch, the bias is close to the optimal solution, but the bound on variance is very weak. We prove Theorems 23 in Appendix D.

Theorem 23 (Classical Sketch) *Let η and θ be defined in Assumption 1. Under Assumption 1.1, it holds that*

$$\frac{1}{1+\eta} \leq \frac{\text{bias}(\mathbf{W}^c)}{\text{bias}(\mathbf{W}^*)} \leq \frac{1}{1-\eta}.$$

Under Assumptions 1.1 and 1.3, it holds that

$$\frac{\text{var}(\mathbf{W}^c)}{\text{var}(\mathbf{W}^*)} \leq \frac{(1+\eta)}{(1-\eta)^2} \frac{\theta n}{s}.$$

Theorem 24 establishes a lower bound on the variance of classical sketch. We prove Theorems 24 in Appendix D.

Theorem 24 (Lower Bound on the Variance) *Under Assumption 1.1 and the additional assumption that $\mathbf{S}^T \mathbf{S} \succeq \frac{\vartheta n}{s} \mathbf{I}_s$, it holds that*

$$\frac{\text{var}(\mathbf{W}^c)}{\text{var}(\mathbf{W}^*)} \geq \frac{1-\eta}{(1+\eta)^2} \frac{\vartheta n}{s}.$$

Theorem 25 holds under the subspace embedding property (Assumption 1.1). In the theorem we define $\rho = \text{rank}(\mathbf{X})$ and $\sigma_1 \geq \dots \geq \sigma_\rho$ as the singular values of \mathbf{X} . We prove Theorems 25 in Appendix D.

Theorem 25 (Hessian Sketch) *Let η be defined in Assumption 1. Under Assumption 1.1, it holds that*

$$\begin{aligned} \frac{\text{bias}(\mathbf{W}^h)}{\text{bias}(\mathbf{W}^*)} &\leq \frac{1}{1-\eta} \left(1 + \frac{\eta \sigma_1^2}{n\gamma}\right), \\ \frac{1}{1+\eta} &\leq \frac{\text{var}(\mathbf{W}^h)}{\text{var}(\mathbf{W}^*)} \leq \frac{1}{1-\eta}. \end{aligned}$$

Further assume that $\sigma_\rho^2 \geq \frac{n\gamma}{\eta}$. Then

$$\frac{\text{bias}(\mathbf{W}^h)}{\text{bias}(\mathbf{W}^*)} \geq \frac{1}{1+\eta} \left(\frac{\eta \sigma_\rho^2}{n\gamma} - 1\right).$$

6.5 Model Averaging: Optimization Perspective

Theorem 26 holds under the subspace embedding property (Assumption 2.1) and the matrix multiplication property (Assumption 2.2). We prove Theorems 26 in Appendix E.

Theorem 26 (Classical Sketch with Model Averaging) *Let η and ϵ be defined in Assumption 2. Let $\alpha = 2[\max\{\sqrt{\frac{\epsilon}{g}}, \frac{\eta}{g}\} + 2\beta \max\{\eta\sqrt{\epsilon}, \eta^2\}]^2$ and $\beta = \frac{\|\mathbf{X}\|_2^2}{\|\mathbf{X}\|_2^2 + n\gamma} \leq 1$. Under Assumption 2.1 and 2.2, we have that*

$$f(\mathbf{W}^c) - f(\mathbf{W}^*) \leq \alpha\beta f(\mathbf{W}^*).$$

Theorem 27 holds under the subspace embedding property (Assumption 2.1). We prove Theorems 27 in Appendix E.

Theorem 27 (Hessian Sketch with Model Averaging) *Let η be defined in Assumption 2. Let $\alpha = (\frac{\eta}{g} + \frac{\eta^2}{1-\eta})$ and $\beta = \frac{\|\mathbf{X}\|_2^2}{\|\mathbf{X}\|_2^2 + n\gamma} \leq 1$. Under Assumption 2.1, we have that*

$$f(\mathbf{W}^h) - f(\mathbf{W}^*) \leq \alpha^2\beta^2 \left(\frac{1}{n} \|\mathbf{Y}\|_F^2 - f(\mathbf{W}^*) \right).$$

6.6 Model Averaging: Statistical Perspective

Theorem 28 requires the subspace embedding property (Assumption 2.1). In addition, to bound the variance, the spectral norms of $\mathbf{S}_1, \dots, \mathbf{S}_g$ and $\mathbf{S} = \frac{1}{\sqrt{g}}[\mathbf{S}_1, \dots, \mathbf{S}_g]$ must be bounded (Assumption 2.3). The theorem shows that model averaging improves the variance without making the bias worse. We prove Theorems 28 in Appendix F.

Theorem 28 (Classical Sketch with Model Averaging) *Under Assumption 2.1, it holds that*

$$\frac{\text{bias}(\mathbf{W}^c)}{\text{bias}(\mathbf{W}^*)} \leq \frac{1}{1-\eta}.$$

Under Assumptions 2.1 and 2.3, it holds that

$$\frac{\text{var}(\mathbf{W}^c)}{\text{var}(\mathbf{W}^*)} \leq \frac{\theta n}{s} \left(\frac{\sqrt{1+\eta/g}}{\sqrt{g}} + \frac{\eta\sqrt{1+\eta}}{1-\eta} \right)^2.$$

Here η and θ are defined in Assumption 2.

Theorem 29 requires the subspace embedding property (Assumption 2.1). It shows that model averaging improves the bias without making the variance worse. We prove Theorems 29 in Appendix F.

Theorem 29 (Hessian Sketch with Model Averaging) *Under Assumption 2.1, it holds that:*

$$\begin{aligned} \frac{\text{bias}(\mathbf{W}^h)}{\text{bias}(\mathbf{W}^*)} &\leq \frac{1}{1-\eta} + \left(\frac{\eta}{g} + \frac{\eta^2}{1-\eta} \right) \frac{\|\mathbf{X}\|_2^2}{n\gamma}, \\ \frac{\text{var}(\mathbf{W}^h)}{\text{var}(\mathbf{W}^*)} &\leq \frac{1}{1-\eta}. \end{aligned}$$

Here η is defined in Assumption 2.

7. Conclusions

We studied sketched matrix ridge regression (MRR) from optimization and statistical perspectives. Using classical sketch, by taking a large enough sketch, one can obtain an ϵ -accurate approximate solution. Counterintuitively and in contrast to classical sketch, the relative error of Hessian sketch increases as the responses \mathbf{Y} are better approximated by linear combinations of the columns of \mathbf{X} . Both classical and Hessian sketches can have statistical risks that are worse than the risk of the optimal solution by an order of magnitude.

We proposed the use of model averaging to attain better optimization and statistical properties. We have shown that model averaging leads to substantial improvements in the theoretical error bounds, suggesting applications in distributed optimization and machine learning. We also empirically verified its practical benefits.

Appendix A. Risk of Fixed Design Model

Let the risk $R(\mathbf{W})$ be defined in (8). The risk $R(\mathbf{W})$ determines how well the learned \mathbf{W} generalize to test data, which is the reason why we care about the risk. We formally explain this in the following.

Under the fixed design model, a test sample \mathbf{x} is uniformly drawn from the set $\{\mathbf{x}_1, \dots, \mathbf{x}_n\} \subset \mathbb{R}^d$. The corresponding response is $\mathbf{y} = \langle \mathbf{W}_0, \mathbf{x} \rangle + \boldsymbol{\xi}' \in \mathbb{R}^m$, where $\boldsymbol{\xi}' \in \mathbb{R}^m$ captures random noise; assume that $\mathbb{E}[\boldsymbol{\xi}'] = \mathbf{0}$ and that $\boldsymbol{\xi}'$ is independent of \mathbf{W} , \mathbf{W}_0 , and \mathbf{x} . The test mean squared error (MSE) is

$$\begin{aligned} \mathbb{E}_{\mathbf{x}, \boldsymbol{\xi}} \|\mathbf{W}^T \mathbf{x} - \mathbf{y}\|_2^2 &= \mathbb{E}_{\mathbf{x}, \boldsymbol{\xi}} \|\mathbf{W}^T \mathbf{x} - \mathbf{W}_0^T \mathbf{x} + \mathbf{W}_0 \mathbf{x} - \mathbf{y}\|_2^2 \\ &= \mathbb{E}_{\mathbf{x}, \boldsymbol{\xi}} \|\mathbf{W}^T \mathbf{x} - \mathbf{W}_0^T \mathbf{x} - \boldsymbol{\xi}'\|_2^2 \\ &= \mathbb{E}_{\mathbf{x}, \boldsymbol{\xi}} \left[\|\mathbf{W}^T \mathbf{x} - \mathbf{W}_0^T \mathbf{x}\|_2^2 + \|\boldsymbol{\xi}'\|_2^2 \right] \\ &= \frac{1}{n} \sum_{i=1}^n \|\mathbf{W}^T \mathbf{x}_i - \mathbf{W}_0^T \mathbf{x}_i\|_2^2 + \mathbb{E} \|\boldsymbol{\xi}'\|_2^2 \\ &= R(\mathbf{W}) + \mathbb{E} \|\boldsymbol{\xi}'\|_2^2. \end{aligned}$$

To this end, it is clear that the test MSE equals to the (training) risk $R(W)$ plus the “intensity” of the noise in test response.

Appendix B. Properties of Matrix Sketching: Proofs

In Section B.1 we prove Theorem 16. In Section B.2, we prove Theorem 17. In Section B.3 we prove Theorem 19.

B.1 Proof of Theorem 16

We prove the six sketching methods considered in this paper all satisfy the three key properties. In Section B.1.1 we show the six sketching methods satisfy Assumptions 1.1 and 1.2. In section B.1.2 we show the six sketching methods satisfy Assumption 1.3.

B.1.1 PROOF OF ASSUMPTIONS 1.1 AND 1.2

For uniform sampling, leverage score sampling, Gaussian projection, SRHT, and CountSketch, the subspace embedding property and matrix multiplication property have been established by the previous work (Drineas et al., 2008, 2011, Meng and Mahoney, 2013, Nelson and Nguyn, 2013, Tropp, 2011, Woodruff, 2014). See also (Wang et al., 2016c) for the summary.

In the following we prove only the **shrinked leverage score sampling**. We cite the following lemma from (Wang et al., 2016b); the lemma was firstly proved by the work (Drineas et al., 2008, Gittens, 2011, Woodruff, 2014).

Lemma 30 (Wang et al. (2016b)) *Let $\mathbf{U} \in \mathbb{R}^{n \times \rho}$ be any fixed matrix with orthonormal columns. The column selection matrix $\mathbf{S} \in \mathbb{R}^{n \times s}$ samples s columns according to arbitrary probabilities p_1, p_2, \dots, p_n . Assume $\alpha \geq \rho$ and*

$$\max_{i \in [n]} \frac{\|\mathbf{u}_{i:}\|_2^2}{p_i} \leq \alpha.$$

When $s \geq \alpha \frac{6+2\eta}{3\eta^2} \log(\rho/\delta_1)$, it holds that

$$\mathbb{P}\left\{\|\mathbf{I}_\rho - \mathbf{U}^T \mathbf{S} \mathbf{S}^T \mathbf{U}\|_2 \geq \eta\right\} \leq \delta_1.$$

When $s \geq \frac{\alpha}{\epsilon\delta_2}$, it holds that

$$\mathbb{E}\|\mathbf{U}\mathbf{B} - \mathbf{U}^T \mathbf{S} \mathbf{S}^T \mathbf{B}\|_F^2 \leq \delta_2 \epsilon \|\mathbf{B}\|_F^2;$$

as a consequence of Markov's inequality, it holds that

$$\mathbb{P}\left\{\|\mathbf{U}\mathbf{B} - \mathbf{U}^T \mathbf{S} \mathbf{S}^T \mathbf{B}\|_F^2 \geq \epsilon \|\mathbf{B}\|_F^2\right\} \leq \delta_2.$$

Here the expectation and probability are all w.r.t. the randomness in \mathbf{S} .

Now we apply the above lemma to analyze **shrinked leverage score sampling**. For the approximate shrinked leverage scores defined in (5), the sampling probabilities satisfy

$$p_i = \frac{1}{2} \left(\frac{1}{n} + \frac{\tilde{l}_i}{\sum_{q=1}^n \tilde{l}_q} \right) \geq \frac{\|\mathbf{u}_{i:}\|_2^2}{2\tau\rho}.$$

Here \tilde{l}_i and τ are defined in (5). Thus for all $i \in [n]$, $\frac{\|\mathbf{u}_{i:}\|_2^2}{\rho} < 2\tau\rho$. We can then apply Lemma 30 to show that Assumption 1.1 holds with probability at least $1 - \delta_1$ when $s \geq 2\tau\rho \frac{6+2\eta}{3\eta^2} \log(\rho/\delta_1)$ and that Assumption 1.2 holds with probability at least $1 - \delta_2$ when $s \geq \frac{2\tau\rho}{\epsilon\delta_2}$.

B.1.2 PROOF OF ASSUMPTION 1.3

For Uniform Sampling and SRHT, it is easy to show that $\mathbf{S}^T \mathbf{S} = \frac{n}{s} \mathbf{I}_s$. Thus $\|\mathbf{S}\|_2^2 = \frac{n}{s}$.

Let $\{p_i^s\}$ and $\{p_i^u\}$ be the sampling probabilities of the leverage score sampling and uniform sampling, respectively. Obviously $p_i^s \geq \frac{1}{2} p_i^u$. Thus for the shrinked leverage score sampling, $\|\mathbf{S}\|_2^2 \leq \frac{2n}{s}$.

[Vershynin \(2010\)](#) showed that the greatest singular value of the standard Gaussian matrix $\mathbf{G} \in \mathbb{R}^{n \times s}$ is at most $\sqrt{n} + \sqrt{s} + t$ with probability at least $1 - 2e^{-t^2/2}$. Thus for Gaussian projection matrix \mathbf{S} ,

$$\|\mathbf{S}\|_2^2 = \frac{1}{s} \|\mathbf{G}\|_2^2 \leq \frac{(\sqrt{n} + \sqrt{s} + t)^2}{s}$$

holds with probability at least $1 - 2e^{-t^2/2}$.

If \mathbf{S} is the CountSketch matrix, then each row of \mathbf{S} has exactly one nonzero entry, either 1 or -1 . Because the columns of \mathbf{S} are orthogonal to each other, it holds that

$$\|\mathbf{S}\|_2^2 = \max_{i \in [s]} \|\mathbf{s}_{:i}\|_2^2 = \max_{i \in [s]} \text{nnz}(\mathbf{s}_{:i}).$$

The problem of bounding $\text{nnz}(\mathbf{s}_{:i})$ is equivalent to assigning n balls into s bins uniformly at random and bounding the number of balls in the bins. [Patrascu and Thorup \(2012\)](#) showed that the maximal number of balls in any bin is at most $n/s + \mathcal{O}(\sqrt{n/s} \log^c n)$ with probability at least $1 - \frac{1}{n}$, where $c = \mathcal{O}(1)$. Thus

$$\|\mathbf{S}\|_2^2 = \max_{i \in [s]} \text{nnz}(\mathbf{s}_{:i}) \leq \frac{n}{s} + \mathcal{O}\left(\frac{\sqrt{n} \log^c n}{\sqrt{s}}\right) = \frac{n}{s}(1 + o(1))$$

holds with probability at least $1 - \frac{1}{n}$.

B.2 Proof of Theorem 17

For uniform sampling and SRHT, it holds that $\mathbf{S}^T \mathbf{S} = \frac{n}{s} \mathbf{I}_s$.

For non-uniform sampling with probabilities p_1, \dots, p_n ($\sum_i p_i = 1$), let $p_{\max} = \max_i p_i$. The smallest entry in \mathbf{S} is $\frac{1}{\sqrt{sp_{\max}}}$, and thus $\mathbf{S}^T \mathbf{S} \succeq \frac{1}{sp_{\max}} \mathbf{I}_s$. For the leverage score sampling, $p_{\max} = \frac{\mu}{n}$. For the shrinked leverage score sampling, $p_{\max} = \frac{1+\mu}{2n}$. The lower bound on $\|\mathbf{S}\|_2^2$ is established.

[Vershynin \(2010\)](#) showed that the smallest singular value of any $n \times s$ standard Gaussian matrix \mathbf{G} is at least $\sqrt{n} - \sqrt{s} - t$ with probability at least $1 - 2e^{-t^2/2}$. If $\mathbf{S} = \frac{1}{\sqrt{s}} \mathbf{G}$ is the Gaussian projection matrix, the smallest eigenvalue of $\mathbf{S}^T \mathbf{S}$ is $(1 - o(1)) \frac{n}{s}$ with probability very close to one.

If \mathbf{S} is the CountSketch matrix, then each row of \mathbf{S} has exactly one nonzero entry, either 1 or -1 . Because the columns of \mathbf{S} are orthogonal to each other, it holds that

$$\sigma_{\min}^2(\mathbf{S}) = \min_{i \in [s]} \|\mathbf{s}_{:i}\|_2^2 = \min_{i \in [s]} \text{nnz}(\mathbf{s}_{:i}).$$

The problem of bounding $\text{nnz}(\mathbf{s}_{:i})$ is equivalent to assigning n balls into s bins uniformly at random and bounding the number of balls in the bins. Standard concentration argument can show that each bin has at least $\frac{n}{s}(1 - o(1))$ balls w.h.p. Hence $\sigma_{\min}^2(\mathbf{S}) \geq \frac{n}{s}(1 - o(1))$ w.h.p.

B.3 Proof of Theorem 19

Assumption 2.1. By Theorem 16 and the union bound, we have that $\|\mathbf{U}^T \mathbf{S}_i \mathbf{S}_i^T - \mathbf{I}_\rho\|_2 \leq \eta$ hold simultaneously for all $i \in [g]$ with probability at least $1 - g\delta_1$. Because $\mathbf{S} \in \mathbb{R}^{n \times gs}$ is the same type of sketching matrix, it follows from Theorem 16 that $\|\mathbf{U}^T \mathbf{S} \mathbf{S}^T \mathbf{U} - \mathbf{I}_\rho\|_2 \leq \frac{\eta}{g}$ holds with probability at least $1 - \delta_1$.

Assumption 2.2. By the same proof of Theorem 16, we can easily show that

$$\mathbb{E} \|\mathbf{U}^T \mathbf{B} - \mathbf{U}^T \mathbf{S}_i \mathbf{S}_i^T \mathbf{B}\|_F^2 \leq \delta_2 \epsilon \|\mathbf{B}\|_F^2,$$

where \mathbf{B} is any fixed matrix and the expectation is taken w.r.t. \mathbf{S} . It follows from Jensen's inequality that

$$\left(\mathbb{E} \|\mathbf{U}^T \mathbf{S}_i \mathbf{S}_i^T \mathbf{B} - \mathbf{U}^T \mathbf{B}\|_F \right)^2 \leq \mathbb{E} \|\mathbf{U}^T \mathbf{S}_i \mathbf{S}_i^T \mathbf{B} - \mathbf{U}^T \mathbf{B}\|_F^2 \leq \delta_2 \epsilon \|\mathbf{B}\|_F^2.$$

It follows that

$$\frac{1}{g} \sum_{i=1}^g \mathbb{E} \|\mathbf{U}^T \mathbf{S}_i \mathbf{S}_i^T \mathbf{B} - \mathbf{U}^T \mathbf{B}\|_F \leq \sqrt{\delta_2 \epsilon} \|\mathbf{B}\|_F,$$

and thus

$$\left(\frac{1}{g} \sum_{i=1}^g \mathbb{E} \|\mathbf{U}^T \mathbf{S}_i \mathbf{S}_i^T \mathbf{B} - \mathbf{U}^T \mathbf{B}\|_F \right)^2 \leq \delta_2 \epsilon \|\mathbf{B}\|_F^2.$$

It follows from Markov's bound that

$$\mathbb{P} \left\{ \left(\frac{1}{g} \sum_{i=1}^g \|\mathbf{U}^T \mathbf{S}_i \mathbf{S}_i^T \mathbf{B} - \mathbf{U}^T \mathbf{B}\|_F \right)^2 \leq \epsilon \|\mathbf{B}\|_F^2 \right\} \geq 1 - \delta_2.$$

Because $\mathbf{S} \in \mathbb{R}^{n \times gs}$ is the same type of sketching matrix, it follows from Theorem 16 that $\|\mathbf{U}^T \mathbf{S} \mathbf{S}^T \mathbf{B} - \mathbf{U}^T \mathbf{B}\|_F^2 \leq \frac{\epsilon}{g} \|\mathbf{B}\|_F^2$ holds with probability at least $1 - \delta_2$.

Assumption 2.3. Theorem 16 shows that $\|\mathbf{S}_i\|_2^2$ can be bounded either surely or with probability very close to 1 (assume n is big enough). Because $g \ll n$, $\|\mathbf{S}_i\|_2^2$ can be bounded simultaneously for all $i \in [g]$ either surely or with probability close to 1. Because $\mathbf{S} \in \mathbb{R}^{n \times gs}$ is the same type of sketching matrix, it follows from Theorem 16 that $\|\mathbf{S}\|_2^2 \leq \frac{n}{gs}$ holds either surely or with probability very close to 1.

Appendix C. Sketched MRR from Optimization Perspective: Proofs

In Section C.1 we establish a key lemma. In Section C.2 we prove Theorem 21. In Section C.3 we prove Theorem 22.

C.1 Key Lemma

Recall that objective function of the matrix ridge regression (MRR) is

$$f(\mathbf{W}) \triangleq \frac{1}{n} \|\mathbf{XW} - \mathbf{Y}\|_F^2 + \gamma \|\mathbf{W}\|_F^2.$$

The optimal solution is $\mathbf{W}^* = \operatorname{argmin}_{\mathbf{W}} f(\mathbf{W})$. The following is the key lemma for decomposing difference between any \mathbf{W} and \mathbf{W}^* .

Lemma 31 *For any matrix \mathbf{W} and any nonsingular matrix \mathbf{M} of proper size, it holds that*

$$\begin{aligned} f(\mathbf{W}) &= \frac{1}{n} \operatorname{tr} \left[\mathbf{Y}^T \mathbf{Y} - (2\mathbf{W}^* - \mathbf{W})^T (\mathbf{X}^T \mathbf{X} + n\gamma \mathbf{I}_n) \mathbf{W} \right], \\ f(\mathbf{W}^*) &= \frac{1}{n} \left[\|\mathbf{Y}^\perp\|_F^2 + n\gamma \|(\Sigma^2 + n\gamma \mathbf{I}_\rho)^{-1/2} \mathbf{U}^T \mathbf{Y}\|_F^2 \right], \\ f(\mathbf{W}) - f(\mathbf{W}^*) &= \frac{1}{n} \left\| (\mathbf{X}^T \mathbf{X} + n\gamma \mathbf{I}_d)^{1/2} (\mathbf{W} - \mathbf{W}^*) \right\|_F^2, \\ \|\mathbf{M}^{-1}(\mathbf{W} - \mathbf{W}^*)\|_F^2 &\leq \sigma_{\min}^{-2} \left[(\mathbf{X}^T \mathbf{X} + n\gamma \mathbf{I}_d)^{1/2} \mathbf{M} \right] \left\| (\mathbf{X}^T \mathbf{X} + n\gamma \mathbf{I}_d)^{1/2} (\mathbf{W} - \mathbf{W}^*) \right\|_F^2. \end{aligned}$$

Here $\mathbf{X} = \mathbf{U}\Sigma\mathbf{V}^T$ is the SVD; $\mathbf{Y}^\perp = \mathbf{Y} - \mathbf{X}\mathbf{X}^\dagger \mathbf{Y}$.

Proof Let \mathbf{U} be the left singular vectors of \mathbf{X} . The objective function $f(\mathbf{W})$ can be written as

$$\begin{aligned} f(\mathbf{W}) &= \frac{1}{n} \|\mathbf{XW} - \mathbf{Y}\|_F^2 + \gamma \|\mathbf{W}\|_F^2 \\ &= \frac{1}{n} \operatorname{tr} \left[\mathbf{Y}^T \mathbf{Y} - (2\mathbf{W}^* - \mathbf{W})^T (\mathbf{X}^T \mathbf{X} + n\gamma \mathbf{I}_n) \mathbf{W} \right]. \end{aligned}$$

Then

$$\begin{aligned} f(\mathbf{W}^*) &= \frac{1}{n} \operatorname{tr} \left[\mathbf{Y}^T \left(\mathbf{I}_n - \mathbf{X}(\mathbf{X}^T \mathbf{X} + n\gamma \mathbf{I}_d)^{-1} \mathbf{X}^T \right) \mathbf{Y} \right] \\ &= \frac{1}{n} \operatorname{tr} \left[\mathbf{Y}^T \left(\mathbf{I}_n - \mathbf{U}(\mathbf{I}_\rho + n\gamma \Sigma^{-2})^{-1} \mathbf{U}^T \right) \mathbf{Y} \right] \\ &= \frac{1}{n} \operatorname{tr} \left[\mathbf{Y}^T \mathbf{Y} - \mathbf{Y}^T \mathbf{U} \mathbf{U}^T \mathbf{Y} + \mathbf{Y}^T \mathbf{U} \mathbf{U}^T \mathbf{Y} - \mathbf{Y}^T \mathbf{U} (\mathbf{I}_\rho + n\gamma \Sigma^{-2})^{-1} \mathbf{U}^T \mathbf{Y} \right] \\ &= \frac{1}{n} \left\{ \operatorname{tr} \left[\mathbf{Y}^T (\mathbf{I}_n - \mathbf{U} \mathbf{U}^T) \mathbf{Y} \right] + n\gamma \cdot \operatorname{tr} \left[\mathbf{Y}^T \mathbf{U} (\Sigma^2 + n\gamma \mathbf{I}_\rho)^{-1} \mathbf{U}^T \mathbf{Y} \right] \right\} \\ &= \frac{1}{n} \left[\|\mathbf{Y}^\perp\|_F^2 + n\gamma \|(\Sigma^2 + n\gamma \mathbf{I}_\rho)^{-1/2} \mathbf{U}^T \mathbf{Y}\|_F^2 \right]. \end{aligned}$$

The difference in the objective function value is

$$\begin{aligned} f(\mathbf{W}) - f(\mathbf{W}^*) &= \frac{1}{n} \operatorname{tr} \left[(\mathbf{W} - \mathbf{W}^*)^T (\mathbf{X}^T \mathbf{X} + n\gamma \mathbf{I}_d) (\mathbf{W} - \mathbf{W}^*) \right] \\ &= \frac{1}{n} \left\| (\mathbf{X}^T \mathbf{X} + n\gamma \mathbf{I}_d)^{1/2} (\mathbf{W} - \mathbf{W}^*) \right\|_F^2. \end{aligned}$$

Because $\sigma_{\min}(\mathbf{A})\|\mathbf{B}\|_F \leq \|\mathbf{AB}\|_F$ holds for any nonsingular \mathbf{A} and any \mathbf{B} , it holds for any nonsingular matrix \mathbf{M} that

$$\begin{aligned}\sigma_{\min}^2\left[(\mathbf{X}^T\mathbf{X} + n\gamma\mathbf{I}_d)^{1/2}\mathbf{M}\right]\left\|\mathbf{M}^{-1}(\mathbf{W} - \mathbf{W}^*)\right\|_F^2 &\leq \left\|(\mathbf{X}^T\mathbf{X} + n\gamma\mathbf{I}_d)^{1/2}\mathbf{M}\mathbf{M}^{-1}(\mathbf{W} - \mathbf{W}^*)\right\|_F^2 \\ &= \left\|(\mathbf{X}^T\mathbf{X} + n\gamma\mathbf{I}_d)^{1/2}(\mathbf{W} - \mathbf{W}^*)\right\|_F^2.\end{aligned}$$

The last claim in the lemma follows from the above inequality. \blacksquare

C.2 Proof of Theorem 21

Proof Let $\rho = \text{rank}(\mathbf{X})$, $\mathbf{U} \in \mathbb{R}^{n \times \rho}$ be the left singular vectors of \mathbf{X} , and $\mathbf{Y}^\perp = \mathbf{Y} - \mathbf{XX}^\dagger\mathbf{Y} = \mathbf{Y} - \mathbf{UU}^T\mathbf{Y}$. It follows from the definition of \mathbf{W}^* and \mathbf{W}^c that

$$\mathbf{W}^c - \mathbf{W}^* = (\mathbf{X}^T\mathbf{SS}^T\mathbf{X} + n\gamma\mathbf{I}_d)^{-1}\mathbf{X}^T\mathbf{SS}^T\mathbf{Y} - (\mathbf{X}^T\mathbf{X} + n\gamma\mathbf{I}_d)^{-1}\mathbf{X}^T\mathbf{Y}.$$

It follows that

$$\begin{aligned} &(\mathbf{X}^T\mathbf{SS}^T\mathbf{X} + n\gamma\mathbf{I}_d)(\mathbf{W}^c - \mathbf{W}^*) \\ &= \mathbf{X}^T\mathbf{SS}^T\mathbf{Y}^\perp + \mathbf{X}^T\mathbf{SS}^T\mathbf{XX}^\dagger\mathbf{Y} - (\mathbf{X}^T\mathbf{SS}^T\mathbf{X} + n\gamma\mathbf{I}_d)(\mathbf{X}^T\mathbf{X} + n\gamma\mathbf{I}_d)^{-1}\mathbf{X}^T\mathbf{Y} \\ &= \mathbf{X}^T\mathbf{SS}^T\mathbf{Y}^\perp - n\gamma\mathbf{X}^\dagger\mathbf{Y} + (\mathbf{X}^T\mathbf{SS}^T\mathbf{X} + n\gamma\mathbf{I}_d)[\mathbf{X}^\dagger - (\mathbf{X}^T\mathbf{X} + n\gamma\mathbf{I}_d)^{-1}\mathbf{X}^T]\mathbf{Y} \\ &= \mathbf{X}^T\mathbf{SS}^T\mathbf{Y}^\perp - n\gamma\mathbf{X}^\dagger\mathbf{Y} + n\gamma(\mathbf{X}^T\mathbf{SS}^T\mathbf{X} + n\gamma\mathbf{I}_d)(\mathbf{X}^T\mathbf{X} + n\gamma\mathbf{I}_d)^{-1}\mathbf{X}^\dagger\mathbf{Y} \\ &= \mathbf{X}^T\mathbf{SS}^T\mathbf{Y}^\perp + n\gamma(\mathbf{X}^T\mathbf{SS}^T\mathbf{X} - \mathbf{X}^T\mathbf{X})(\mathbf{X}^T\mathbf{X} + n\gamma\mathbf{I}_d)^{-1}\mathbf{X}^\dagger\mathbf{Y}.\end{aligned}$$

It follows that

$$(\mathbf{X}^T\mathbf{X} + n\gamma\mathbf{I}_d)^{-1/2}(\mathbf{X}^T\mathbf{SS}^T\mathbf{X} + n\gamma\mathbf{I}_d)(\mathbf{W}^c - \mathbf{W}^*) = \mathbf{A} + \mathbf{B}, \quad (13)$$

where

$$\begin{aligned}\mathbf{A} &= [(\mathbf{X}^T\mathbf{X} + n\gamma\mathbf{I}_d)^{1/2}]^\dagger\mathbf{X}^T\mathbf{SS}^T\mathbf{Y}^\perp = \mathbf{V}(\Sigma^2 + n\gamma\mathbf{I}_\rho)^{-1/2}\Sigma\mathbf{U}\mathbf{S}\mathbf{S}^T\mathbf{Y}^\perp, \\ \mathbf{B} &= n\gamma[(\mathbf{X}^T\mathbf{X} + n\gamma\mathbf{I}_d)^{1/2}]^\dagger(\mathbf{X}^T\mathbf{SS}^T\mathbf{X} - \mathbf{X}^T\mathbf{X})(\mathbf{X}^T\mathbf{X} + n\gamma\mathbf{I}_d)^\dagger\mathbf{X}^\dagger\mathbf{Y} \\ &= n\gamma\mathbf{V}(\Sigma^2 + n\gamma\mathbf{I}_\rho)^{-1/2}\Sigma(\mathbf{U}^T\mathbf{SS}^T\mathbf{U} - \mathbf{I}_\rho)\Sigma(\Sigma^2 + n\gamma\mathbf{I}_\rho)^{-1}\Sigma^{-1}\mathbf{U}^T\mathbf{Y} \\ &= n\gamma\mathbf{V}\Sigma(\Sigma^2 + n\gamma\mathbf{I}_\rho)^{-1/2}(\mathbf{U}^T\mathbf{SS}^T\mathbf{U} - \mathbf{I}_\rho)(\Sigma^2 + n\gamma\mathbf{I}_\rho)^{-1}\mathbf{U}^T\mathbf{Y}.\end{aligned}$$

It follows from (13) that

$$\begin{aligned} &(\mathbf{X}^T\mathbf{X} + n\gamma\mathbf{I}_d)^{1/2}(\mathbf{W}^c - \mathbf{W}^*) \\ &= [(\mathbf{X}^T\mathbf{X} + n\gamma\mathbf{I}_d)^{-1/2}(\mathbf{X}^T\mathbf{SS}^T\mathbf{X} + n\gamma\mathbf{I}_d)(\mathbf{X}^T\mathbf{X} + n\gamma\mathbf{I}_d)^{-1/2}]^\dagger(\mathbf{A} + \mathbf{B})\end{aligned}$$

By Assumption 1.1, we have that

$$(1 - \eta)(\mathbf{X}^T\mathbf{X} + n\gamma\mathbf{I}_d) \preceq (\mathbf{X}^T\mathbf{SS}^T\mathbf{X} + n\gamma\mathbf{I}_d) \preceq (1 + \eta)(\mathbf{X}^T\mathbf{X} + n\gamma\mathbf{I}_d)$$

It follows that

$$\left\| [(\mathbf{X}^T \mathbf{X} + n\gamma \mathbf{I}_d)^{-1/2} (\mathbf{X}^T \mathbf{S} \mathbf{S}^T \mathbf{X} + n\gamma \mathbf{I}_d) (\mathbf{X}^T \mathbf{X} + n\gamma \mathbf{I}_d)^{-1/2}]^\dagger \right\|_2 \leq \frac{1}{1-\eta}.$$

Thus

$$\left\| (\mathbf{X}^T \mathbf{X} + n\gamma \mathbf{I}_d)^{1/2} (\mathbf{W}^c - \mathbf{W}^*) \right\|_F^2 \leq \frac{1}{1-\eta} \left\| \mathbf{A} + \mathbf{B} \right\|_F^2 \leq \frac{2}{1-\eta} \left(\left\| \mathbf{A} \right\|_F^2 + \left\| \mathbf{B} \right\|_F^2 \right).$$

Lemma 31 shows

$$f(\mathbf{W}^c) - f(\mathbf{W}^*) = \frac{1}{n} \left\| (\mathbf{X}^T \mathbf{X} + n\gamma \mathbf{I}_d)^{1/2} (\mathbf{W}^c - \mathbf{W}^*) \right\|_F^2 \leq \frac{2}{n(1-\eta)} \left(\left\| \mathbf{A} \right\|_F^2 + \left\| \mathbf{B} \right\|_F^2 \right). \quad (14)$$

We respectively bound $\left\| \mathbf{A} \right\|_F^2$ and $\left\| \mathbf{B} \right\|_F^2$ in the following. It follows from Assumption 1.2 and $\mathbf{U}^T \mathbf{Y}^\perp = \mathbf{0}$ that

$$\begin{aligned} \left\| \mathbf{A} \right\|_F^2 &= \left\| \mathbf{V} (\Sigma^2 + n\gamma \mathbf{I}_\rho)^{-1/2} \Sigma \mathbf{U} \mathbf{S} \mathbf{S}^T \mathbf{Y}^\perp \right\|_F^2 \\ &\leq \left\| (\Sigma^2 + n\gamma \mathbf{I}_\rho)^{-1/2} \Sigma \right\|_2^2 \left\| \mathbf{U}^T \mathbf{S} \mathbf{S}^T \mathbf{Y}^\perp - \mathbf{U}^T \mathbf{Y}^\perp \right\|_F^2 \\ &\leq \epsilon \left\| (\Sigma^2 + n\gamma \mathbf{I}_\rho)^{-1/2} \Sigma \right\|_2^2 \left\| \mathbf{Y}^\perp \right\|_F^2. \end{aligned}$$

By the definition of \mathbf{B} , we have

$$\begin{aligned} \left\| \mathbf{B} \right\|_F^2 &\leq n^2 \gamma^2 \left\| \Sigma (\Sigma^2 + n\gamma \mathbf{I}_\rho)^{-1/2} (\mathbf{U}^T \mathbf{S} \mathbf{S}^T \mathbf{U} - \mathbf{I}_\rho) (\Sigma^2 + n\gamma \mathbf{I}_\rho)^{-1/2} \mathbf{U}^T \mathbf{Y} \right\|_F^2 \\ &\leq n^2 \gamma^2 \left\| \Sigma (\Sigma^2 + n\gamma \mathbf{I}_\rho)^{-1/2} (\mathbf{U}^T \mathbf{S} \mathbf{S}^T \mathbf{U} - \mathbf{I}_\rho) (\Sigma^2 + n\gamma \mathbf{I}_\rho)^{-1/2} \right\|_2^2 \left\| (\Sigma^2 + n\gamma \mathbf{I}_\rho)^{-1/2} \mathbf{U}^T \mathbf{Y} \right\|_F^2 \\ &= n^2 \gamma^2 \left\| \Sigma \mathbf{N} \right\|_2^2 \left\| (\Sigma^2 + n\gamma \mathbf{I}_\rho)^{-1/2} \mathbf{U}^T \mathbf{Y} \right\|_F^2, \end{aligned}$$

where we define $\mathbf{N} = (\Sigma^2 + n\gamma \mathbf{I}_\rho)^{-1/2} (\mathbf{U}^T \mathbf{S} \mathbf{S}^T \mathbf{U} - \mathbf{I}_\rho) (\Sigma^2 + n\gamma \mathbf{I}_\rho)^{-1/2}$. By Assumption 1.1, we have

$$-\eta (\Sigma^2 + n\gamma \mathbf{I}_\rho)^{-1} \preceq \mathbf{N} \preceq \eta (\Sigma^2 + n\gamma \mathbf{I}_\rho)^{-1}.$$

It follows that

$$\begin{aligned} \left\| \mathbf{B} \right\|_F^2 &\leq n^2 \gamma^2 \left\| \Sigma \mathbf{N}^2 \Sigma \right\|_2 \left\| (\Sigma^2 + n\gamma \mathbf{I}_\rho)^{-1/2} \mathbf{U}^T \mathbf{Y} \right\|_F^2 \\ &\leq \eta^2 n^2 \gamma^2 \left\| \Sigma (\Sigma^2 + n\gamma \mathbf{I}_\rho)^{-1/2} \Sigma \right\|_2 \left\| (\Sigma^2 + n\gamma \mathbf{I}_\rho)^{-1/2} \mathbf{U}^T \mathbf{Y} \right\|_F^2 \\ &= \eta^2 n^2 \gamma^2 \left\| (\Sigma^2 + n\gamma \mathbf{I}_\rho)^{-1} \Sigma \right\|_2^2 \left\| (\Sigma^2 + n\gamma \mathbf{I}_\rho)^{-1/2} \mathbf{U}^T \mathbf{Y} \right\|_F^2 \\ &= \eta^2 n \gamma \left\| (\Sigma^2 + n\gamma \mathbf{I}_\rho)^{-1/2} \Sigma \right\|_2^2 \left\| (\Sigma^2 + n\gamma \mathbf{I}_\rho)^{-1/2} \mathbf{U}^T \mathbf{Y} \right\|_F^2. \end{aligned}$$

The last equality follows from that $\left\| (\Sigma^2 + n\gamma \mathbf{I}_\rho)^{-1/2} \right\|_2 \leq n\gamma$. It follows that

$$\begin{aligned} \left\| \mathbf{A} \right\|_F^2 + \left\| \mathbf{B} \right\|_F^2 &\leq \max \{ \epsilon, \eta^2 \} \left\| (\Sigma^2 + n\gamma \mathbf{I}_d)^{-1} \Sigma \right\|_2 \left[\left\| \mathbf{Y}^\perp \right\|_F^2 + n\gamma \left\| (\Sigma^2 + n\gamma \mathbf{I}_d)^{-1/2} \mathbf{U}^T \mathbf{Y} \right\|_F^2 \right] \\ &\leq \max \{ \epsilon, \eta^2 \} \frac{\sigma_{\max}^2}{\sigma_{\max}^2 + n\gamma} \left[\left\| \mathbf{Y}^\perp \right\|_F^2 + n\gamma \left\| (\Sigma^2 + n\gamma \mathbf{I}_d)^{-1/2} \mathbf{U}^T \mathbf{Y} \right\|_F^2 \right] \\ &\leq \max \{ \epsilon, \eta^2 \} \beta n f(\mathbf{W}^*). \end{aligned} \quad (15)$$

Here the last inequality follows from Lemma 31. Then the theorem follows from (15) and (14). \blacksquare

C.3 Proof of Theorem 22

Proof By the definition of \mathbf{W}^h and \mathbf{W}^* , we have

$$\begin{aligned} & (\mathbf{X}^T \mathbf{X} + n\gamma \mathbf{I}_d)^{1/2} (\mathbf{W}^h - \mathbf{W}^*) \\ &= (\mathbf{X}^T \mathbf{X} + n\gamma \mathbf{I}_d)^{1/2} \left[(\mathbf{X}^T \mathbf{S} \mathbf{S}^T \mathbf{X} + n\gamma \mathbf{I}_d)^\dagger - (\mathbf{X}^T \mathbf{X} + n\gamma \mathbf{I}_d)^\dagger \right] \mathbf{X}^T \mathbf{Y} \\ &= \mathbf{V} (\Sigma^2 + n\gamma \mathbf{I}_\rho)^{1/2} \left[(\Sigma \mathbf{U}^T \mathbf{S} \mathbf{S}^T \mathbf{U} \Sigma + n\gamma \mathbf{I}_\rho)^\dagger - (\Sigma^2 + n\gamma \mathbf{I}_\rho)^{-1} \right] \Sigma \mathbf{U}^T \mathbf{Y}. \end{aligned}$$

It follows from Assumption 1.1 that $\mathbf{U}^T \mathbf{S} \mathbf{S}^T \mathbf{U}$ has full rank, and thus

$$\begin{aligned} & (\mathbf{X}^T \mathbf{X} + n\gamma \mathbf{I}_d)^{1/2} (\mathbf{W}^h - \mathbf{W}^*) \\ &= \mathbf{V} (\Sigma^2 + n\gamma \mathbf{I}_\rho)^{1/2} \left[(\Sigma \mathbf{U}^T \mathbf{S} \mathbf{S}^T \mathbf{U} \Sigma + n\gamma \mathbf{I}_\rho)^{-1} - (\Sigma^2 + n\gamma \mathbf{I}_\rho)^{-1} \right] \Sigma \mathbf{U}^T \mathbf{Y} \\ &= \mathbf{V} (\Sigma^2 + n\gamma \mathbf{I}_\rho)^{1/2} (\Sigma^2 + n\gamma \mathbf{I}_\rho)^{-1} (\Sigma^2 - \Sigma \mathbf{U}^T \mathbf{S} \mathbf{S}^T \mathbf{U} \Sigma) (\Sigma \mathbf{U}^T \mathbf{S} \mathbf{S}^T \mathbf{U} \Sigma + n\gamma \mathbf{I}_\rho)^{-1} \Sigma \mathbf{U}^T \mathbf{Y} \\ &= \mathbf{V} (\Sigma^2 + n\gamma \mathbf{I}_\rho)^{-1/2} \Sigma (\mathbf{I}_\rho - \mathbf{U}^T \mathbf{S} \mathbf{S}^T \mathbf{U}) \Sigma (\Sigma \mathbf{U}^T \mathbf{S} \mathbf{S}^T \mathbf{U} \Sigma + n\gamma \mathbf{I}_\rho)^{-1} \Sigma \mathbf{U}^T \mathbf{Y}. \end{aligned}$$

where the second equality follow from $\mathbf{M}^{-1} - \mathbf{N}^{-1} = \mathbf{N}^{-1}(\mathbf{N} - \mathbf{M})\mathbf{M}^{-1}$. We define

$$(\mathbf{X}^T \mathbf{X} + n\gamma \mathbf{I}_d)^{1/2} (\mathbf{W}^h - \mathbf{W}^*) = \mathbf{V} \mathbf{A} \mathbf{B} \mathbf{C},$$

where

$$\begin{aligned} \mathbf{A} &= (\Sigma^2 + n\gamma \mathbf{I}_\rho)^{-1/2} \Sigma (\mathbf{I}_\rho - \mathbf{U}^T \mathbf{S} \mathbf{S}^T \mathbf{U}) \Sigma (\Sigma^2 + n\gamma \mathbf{I}_\rho)^{-1/2}, \\ \mathbf{B} &= (\Sigma^2 + n\gamma \mathbf{I}_\rho)^{1/2} (\Sigma \mathbf{U}^T \mathbf{S} \mathbf{S}^T \mathbf{U} \Sigma + n\gamma \mathbf{I}_\rho)^{-1} (\Sigma^2 + n\gamma \mathbf{I}_\rho)^{1/2}, \\ \mathbf{C} &= (\Sigma^2 + n\gamma \mathbf{I}_\rho)^{-1/2} \Sigma \mathbf{U}^T \mathbf{Y}. \end{aligned}$$

It follows from Assumption 1.1 that

$$\begin{aligned} \|\mathbf{A}\|_2 &\leq \eta \left\| (\Sigma^2 + n\gamma \mathbf{I}_\rho)^{-1/2} \Sigma^2 (\Sigma^2 + n\gamma \mathbf{I}_\rho)^{-1/2} \right\|_2 \leq \eta \beta, \\ \|\mathbf{B}\|_2 &\leq (1 - \eta)^{-1}. \end{aligned}$$

It holds that

$$\begin{aligned} \|\mathbf{C}\|_F^2 &\leq \left\| (\Sigma^2 + n\gamma \mathbf{I}_\rho)^{-1/2} \Sigma \mathbf{U}^T \mathbf{Y} \right\|_F^2 \\ &= \left[\text{tr}(\mathbf{Y}^T \mathbf{U} \mathbf{U}^T \mathbf{Y}) - n\gamma \text{tr}(\mathbf{Y}^T \mathbf{U} (\Sigma^2 + n\gamma \mathbf{I}_d)^{-1} \mathbf{U}^T \mathbf{Y}) \right] \\ &= \left[-\text{tr}(\mathbf{Y}^T (\mathbf{I}_d - \mathbf{U} \mathbf{U}^T) \mathbf{Y}) - n\gamma \text{tr}(\mathbf{Y}^T \mathbf{U} (\Sigma^2 + n\gamma \mathbf{I}_d)^\dagger \mathbf{U}^T \mathbf{Y}) + \text{tr}(\mathbf{Y}^T \mathbf{Y}) \right] \\ &= \left(-nf(\mathbf{W}^*) + \|\mathbf{Y}\|_F^2 \right), \end{aligned}$$

where the last equality follows from Lemma 31. It follows from Lemma 31 that

$$\begin{aligned} f(\mathbf{W}^h) - f(\mathbf{W}^*) &= \frac{1}{n} \|(\mathbf{X}^T \mathbf{X} + n\gamma \mathbf{I}_d)^{1/2} (\mathbf{W}^h - \mathbf{W}^*)\|_F^2 \\ &= \frac{1}{n} \|\mathbf{A} \mathbf{B} \mathbf{C}\|_F^2 \leq \frac{\eta^2 \beta^2}{(1 - \eta)^2} \left(\frac{1}{n} \|\mathbf{Y}\|_F^2 - f(\mathbf{W}^*) \right). \end{aligned}$$

■

Appendix D. Sketched MRR from Statistical Perspective: Proofs

In Section D.1 we prove Theorem 4. In Section D.2 we prove Theorem 23. In Section D.3 we prove Theorem 24. In Section B.2 we prove Theorem 17. In Section D.4 we prove Theorem 25. Recall that the fixed design model is $\mathbf{Y} = \mathbf{X}\mathbf{W}_0 + \mathbf{\Xi}$ where $\mathbf{\Xi}$ is random, $\mathbb{E}\mathbf{\Xi} = \mathbf{0}$, and $\mathbb{E}[\mathbf{\Xi}\mathbf{\Xi}^T] = \xi^2\mathbf{I}_n$.

D.1 Proofs of Theorem 4

We prove Theorem 4 in the following. In the proof we exploit several identities. The Frobenius norm and matrix trace satisfies that for any matrix \mathbf{A} and \mathbf{B} ,

$$\|\mathbf{A} - \mathbf{B}\|_F^2 = \text{tr}[(\mathbf{A} - \mathbf{B})(\mathbf{A} - \mathbf{B})^T] = \text{tr}(\mathbf{A}\mathbf{A}^T) + \text{tr}(\mathbf{B}\mathbf{B}^T) - 2\text{tr}(\mathbf{A}\mathbf{B}^T).$$

The trace is linear function, and thus for any fixed \mathbf{A} and \mathbf{B} and random matrix $\mathbf{\Psi}$ of proper size,

$$\mathbb{E}[\text{tr}(\mathbf{A}\mathbf{\Psi}\mathbf{B})] = \text{tr}[\mathbf{A}(\mathbb{E}\mathbf{\Psi})\mathbf{B}]$$

where the expectation is taken w.r.t. $\mathbf{\Psi}$.

Proof It follows from the definition of the optimal solution \mathbf{W}^* in (2) that

$$\begin{aligned} \mathbf{X}\mathbf{W}^* &= \mathbf{X}(\mathbf{X}^T\mathbf{X} + n\gamma\mathbf{I}_d)^\dagger\mathbf{X}^T(\mathbf{X}\mathbf{W}_0 + \mathbf{\Xi}) \\ &= \mathbf{U}(\mathbf{\Sigma}^2 + n\gamma\mathbf{I}_\rho)^{-1}\mathbf{\Sigma}^3\mathbf{V}^T\mathbf{W}_0 + \mathbf{U}(\mathbf{\Sigma}^2 + n\gamma\mathbf{I}_\rho)^{-1}\mathbf{\Sigma}^2\mathbf{U}^T\mathbf{\Xi} \\ &= \mathbf{U}\left[\mathbf{I}_\rho - n\gamma(\mathbf{\Sigma}^2 + n\gamma\mathbf{I}_\rho)^{-1}\right]\mathbf{\Sigma}\mathbf{V}^T\mathbf{W}_0 + \mathbf{U}(\mathbf{\Sigma}^2 + n\gamma\mathbf{I}_\rho)^{-1}\mathbf{\Sigma}^2\mathbf{U}^T\mathbf{\Xi} \\ &= \mathbf{X}\mathbf{W}_0 - n\gamma\mathbf{U}(\mathbf{\Sigma}^2 + n\gamma\mathbf{I}_\rho)^{-1}\mathbf{\Sigma}\mathbf{V}^T\mathbf{W}_0 + \mathbf{U}(\mathbf{\Sigma}^2 + n\gamma\mathbf{I}_\rho)^{-1}\mathbf{\Sigma}^2\mathbf{U}^T\mathbf{\Xi}. \end{aligned}$$

Since $\mathbb{E}[\mathbf{\Xi}] = \mathbf{0}$ and $\mathbb{E}[\mathbf{\Xi}\mathbf{\Xi}^T] = \xi^2\mathbf{I}_n$, it holds that

$$\begin{aligned} R(\mathbf{W}^*) &= \frac{1}{n}\mathbb{E}\|\mathbf{X}\mathbf{W}^* - \mathbf{X}\mathbf{W}_0\|_F^2 \\ &= \frac{1}{n}\left\| -n\gamma(\mathbf{\Sigma}^2 + n\gamma\mathbf{I}_\rho)^{-1}\mathbf{\Sigma}\mathbf{V}^T\mathbf{W}_0 + (\mathbf{\Sigma}^2 + n\gamma\mathbf{I}_\rho)^{-1}\mathbf{\Sigma}^2\mathbf{U}^T\mathbf{\Xi} \right\|_F^2 \\ &= n\gamma^2\left\|(\mathbf{\Sigma}^2 + n\gamma\mathbf{I}_\rho)^{-1}\mathbf{\Sigma}\mathbf{V}^T\mathbf{W}_0\right\|_F^2 + \frac{\xi^2}{n}\left\|(\mathbf{\Sigma}^2 + n\gamma\mathbf{I}_\rho)^{-1}\mathbf{\Sigma}^2\right\|_F^2. \end{aligned}$$

This shows the bias and variance of the optimal solution \mathbf{W}^* .

We then decompose the risk function $R(\mathbf{W}^c)$. It follows from the definition of \mathbf{W}^c in (3) that

$$\begin{aligned} \mathbf{X}\mathbf{W}^c &= \mathbf{X}(\mathbf{X}^T\mathbf{S}\mathbf{S}^T\mathbf{X} + n\gamma\mathbf{I}_d)^\dagger\mathbf{X}^T\mathbf{S}\mathbf{S}^T(\mathbf{X}\mathbf{W}_0 + \mathbf{\Xi}) \\ &= \mathbf{U}\mathbf{\Sigma}(\mathbf{\Sigma}\mathbf{U}^T\mathbf{S}\mathbf{S}^T\mathbf{U}\mathbf{\Sigma} + n\gamma\mathbf{I}_d)^\dagger\mathbf{\Sigma}(\mathbf{U}^T\mathbf{S}\mathbf{S}^T\mathbf{U}\mathbf{\Sigma}\mathbf{V}^T\mathbf{W}_0 + \mathbf{U}^T\mathbf{S}\mathbf{S}^T\mathbf{\Xi}) \\ &= \mathbf{U}(\mathbf{U}^T\mathbf{S}\mathbf{S}^T\mathbf{U} + n\gamma\mathbf{\Sigma}^{-2})^{-1}\left[(\mathbf{U}^T\mathbf{S}\mathbf{S}^T\mathbf{U} + n\gamma\mathbf{\Sigma}^{-2})\mathbf{\Sigma}\mathbf{V}^T\mathbf{W}_0 - n\gamma\mathbf{\Sigma}^{-1}\mathbf{V}^T\mathbf{W}_0 + \mathbf{U}^T\mathbf{S}\mathbf{S}^T\mathbf{\Xi}\right] \\ &= \mathbf{X}\mathbf{W}_0 + \mathbf{U}(\mathbf{U}^T\mathbf{S}\mathbf{S}^T\mathbf{U} + n\gamma\mathbf{\Sigma}^{-2})^{-1}(-n\gamma\mathbf{\Sigma}^{-1}\mathbf{V}^T\mathbf{W}_0 + \mathbf{U}^T\mathbf{S}\mathbf{S}^T\mathbf{\Xi}). \end{aligned}$$

Since $\mathbb{E}[\boldsymbol{\Xi}] = \mathbf{0}$ and $\mathbb{E}[\boldsymbol{\Xi}\boldsymbol{\Xi}^T] = \xi^2\mathbf{I}_n$, it follows that

$$\begin{aligned} R(\mathbf{W}^c) &= \frac{1}{n}\mathbb{E}\|\mathbf{X}\mathbf{W}^c - \mathbf{X}\mathbf{W}_0\|_F^2 \\ &= \frac{1}{n}\left\| -n\gamma(\mathbf{U}^T\mathbf{S}\mathbf{S}^T\mathbf{U} + n\gamma\boldsymbol{\Sigma}^{-2})^{-1}\boldsymbol{\Sigma}^{-1}\mathbf{V}^T\mathbf{W}_0 + (\mathbf{U}^T\mathbf{S}\mathbf{S}^T\mathbf{U} + n\gamma\boldsymbol{\Sigma}^{-2})^{-1}\mathbf{U}^T\mathbf{S}\mathbf{S}^T\boldsymbol{\Xi} \right\|_F^2 \\ &= n\gamma^2\left\|(\mathbf{U}^T\mathbf{S}\mathbf{S}^T\mathbf{U} + n\gamma\boldsymbol{\Sigma}^{-2})^{-1}\boldsymbol{\Sigma}^{-1}\mathbf{V}^T\mathbf{W}_0\right\|_F^2 + \frac{\xi^2}{n}\left\|(\mathbf{U}^T\mathbf{S}\mathbf{S}^T\mathbf{U} + n\gamma\boldsymbol{\Sigma}^{-2})^{-1}\mathbf{U}^T\mathbf{S}\mathbf{S}^T\right\|_F^2. \end{aligned}$$

This shows the bias and variance of the approximate solution \mathbf{W}^c .

We then decompose the risk function $R(\mathbf{W}^h)$. It follows from the definition of \mathbf{W}^h in (4) that

$$\begin{aligned} \mathbf{X}\mathbf{W}^h - \mathbf{X}\mathbf{W}_0 &= \mathbf{X}(\mathbf{X}^T\mathbf{S}\mathbf{S}^T\mathbf{X} + n\gamma\mathbf{I}_n)^\dagger\mathbf{X}^T(\mathbf{X}\mathbf{W}_0 + \boldsymbol{\Xi}) - \mathbf{X}\mathbf{W}_0 \\ &= \mathbf{X}(\mathbf{X}^T\mathbf{S}\mathbf{S}^T\mathbf{X} + n\gamma\mathbf{I}_d)^\dagger\mathbf{X}^T\mathbf{X}\mathbf{W}_0 - \mathbf{X}\mathbf{W}_0 + \mathbf{X}(\mathbf{X}^T\mathbf{S}\mathbf{S}^T\mathbf{X} + n\gamma\mathbf{I}_d)^\dagger\mathbf{X}^T\boldsymbol{\Xi} \\ &= \mathbf{U}[(\mathbf{U}^T\mathbf{S}\mathbf{S}^T\mathbf{U} + n\gamma\boldsymbol{\Sigma}^{-2})^{-1} - \mathbf{I}_\rho^{-1}]\mathbf{U}^T\mathbf{X}\mathbf{W}_0 + \mathbf{U}(\mathbf{U}^T\mathbf{S}\mathbf{S}^T\mathbf{U}^T + n\gamma\boldsymbol{\Sigma}^{-2})^\dagger\mathbf{U}^T\boldsymbol{\Xi} \\ &= \mathbf{U}(\mathbf{I}_\rho - \mathbf{U}^T\mathbf{S}\mathbf{S}^T\mathbf{U} - n\gamma\boldsymbol{\Sigma}^{-2})(\mathbf{U}^T\mathbf{S}\mathbf{S}^T\mathbf{U} + n\gamma\boldsymbol{\Sigma}^{-2})^{-1}\boldsymbol{\Sigma}\mathbf{V}^T\mathbf{W}_0 \\ &\quad + \mathbf{U}(\mathbf{U}^T\mathbf{S}\mathbf{S}^T\mathbf{U}^T + n\gamma\boldsymbol{\Sigma}^{-2})^\dagger\mathbf{U}^T\boldsymbol{\Xi}, \end{aligned}$$

where the last equality follows from that $\mathbf{A}^{-1} - \mathbf{B}^{-1} = \mathbf{B}^{-1}(\mathbf{B} - \mathbf{A})\mathbf{A}^{-1}$ for any nonsingular matrices \mathbf{A} and \mathbf{B} of proper size. Since $\mathbb{E}[\boldsymbol{\Xi}] = \mathbf{0}$ and $\mathbb{E}[\boldsymbol{\Xi}\boldsymbol{\Xi}^T] = \xi^2\mathbf{I}_n$, it follows that

$$R(\mathbf{W}^h) = \text{bias}^2(\mathbf{W}^h) + \text{var}(\mathbf{W}^h)$$

where

$$\begin{aligned} \text{bias}^2(\mathbf{W}^h) &= \frac{1}{n}\left\| (n\gamma\boldsymbol{\Sigma}^{-2} + \mathbf{U}^T\mathbf{S}\mathbf{S}^T\mathbf{U} - \mathbf{I}_\rho)(\mathbf{U}^T\mathbf{S}\mathbf{S}^T\mathbf{U} + n\gamma\boldsymbol{\Sigma}^{-2})^{-1}\boldsymbol{\Sigma}\mathbf{V}^T\mathbf{W}_0 \right\|_F^2, \\ \text{var}(\mathbf{W}^h) &= \frac{\xi^2}{n}\left\|(\mathbf{U}^T\mathbf{S}\mathbf{S}^T\mathbf{U} + n\gamma\boldsymbol{\Sigma}^{-2})^{-1}\right\|_F^2. \end{aligned}$$

This shows the bias and variance of \mathbf{W}^h . ■

D.2 Proof of Theorem 23

Proof Assumption 1.1 ensures that $(1 - \eta)\mathbf{I}_\rho \preceq \mathbf{U}^T\mathbf{S}\mathbf{S}^T\mathbf{U} \preceq (1 + \eta)\mathbf{I}_\rho$. It follows that

$$(1 - \eta)(\mathbf{I}_\rho + n\gamma\boldsymbol{\Sigma}^{-2}) \preceq \mathbf{U}^T\mathbf{S}\mathbf{S}^T\mathbf{U} + n\gamma\boldsymbol{\Sigma}^{-2} \preceq (1 + \eta)(\mathbf{I}_\rho + n\gamma\boldsymbol{\Sigma}^{-2}).$$

The bias term can be written as

$$\begin{aligned} \text{bias}^2(\mathbf{W}^c) &= n\gamma^2\left\|(\mathbf{U}^T\mathbf{S}\mathbf{S}^T\mathbf{U} + n\gamma\boldsymbol{\Sigma}^{-2})^\dagger\boldsymbol{\Sigma}^{-1}\mathbf{V}^T\mathbf{W}_0\right\|_F^2 \\ &= n\gamma^2 \text{tr}\left(\mathbf{W}_0^T\mathbf{V}\boldsymbol{\Sigma}^{-1}[(\mathbf{U}^T\mathbf{S}\mathbf{S}^T\mathbf{U} + n\gamma\boldsymbol{\Sigma}^{-2})^\dagger]^2\boldsymbol{\Sigma}^{-1}\mathbf{V}^T\mathbf{W}_0\right) \\ &\leq \frac{n\gamma^2}{(1-\eta)^2}\left\|(\mathbf{I}_\rho + n\gamma\boldsymbol{\Sigma}^{-2})^{-1}\boldsymbol{\Sigma}^{-1}\mathbf{V}^T\mathbf{W}_0\right\|_F^2 \\ &= \frac{n\gamma^2}{(1-\eta)^2}\left\|(\boldsymbol{\Sigma}^2 + n\gamma\mathbf{I}_\rho)^{-1}\boldsymbol{\Sigma}\mathbf{V}^T\mathbf{W}_0\right\|_F^2 \\ &= \frac{1}{(1-\eta)^2}\text{bias}^2(\mathbf{W}^*). \end{aligned}$$

We can analogously show $\text{bias}^2(\mathbf{W}^c) \geq \frac{1}{(1+\eta)^2} \text{bias}^2(\mathbf{W}^*)$.

Let $\mathbf{B} = (\mathbf{U}^T \mathbf{S} \mathbf{S}^T \mathbf{U} + n\gamma \boldsymbol{\Sigma}^{-2})^\dagger \mathbf{U}^T \mathbf{S} \in \mathbb{R}^{\rho \times s}$. By Assumption 1.1, it holds that

$$(1-\eta)[(\mathbf{U}^T \mathbf{S} \mathbf{S}^T \mathbf{U} + n\gamma \boldsymbol{\Sigma}^{-2})^2]^\dagger \preceq \mathbf{B} \mathbf{B}^T \preceq (1+\eta)[(\mathbf{U}^T \mathbf{S} \mathbf{S}^T \mathbf{U} + n\gamma \boldsymbol{\Sigma}^{-2})^2]^\dagger.$$

Applying Assumption 1.1 again, we obtain

$$(1-\eta)^2 (\mathbf{I}_\rho + n\gamma \boldsymbol{\Sigma}^{-2})^2 \preceq (\mathbf{U}^T \mathbf{S} \mathbf{S}^T \mathbf{U} + n\gamma \boldsymbol{\Sigma}^{-2})^2 \preceq (1+\eta)^2 (\mathbf{I}_\rho + n\gamma \boldsymbol{\Sigma}^{-2})^2$$

Note that both sides are nonsingular. Combining the above two equations, we have

$$\frac{1-\eta}{(1+\eta)^2} (\mathbf{I}_\rho + n\gamma \boldsymbol{\Sigma}^{-2})^{-2} \preceq \mathbf{B} \mathbf{B}^T \preceq \frac{1+\eta}{(1-\eta)^2} (\mathbf{I}_\rho + n\gamma \boldsymbol{\Sigma}^{-2})^{-2}.$$

Taking the trace of all the terms, we obtain

$$\frac{1-\eta}{(1+\eta)^2} \leq \frac{\|\mathbf{B}\|_F^2}{\|(\mathbf{I}_\rho + n\gamma \boldsymbol{\Sigma}^{-2})^{-1}\|_F^2} \leq \frac{1+\eta}{(1-\eta)^2}$$

The variance term can be written as

$$\begin{aligned} \text{var}(\mathbf{W}^c) &= \frac{\xi^2}{n} \|\mathbf{B} \mathbf{S}^T\|_F^2 \leq \frac{\xi^2}{n} \|\mathbf{B}\|_F^2 \|\mathbf{S}\|_2^2 \\ &\leq \frac{\xi^2(1+\eta)}{n(1-\eta)^2} \|(\mathbf{I}_\rho + n\gamma \boldsymbol{\Sigma}^{-2})^{-1}\|_F^2 \|\mathbf{S}\|_2^2 \\ &= \frac{(1+\eta)\|\mathbf{S}\|_2^2}{(1-\eta)^2} \text{var}(\mathbf{W}^*). \end{aligned}$$

The upper bound the the variance follows from Assumption 1.3. ■

D.3 Proof of Theorem 24

Proof Let $\mathbf{B} = (\mathbf{U}^T \mathbf{S} \mathbf{S}^T \mathbf{U} + n\gamma \boldsymbol{\Sigma}^{-2})^\dagger \mathbf{U}^T \mathbf{S} \in \mathbb{R}^{\rho \times s}$. In the proof of Theorem 5 we show that

$$\text{var}(\mathbf{W}^c) = \frac{\xi^2}{n} \|\mathbf{B} \mathbf{S}^T\|_F^2.$$

If $\mathbf{S}^T \mathbf{S} \succeq \frac{\vartheta n}{s} \mathbf{I}_s$, then it holds that

$$\text{var}(\mathbf{W}^c) = \frac{\xi^2}{n} \|\mathbf{B} \mathbf{S}^T\|_F^2 \geq \frac{\vartheta n}{s} \frac{\xi^2}{n} \|\mathbf{B}\|_F^2 \geq \frac{\vartheta n}{s} \frac{1-\eta}{(1+\eta)^2} \text{var}(\mathbf{W}^*).$$

This established the lower bounds on the variance. ■

D.4 Proof of Theorem 25

Proof Theorem 4 shows that

$$\begin{aligned}\text{bias}(\mathbf{W}^h) &= \gamma\sqrt{n}\left\|\left(\Sigma^{-2} + \frac{\mathbf{U}^T\mathbf{S}\mathbf{S}^T\mathbf{U} - \mathbf{I}_\rho}{n\gamma}\right)(\mathbf{U}^T\mathbf{S}\mathbf{S}^T\mathbf{U} + n\gamma\Sigma^{-2})^\dagger\Sigma\mathbf{V}^T\mathbf{W}_0\right\|_F \\ &= \gamma\sqrt{n}\|\mathbf{A}\Sigma^2\mathbf{B}\|_F \leq \gamma\sqrt{n}\|\mathbf{A}\Sigma^2\|_2\|\mathbf{B}\|_F, \\ \text{var}(\mathbf{W}^h) &= \frac{\xi^2}{n}\left\|(\mathbf{U}^T\mathbf{S}\mathbf{S}^T\mathbf{U} + n\gamma\Sigma^{-2})^\dagger\right\|_F^2.\end{aligned}$$

where we define

$$\begin{aligned}\mathbf{A} &= \Sigma^{-2} + \frac{\mathbf{U}^T\mathbf{S}\mathbf{S}^T\mathbf{U} - \mathbf{I}_\rho}{n\gamma}, \\ \mathbf{B} &= \Sigma^{-2}(\mathbf{U}^T\mathbf{S}\mathbf{S}^T\mathbf{U} + n\gamma\Sigma^{-2})^\dagger\Sigma\mathbf{V}^T\mathbf{W}_0.\end{aligned}$$

We first analyze then bias. It follows from Assumption 1.1 that

$$\Sigma^{-2}\left(\mathbf{I}_\rho - \frac{\eta}{n\gamma}\Sigma^2\right) \preceq \mathbf{A} \preceq \Sigma^{-2}\left(\mathbf{I}_\rho + \frac{\eta}{n\gamma}\Sigma^2\right). \quad (16)$$

Since $(\mathbf{I}_\rho - \frac{\eta}{n\gamma}\Sigma^2)^2 \preceq (\mathbf{I}_\rho + \frac{\eta}{n\gamma}\Sigma^2)^2 \preceq (1 + \frac{\eta\sigma_1^2}{n\gamma})^2\mathbf{I}_\rho$, it follows that

$$\mathbf{A}^2 \preceq \Sigma^{-4}\left(\mathbf{I}_\rho + \frac{\eta}{n\gamma}\Sigma^2\right)^2 \preceq \left(1 + \frac{\eta\sigma_1^2}{n\gamma}\right)^2\Sigma^{-4}.$$

Thus

$$\|\mathbf{A}\Sigma^2\|_2^2 = \|\Sigma^T\mathbf{A}^2\Sigma^2\|_2 \leq \left(1 + \frac{\eta\sigma_1^2}{n\gamma}\right)^2.$$

It follows from Assumption 1.1 that

$$\begin{aligned}(1 + \eta)^{-1}(\mathbf{I}_\rho + n\gamma\Sigma^{-2})^{-1} &\preceq ((1 + \eta)\mathbf{I}_\rho + n\gamma\Sigma^{-2})^{-1} \\ &\preceq (\mathbf{U}^T\mathbf{S}\mathbf{S}^T\mathbf{U} + n\gamma\Sigma^{-2})^\dagger \preceq ((1 - \eta)\mathbf{I}_\rho + n\gamma\Sigma^{-2})^{-1} \preceq (1 - \eta)^{-1}(\mathbf{I}_\rho + n\gamma\Sigma^{-2})^{-1}.\end{aligned}$$

Thus

$$\begin{aligned}\mathbf{B}^T\mathbf{B} &= \mathbf{W}_0^T\mathbf{V}\Sigma^3(\Sigma^{-2}(\mathbf{U}^T\mathbf{S}\mathbf{S}^T\mathbf{U} + n\gamma\Sigma^{-2})^\dagger\Sigma^{-2})^2\Sigma^3\mathbf{V}^T\mathbf{W}_0 \quad (17) \\ &\preceq (1 - \eta)^{-2}\mathbf{W}_0^T\mathbf{V}\Sigma^3(\Sigma^{-2}(\mathbf{I}_\rho + n\gamma\Sigma^{-2})^{-1}\Sigma^{-2})^2\Sigma^3\mathbf{V}^T\mathbf{W}_0 \\ &= (1 - \eta)^{-2}\mathbf{W}_0^T\mathbf{V}\Sigma(\Sigma^2 + n\gamma\mathbf{I}_\rho)^{-2}\Sigma\mathbf{V}^T\mathbf{W}_0.\end{aligned}$$

It follows that

$$\|\mathbf{B}\|_F^2 = \text{tr}(\mathbf{B}^T\mathbf{B}) \leq (1 - \eta)^{-2}\|(\Sigma^{-2} + n\gamma\mathbf{I}_\rho)^{-1}\Sigma\mathbf{V}^T\mathbf{W}_0\|_F^2 = \frac{\text{bias}^2(\mathbf{W}^*)}{n\gamma^2(1 - \eta)^2}.$$

where the last equality follows from the definition of $\text{bias}(\mathbf{W}^*)$. By the definition of \mathbf{A} and \mathbf{B} , we have

$$\text{bias}^2(\mathbf{W}^h) \leq \gamma^2 n \|\mathbf{A}\Sigma^2\|_2^2 \|\mathbf{B}\|_F^2 = \frac{1}{(1 - \eta)^2} \left(1 + \frac{\eta\sigma_1^2}{n\gamma}\right)^2 \text{bias}^2(\mathbf{W}^*).$$

To this end, the upper bound on $\text{bias}(\mathbf{W}^h)$ is established.

By the same definition of \mathbf{A} and \mathbf{B} , we can also show that

$$\text{bias}(\mathbf{W}^h) = \gamma\sqrt{n}\|\mathbf{A}\Sigma^2\mathbf{B}\|_F \geq \gamma\sqrt{n}\sigma_{\min}(\mathbf{A}\Sigma^2)\|\mathbf{B}\|_F.$$

Assume that $\sigma_\rho^2 \geq \frac{n\gamma}{\eta}$. It follows from (16) that

$$\mathbf{A}^2 \succeq \left(\frac{\eta\sigma_\rho^2}{n\gamma} - 1\right)^2 \Sigma^{-4}.$$

Thus

$$\sigma_{\min}^2(\mathbf{A}\Sigma^2) = \sigma_{\min}(\Sigma^2\mathbf{A}^2\Sigma^2) \geq \left(\frac{\eta\sigma_\rho^2}{n\gamma} - 1\right)^2.$$

It follows from (17) that

$$\mathbf{B}^T\mathbf{B} \succeq (1+\eta)^{-2}\mathbf{W}_0^T\mathbf{V}\Sigma(\Sigma^2 + n\gamma\mathbf{I}_\rho)^{-2}\Sigma\mathbf{V}^T\mathbf{W}_0.$$

Thus

$$\|\mathbf{B}\|_F^2 = \text{tr}(\mathbf{B}^T\mathbf{B}) \geq (1+\eta)^{-2}\|(\Sigma^{-2} + n\gamma\mathbf{I}_\rho)^{-1}\Sigma\mathbf{V}^T\mathbf{W}_0\|_F^2 = \frac{\text{bias}^2(\mathbf{W}^*)}{n\gamma^2(1+\eta)^2}.$$

In sum, we obtain

$$\text{bias}^2(\mathbf{W}^h) \geq \gamma^2 n \sigma_{\min}^2(\mathbf{A}\Sigma^2) \|\mathbf{B}\|_F^2 = (1+\eta)^{-2} \left(\frac{\eta\sigma_\rho^2}{n\gamma} - 1\right)^2 \text{bias}^2(\mathbf{W}^*).$$

To this end the lower bound on $\text{bias}(\mathbf{W}^h)$ is established.

It follows from Assumption 1.1 that

$$(1+\eta)^{-1}(\mathbf{I}_\rho + n\gamma\Sigma^{-2})^{-1} \preceq (\mathbf{U}^T\mathbf{S}\mathbf{S}^T\mathbf{U} + n\gamma\Sigma^{-2})^{-1} \preceq (1-\eta)^{-1}(\mathbf{I}_\rho + n\gamma\Sigma^{-2})^{-1}$$

It follows from Theorem 4 that

$$\begin{aligned} \text{var}(\mathbf{W}^h) &= \frac{\xi^2}{n}\|(\mathbf{U}^T\mathbf{S}\mathbf{S}^T\mathbf{U} + n\gamma\Sigma^{-2})^{-1}\|_F^2 \\ &\in \frac{1}{1\mp\eta}\frac{\xi^2}{n}\|(\mathbf{I}_\rho + n\gamma\Sigma^{-2})^{-1}\|_F^2 \\ &= \frac{1}{1\mp\eta}\text{var}(\mathbf{W}^*). \end{aligned}$$

This concludes the proof. ■

Appendix E. Model Averaging from Optimization Perspective: Proofs

In Section E.1 we prove Theorem 26. In Section E.2 we prove Theorem 27.

E.1 Proof of Theorem 26

Proof By Lemma 31, we only need to show $\|(\mathbf{X}^T \mathbf{X} + n\gamma \mathbf{I}_d)^{1/2}(\mathbf{W}^c - \mathbf{W}^*)\|_F^2 \leq n\alpha\beta f(\mathbf{W}^*)$. In the proof, we define $\rho = \text{rank}(\mathbf{X})$ and $\sigma_1 \geq \dots \geq \sigma_\rho$ be the singular values of \mathbf{X} .

In the proof of Theorem 21 we show that

$$\begin{aligned} & (\mathbf{X}^T \mathbf{X} + n\gamma \mathbf{I}_d)^{1/2}(\mathbf{W}_i^c - \mathbf{W}^*) \\ &= [(\mathbf{X}^T \mathbf{X} + n\gamma \mathbf{I}_d)^{-1/2}(\mathbf{X}^T \mathbf{S}_i \mathbf{S}_i^T \mathbf{X} + n\gamma \mathbf{I}_d)(\mathbf{X}^T \mathbf{X} + n\gamma \mathbf{I}_d)^{-1/2}]^\dagger (\mathbf{A}_i + \mathbf{B}_i) \\ &= \mathbf{C}_i^\dagger (\mathbf{A}_i + \mathbf{B}_i), \end{aligned}$$

where

$$\begin{aligned} \mathbf{A}_i &= \mathbf{V}(\Sigma^2 + n\gamma \mathbf{I}_\rho)^{-1/2} \Sigma \mathbf{U} \mathbf{S}_i \mathbf{S}_i^T \mathbf{Y}^\perp, \\ \mathbf{B}_i &= n\gamma \mathbf{V} \Sigma (\Sigma^2 + n\gamma \mathbf{I}_\rho)^{-1/2} (\mathbf{U}^T \mathbf{S}_i \mathbf{S}_i^T \mathbf{U} - \mathbf{I}_\rho) (\Sigma^2 + n\gamma \mathbf{I}_\rho)^{-1} \mathbf{U}^T \mathbf{Y} \\ \mathbf{C}_i &= [(\mathbf{X}^T \mathbf{X} + n\gamma \mathbf{I}_d)^{1/2}]^\dagger (\mathbf{X}^T \mathbf{S}_i \mathbf{S}_i^T \mathbf{X} + n\gamma \mathbf{I}_d) [(\mathbf{X}^T \mathbf{X} + n\gamma \mathbf{I}_d)^{1/2}]^\dagger \\ &= \mathbf{V}(\mathbf{I}_\rho + n\gamma \Sigma^{-2})^{-1/2} (\mathbf{U}^T \mathbf{S}_i \mathbf{S}_i^T \mathbf{U} + n\gamma \Sigma^{-2}) (\mathbf{I}_\rho + n\gamma \Sigma^{-2})^{-1/2} \mathbf{V}^T \\ &= \mathbf{V} \mathbf{V}^T + \mathbf{V}(\mathbf{I}_\rho + n\gamma \Sigma^{-2})^{-1/2} (\mathbf{U}^T \mathbf{S}_i \mathbf{S}_i^T \mathbf{U} - \mathbf{I}_\rho) (\mathbf{I}_\rho + n\gamma \Sigma^{-2})^{-1/2} \mathbf{V}^T. \end{aligned}$$

By Assumption 2.1, we have that $\mathbf{C}_i \succeq (1 - \frac{\eta \sigma_{\max}^2}{\sigma_{\max}^2 + n\gamma}) \mathbf{V} \mathbf{V}^T$. Since $\eta \leq 1/2$, it follows that $\mathbf{C}_i^\dagger \preceq (1 + \frac{2\eta \sigma_{\max}^2}{\sigma_{\max}^2 + n\gamma}) \mathbf{V} \mathbf{V}^T$. Let $\mathbf{C}_i^\dagger = \mathbf{V} \mathbf{V}^T + \mathbf{V} \Delta_i \mathbf{V}^T$. It holds that $\Delta_i \preceq \frac{2\eta \sigma_{\max}^2}{\sigma_{\max}^2 + n\gamma} \mathbf{V} \mathbf{V}^T \preceq 2\eta \beta \mathbf{V} \mathbf{V}^T$. By definition, $\mathbf{W}^c = \frac{1}{g} \sum_{i=1}^g \mathbf{W}_i^c$. It follows that

$$\begin{aligned} \left\| (\mathbf{X}^T \mathbf{X} + n\gamma \mathbf{I}_d)^{1/2}(\mathbf{W}_i^c - \mathbf{W}^*) \right\|_F &= \left\| \frac{1}{g} \sum_{i=1}^g \mathbf{C}_i^\dagger (\mathbf{A}_i + \mathbf{B}_i) \right\|_F \\ &\leq \left\| \frac{1}{g} \sum_{i=1}^g (\mathbf{A}_i + \mathbf{B}_i) \right\|_F + \left\| \frac{1}{g} \sum_{i=1}^g \mathbf{V} \Delta_i \mathbf{V}^T (\mathbf{A}_i + \mathbf{B}_i) \right\|_F \\ &\leq \left\| \frac{1}{g} \sum_{i=1}^g \mathbf{A}_i \right\|_F + \left\| \frac{1}{g} \sum_{i=1}^g \mathbf{B}_i \right\|_F + \frac{1}{g} \sum_{i=1}^g \|\Delta_i\|_2 (\|\mathbf{A}_i\|_F + \|\mathbf{B}_i\|_F) \\ &\leq \left\| \frac{1}{g} \sum_{i=1}^g \mathbf{A}_i \right\|_F + \left\| \frac{1}{g} \sum_{i=1}^g \mathbf{B}_i \right\|_F + 2\eta \beta \frac{1}{g} \sum_{i=1}^g (\|\mathbf{A}_i\|_F + \|\mathbf{B}_i\|_F). \end{aligned} \tag{18}$$

By Assumption 2.3, we have that

$$\frac{1}{g} \sum_{i=1}^g \|\mathbf{A}_i\|_F = \|(\Sigma^2 + n\gamma \mathbf{I}_d)^{-1/2} \Sigma\|_2 \cdot \frac{1}{g} \sum_{i=1}^g \|\mathbf{U}^T \mathbf{S}_i \mathbf{S}_i^T \mathbf{Y}^\perp\|_F \leq \sqrt{\frac{\epsilon \sigma_{\max}^2}{\sigma_{\max}^2 + n\gamma}} \|\mathbf{Y}^\perp\|_F.$$

We apply Assumption 2.1 and follow the proof of Theorem 21 to show that

$$\|\mathbf{B}_i\|_F^2 \leq \eta^2 n\gamma \frac{\sigma_{\max}^2}{\sigma_{\max}^2 + n\gamma} \left\| (\Sigma^2 + n\gamma \mathbf{I}_d)^{-1/2} \mathbf{U}^T \mathbf{Y} \right\|_F^2.$$

It follows that

$$\begin{aligned}
& \frac{1}{g} \sum_{i=1}^g \left(\|\mathbf{A}_i\|_F + \|\mathbf{B}_i\|_F \right) \\
& \leq \max \left\{ \sqrt{\epsilon}, \eta \right\} \sqrt{\frac{\sigma_{\max}^2}{\sigma_{\max}^2 + n\gamma}} \left(\|\mathbf{Y}^\perp\|_F + \sqrt{n\gamma} \|(\Sigma^2 + n\gamma\mathbf{I}_d)^{-1/2} \mathbf{U}^T \mathbf{Y}\|_F \right) \\
& \leq \max \left\{ \sqrt{\epsilon}, \eta \right\} \sqrt{\beta} \sqrt{2\|\mathbf{Y}^\perp\|_F^2 + 2n\gamma \|(\Sigma^2 + n\gamma\mathbf{I}_d)^{-1/2} \mathbf{U}^T \mathbf{Y}\|_F^2} \\
& = \max \left\{ \sqrt{\epsilon}, \eta \right\} \sqrt{\beta} \sqrt{2n f(\mathbf{W}^*)}.
\end{aligned} \tag{19}$$

Here the equality follows from Lemma 31. Let $\mathbf{S} = \frac{1}{g} [\mathbf{S}_1, \dots, \mathbf{S}_g] \in \mathbb{R}^{n \times sg}$. We have that

$$\begin{aligned}
\frac{1}{g} \sum_{i=1}^g \mathbf{A}_i &= \mathbf{V}(\Sigma^2 + n\gamma\mathbf{I}_d)^{-1/2} \Sigma \mathbf{U}^T \mathbf{S} \mathbf{S}^T \mathbf{Y}^\perp \\
\frac{1}{g} \sum_{i=1}^g \mathbf{B}_i &= n\gamma \mathbf{V} \Sigma (\Sigma^2 + n\gamma\mathbf{I}_d)^{-1/2} (\mathbf{U}^T \mathbf{S} \mathbf{S}^T \mathbf{U} - \mathbf{I}_\rho) (\Sigma^2 + n\gamma\mathbf{I}_\rho)^{-1} \mathbf{U}^T \mathbf{Y}.
\end{aligned}$$

Following the proof Theorem 21 and applying Assumptions 2.1 and 2.2, we have that

$$\begin{aligned}
\left\| \frac{1}{g} \sum_{i=1}^g \mathbf{A}_i \right\|_F + \left\| \frac{1}{g} \sum_{i=1}^g \mathbf{B}_i \right\|_F &\leq \sqrt{2 \left\| \frac{1}{g} \sum_{i=1}^g \mathbf{A}_i \right\|_F^2 + 2 \left\| \frac{1}{g} \sum_{i=1}^g \mathbf{B}_i \right\|_F^2} \\
&\leq \max \left\{ \sqrt{\frac{\epsilon}{g}}, \frac{\eta}{g} \right\} \sqrt{\frac{\sigma_{\max}^2}{\sigma_{\max}^2 + n\gamma}} \sqrt{2n f(\mathbf{W}^*)} = \max \left\{ \sqrt{\frac{\epsilon}{g}}, \frac{\eta}{g} \right\} \sqrt{\beta} \sqrt{2n f(\mathbf{W}^*)}.
\end{aligned} \tag{20}$$

It follows from (18), (19), and (20) that

$$\begin{aligned}
& \left\| (\mathbf{X}^T \mathbf{X} + n\gamma \mathbf{I}_d)^{1/2} (\mathbf{W}_i^c - \mathbf{W}^*) \right\|_F \\
& \leq \left\| \frac{1}{g} \sum_{i=1}^g \mathbf{A}_i \right\|_F + \left\| \frac{1}{g} \sum_{i=1}^g \mathbf{B}_i \right\|_F + 2\eta\beta \frac{1}{g} \sum_{i=1}^g \left(\|\mathbf{A}_i\|_F + \|\mathbf{B}_i\|_F \right) \\
& \leq \left[\max \left\{ \sqrt{\frac{\epsilon}{g}}, \frac{\eta}{g} \right\} + 2\beta \cdot \max \left\{ \eta\sqrt{\epsilon}, \eta^2 \right\} \right] \sqrt{\beta} \sqrt{2n f(\mathbf{W}^*)} \\
& = \sqrt{\alpha\beta n f(\mathbf{W}^*)}.
\end{aligned}$$

This concludes our proof. ■

E.2 Proof of Theorem 27

Proof By Lemma 31, we only need to show $\|(\mathbf{X}^T \mathbf{X} + n\gamma \mathbf{I}_d)^{1/2} (\mathbf{W}^h - \mathbf{W}^*)\|_F^2 \leq \alpha^2 \beta^2 (-nf(\mathbf{W}^*) + \|\mathbf{Y}\|_F^2)$.

In the proof of Theorem 2 we show that

$$(\mathbf{X}^T \mathbf{X} + n\gamma \mathbf{I}_d)^{1/2} (\mathbf{W}_i^h - \mathbf{W}^*) = \mathbf{V} \mathbf{A}_i \mathbf{B}_i \mathbf{C},$$

where

$$\begin{aligned} \mathbf{A}_i &= (\Sigma^2 + n\gamma \mathbf{I}_\rho)^{-1/2} \Sigma (\mathbf{I}_\rho - \mathbf{U}^T \mathbf{S}_i \mathbf{S}_i^T \mathbf{U}) \Sigma (\Sigma^2 + n\gamma \mathbf{I}_\rho)^{-1/2}, \\ \mathbf{B}_i &= (\Sigma^2 + n\gamma \mathbf{I}_\rho)^{1/2} (\Sigma \mathbf{U}^T \mathbf{S}_i \mathbf{S}_i^T \mathbf{U} \Sigma + n\gamma \mathbf{I}_\rho)^{-1} (\Sigma^2 + n\gamma \mathbf{I}_\rho)^{1/2}, \\ \mathbf{C} &= (\Sigma^2 + n\gamma \mathbf{I}_\rho)^{-1/2} \Sigma \mathbf{U}^T \mathbf{Y}. \end{aligned}$$

It follows from Assumption 2.1 that for all $i \in [g]$,

$$\frac{1}{1+\eta} (\Sigma^2 + n\gamma \mathbf{I}_\rho)^{-1} \preceq (\Sigma \mathbf{U}^T \mathbf{S}_i \mathbf{S}_i^T \mathbf{U} \Sigma + n\gamma \mathbf{I}_\rho)^{-1} \preceq \frac{1}{1-\eta} (\Sigma^2 + n\gamma \mathbf{I}_\rho)^{-1}.$$

We let $\mathbf{B}_i = \mathbf{I}_\rho + \Delta_i$. Thus $-\frac{\eta}{1+\eta} \mathbf{I}_\rho \preceq \Delta_i \preceq \frac{\eta}{1-\eta} \mathbf{I}_\rho$. It follows that

$$\begin{aligned} (\mathbf{X}^T \mathbf{X} + n\gamma \mathbf{I}_d)^{1/2} (\mathbf{W}_i^h - \mathbf{W}^*) &= \frac{1}{g} \sum_{i=1}^g (\mathbf{X}^T \mathbf{X} + n\gamma \mathbf{I}_d)^{1/2} (\mathbf{W}_i^h - \mathbf{W}^*) \\ &= \frac{1}{g} \sum_{i=1}^g \mathbf{V} \mathbf{A}_i (\mathbf{I}_\rho + \Delta_i) \mathbf{C} = \frac{1}{g} \sum_{i=1}^g \mathbf{V} \mathbf{A}_i \mathbf{C} + \frac{1}{g} \sum_{i=1}^g \mathbf{V} \mathbf{A}_i \Delta_i \mathbf{C}. \end{aligned}$$

It follows that

$$\begin{aligned} \left\| (\mathbf{X}^T \mathbf{X} + n\gamma \mathbf{I}_d)^{1/2} (\mathbf{W}_i^h - \mathbf{W}^*) \right\|_F &\leq \left\| \frac{1}{g} \sum_{i=1}^g \mathbf{A}_i \right\|_2 \left\| \mathbf{C} \right\|_F + \frac{1}{g} \sum_{i=1}^g \left\| \mathbf{A}_i \right\|_2 \left\| \Delta_i \right\|_2 \left\| \mathbf{C} \right\|_F \\ &\leq \left\| \frac{1}{g} \sum_{i=1}^g \mathbf{A}_i \right\|_2 \left\| \mathbf{C} \right\|_F + \frac{\eta}{1-\eta} \left(\frac{1}{g} \sum_{i=1}^g \left\| \mathbf{A}_i \right\|_2 \right) \left\| \mathbf{C} \right\|_F. \end{aligned} \tag{21}$$

Let $\mathbf{S} = \frac{1}{g} [\mathbf{S}_1, \dots, \mathbf{S}_g] \in \mathbb{R}^{n \times gs}$. It follows from the definition of \mathbf{A}_i that

$$\begin{aligned} \left\| \mathbf{A}_i \right\|_2 &= \left\| (\Sigma^2 + n\gamma \mathbf{I}_\rho)^{-1/2} \Sigma (\mathbf{I}_\rho - \mathbf{U}^T \mathbf{S}_i \mathbf{S}_i^T \mathbf{U}) \Sigma (\Sigma^2 + n\gamma \mathbf{I}_\rho)^{-1/2} \right\|_2 \\ &\leq \eta \left\| (\Sigma^2 + n\gamma \mathbf{I}_\rho)^{-1/2} \Sigma \Sigma (\Sigma^2 + n\gamma \mathbf{I}_\rho)^{-1/2} \right\|_2 = \eta \frac{\sigma_{\max}^2}{\sigma_{\max}^2 + n\gamma} = \eta\beta, \\ \left\| \frac{1}{g} \sum_{i=1}^g \mathbf{A}_i \right\|_2 &= \left\| (\Sigma^2 + n\gamma \mathbf{I}_\rho)^{-1/2} \Sigma (\mathbf{I}_\rho - \mathbf{U}^T \mathbf{S} \mathbf{S}^T \mathbf{U}) \Sigma (\Sigma^2 + n\gamma \mathbf{I}_\rho)^{-1/2} \right\|_2 \\ &\leq \frac{\eta}{g} \left\| (\Sigma^2 + n\gamma \mathbf{I}_\rho)^{-1/2} \Sigma \Sigma (\Sigma^2 + n\gamma \mathbf{I}_\rho)^{-1/2} \right\|_2 = \frac{\eta}{g} \frac{\sigma_{\max}^2}{\sigma_{\max}^2 + n\gamma} = \frac{\eta\beta}{g}. \end{aligned}$$

It follows from (21) that

$$\begin{aligned} \left\| (\mathbf{X}^T \mathbf{X} + n\gamma \mathbf{I}_d)^{1/2} (\mathbf{W}_i^h - \mathbf{W}^*) \right\|_F &\leq \left(\frac{\eta}{g} + \frac{\eta^2}{1-\eta} \right) \beta \left\| \mathbf{C} \right\|_F \\ &\leq \left(\frac{\eta}{g} + \frac{\eta^2}{1-\eta} \right) \beta \sqrt{-nf(\mathbf{W}^*) + \|\mathbf{Y}\|_F^2}, \end{aligned}$$

where the latter inequality follows from the proof of Theorem 22. This concludes the proof. \blacksquare

Appendix F. Model Averaging from Statistical Perspective: Proofs

In Section F.1 we prove Theorem 28. In Section F.2 we prove Theorem 29

F.1 Proof of Theorem 28

Proof The bound on $\text{bias}(\mathbf{W}^c)$ can be shown in the same way as the proof of Theorem 23.

We prove the bound on $\text{var}(\mathbf{W}^c)$ in the following. It follows from Assumption 2.1 that

$$(1 + \eta)^{-1}(\mathbf{I}_\rho + n\gamma\boldsymbol{\Sigma}^{-2})^{-1} \preceq (\mathbf{U}^T \mathbf{S}_i \mathbf{S}_i^T \mathbf{U} + n\gamma\boldsymbol{\Sigma}^{-2})^\dagger \preceq (1 - \eta)^{-1}(\mathbf{I}_\rho + n\gamma\boldsymbol{\Sigma}^{-2})^{-1}$$

Let

$$(\mathbf{U}^T \mathbf{S}_i \mathbf{S}_i^T \mathbf{U} + n\gamma\boldsymbol{\Sigma}^{-2})^\dagger = (\mathbf{I}_\rho + n\gamma\boldsymbol{\Sigma}^{-2})^{-1/2}(\mathbf{I}_\rho + \boldsymbol{\Delta}_i)(\mathbf{I}_\rho + n\gamma\boldsymbol{\Sigma}^{-2})^{-1/2}.$$

It holds that

$$-\frac{\eta}{1 + \eta} \mathbf{I}_\rho \preceq \boldsymbol{\Delta}_i \preceq \frac{\eta}{1 - \eta} \mathbf{I}_\rho.$$

By the definition of $\text{var}(\mathbf{W}^c)$ in Theorem 10, we have that

$$\begin{aligned} & \sqrt{\text{var}(\mathbf{W}^c)} \\ &= \frac{\xi}{\sqrt{n}} \left\| \frac{1}{g} \sum_{i=1}^g (\mathbf{I}_\rho + n\gamma\boldsymbol{\Sigma}^{-2})^{-1} \mathbf{U}^T \mathbf{S}_i \mathbf{S}_i^T + \frac{1}{g} \sum_{i=1}^g (\mathbf{I}_\rho + n\gamma\boldsymbol{\Sigma}^{-2})^{-1/2} \boldsymbol{\Delta}_i (\mathbf{I}_\rho + n\gamma\boldsymbol{\Sigma}^{-2})^{-1/2} \mathbf{U}^T \mathbf{S}_i \mathbf{S}_i^T \right\|_F \\ &\leq \frac{\xi}{\sqrt{n}} \left(\left\| (\mathbf{I}_\rho + n\gamma\boldsymbol{\Sigma}^{-2})^{-1} \mathbf{U}^T \mathbf{S} \mathbf{S}^T \right\|_F + \frac{1}{g} \sum_{i=1}^g \left\| (\mathbf{I}_\rho + n\gamma\boldsymbol{\Sigma}^{-2})^{-1/2} \boldsymbol{\Delta}_i (\mathbf{I}_\rho + n\gamma\boldsymbol{\Sigma}^{-2})^{-1/2} \mathbf{U}^T \mathbf{S}_i \mathbf{S}_i^T \right\|_F \right) \\ &\leq \frac{\xi}{\sqrt{n}} \|(\mathbf{I}_\rho + n\gamma\boldsymbol{\Sigma}^{-2})^{-1}\|_F \left(\|\mathbf{U}^T \mathbf{S}\|_2 \|\mathbf{S}\|_2 + \frac{\eta}{1 - \eta} \frac{1}{g} \sum_{i=1}^g \|\mathbf{U}^T \mathbf{S}_i\|_2 \|\mathbf{S}_i\|_2 \right) \\ &= \sqrt{\text{var}(\mathbf{W}^*)} \left(\|\mathbf{U}^T \mathbf{S}\|_2 \|\mathbf{S}\|_2 + \frac{\eta}{1 - \eta} \frac{1}{g} \sum_{i=1}^g \|\mathbf{U}^T \mathbf{S}_i\|_2 \|\mathbf{S}_i\|_2 \right). \end{aligned}$$

Under Assumption 2.1, we have that $\|\mathbf{S}_i^T \mathbf{U}\|_2^2 \leq 1 + \eta$ and $\|\mathbf{S}^T \mathbf{U}\|_2^2 \leq 1 + \frac{\eta}{g}$. It follows that

$$\sqrt{\frac{\text{var}(\mathbf{W}^c)}{\text{var}(\mathbf{W}^*)}} \leq \sqrt{1 + \frac{\eta}{g}} \|\mathbf{S}\|_2 + \frac{\eta\sqrt{1 + \eta}}{1 - \eta} \frac{1}{g} \sum_{i=1}^g \|\mathbf{S}_i\|_2.$$

Then the theorem follows from Assumption 2.3. \blacksquare

F.2 Proof of Theorem 29

Proof The bound on $\text{var}(\mathbf{W}^h)$ can be established in the same way as Theorem 25.

We prove the bound on $\text{bias}(\mathbf{W}^h)$ in the following. Let

$$(\mathbf{U}^T \mathbf{S}_i \mathbf{S}_i^T \mathbf{U} + n\gamma \boldsymbol{\Sigma}^{-2})^\dagger = (\mathbf{I}_\rho + n\gamma \boldsymbol{\Sigma}^{-2})^{-1/2} (\mathbf{I}_\rho + \boldsymbol{\Delta}_i) (\mathbf{I}_\rho + n\gamma \boldsymbol{\Sigma}^{-2})^{-1/2}.$$

Under Assumption 2.1, we have that $\boldsymbol{\Delta}_i \preceq \frac{\eta}{1-\eta} \mathbf{I}_\rho$. It follows from Theorem 10 that

$$\begin{aligned} \text{bias}(\mathbf{W}^h) &= \gamma \sqrt{n} \left\| \frac{1}{g} \sum_{i=1}^g \left(\boldsymbol{\Sigma}^{-2} + \frac{\mathbf{U}^T \mathbf{S}_i \mathbf{S}_i^T \mathbf{U} - \mathbf{I}_\rho}{n\gamma} \right) (\mathbf{U}^T \mathbf{S}_i \mathbf{S}_i^T \mathbf{U} + n\gamma \boldsymbol{\Sigma}^{-2})^\dagger \boldsymbol{\Sigma} \mathbf{V}^T \mathbf{W}_0 \right\|_F \\ &\leq \gamma \sqrt{n} \left\| \frac{1}{g} \sum_{i=1}^g \left(\boldsymbol{\Sigma}^{-2} + \frac{\mathbf{U}^T \mathbf{S}_i \mathbf{S}_i^T \mathbf{U} - \mathbf{I}_\rho}{n\gamma} \right) (\mathbf{I}_\rho + n\gamma \boldsymbol{\Sigma}^{-2})^{-1} \boldsymbol{\Sigma} \mathbf{V}^T \mathbf{W}_0 \right\|_F \\ &\quad + \gamma \sqrt{n} \left\| \frac{1}{g} \sum_{i=1}^g \left(\boldsymbol{\Sigma}^{-2} + \frac{\mathbf{U}^T \mathbf{S}_i \mathbf{S}_i^T \mathbf{U} - \mathbf{I}_\rho}{n\gamma} \right) (\mathbf{I}_\rho + n\gamma \boldsymbol{\Sigma}^{-2})^{-1/2} \boldsymbol{\Delta}_i (\mathbf{I}_\rho + n\gamma \boldsymbol{\Sigma}^{-2})^{-1/2} \boldsymbol{\Sigma} \mathbf{V}^T \mathbf{W}_0 \right\|_F \\ &\triangleq \gamma \sqrt{n} (A + B), \end{aligned}$$

where

$$\begin{aligned} A &= \left\| \frac{1}{g} \sum_{i=1}^g \left(\boldsymbol{\Sigma}^{-2} + \frac{\mathbf{U}^T \mathbf{S}_i \mathbf{S}_i^T \mathbf{U} - \mathbf{I}_\rho}{n\gamma} \right) (\mathbf{I}_\rho + n\gamma \boldsymbol{\Sigma}^{-2})^{-1} \boldsymbol{\Sigma} \mathbf{V}^T \mathbf{W}_0 \right\|_F \\ &= \left\| \left(\boldsymbol{\Sigma}^{-2} + \frac{\mathbf{U}^T \mathbf{S} \mathbf{S}^T \mathbf{U} - \mathbf{I}_\rho}{n\gamma} \right) (\mathbf{I}_\rho + n\gamma \boldsymbol{\Sigma}^{-2})^{-1} \boldsymbol{\Sigma} \mathbf{V}^T \mathbf{W}_0 \right\|_F, \\ B &= \left\| \frac{1}{g} \sum_{i=1}^g \left(\boldsymbol{\Sigma}^{-2} + \frac{\mathbf{U}^T \mathbf{S}_i \mathbf{S}_i^T \mathbf{U} - \mathbf{I}_\rho}{n\gamma} \right) (\mathbf{I}_\rho + n\gamma \boldsymbol{\Sigma}^{-2})^{-1/2} \boldsymbol{\Delta}_i (\mathbf{I}_\rho + n\gamma \boldsymbol{\Sigma}^{-2})^{-1/2} \boldsymbol{\Sigma} \mathbf{V}^T \mathbf{W}_0 \right\|_F \\ &\leq \frac{1}{g} \sum_{i=1}^g \left\| \left(\boldsymbol{\Sigma}^{-2} + \frac{\mathbf{U}^T \mathbf{S}_i \mathbf{S}_i^T \mathbf{U} - \mathbf{I}_\rho}{n\gamma} \right) (\mathbf{I}_\rho + n\gamma \boldsymbol{\Sigma}^{-2})^{-1/2} \boldsymbol{\Delta}_i (\mathbf{I}_\rho + n\gamma \boldsymbol{\Sigma}^{-2})^{-1/2} \boldsymbol{\Sigma} \mathbf{V}^T \mathbf{W}_0 \right\|_F. \end{aligned}$$

It follows from Assumption 2.1 that

$$\left(1 - \frac{\eta \sigma_{\max}^2}{gn\gamma}\right) \boldsymbol{\Sigma}^{-2} \preceq \boldsymbol{\Sigma}^{-2} + \frac{\mathbf{U}^T \mathbf{S} \mathbf{S}^T \mathbf{U} - \mathbf{I}_\rho}{n\gamma} \preceq \left(1 + \frac{\eta \sigma_{\max}^2}{gn\gamma}\right) \boldsymbol{\Sigma}^{-2},$$

and thus

$$\left(\boldsymbol{\Sigma}^{-2} + \frac{\mathbf{U}^T \mathbf{S} \mathbf{S}^T \mathbf{U} - \mathbf{I}_\rho}{n\gamma} \right)^2 \preceq \left(1 + \frac{\eta \sigma_{\max}^2}{gn\gamma}\right)^2 \boldsymbol{\Sigma}^{-4}.$$

It follows that

$$\begin{aligned} A &= \left\| \left(\boldsymbol{\Sigma}^{-2} + \frac{\mathbf{U}^T \mathbf{S} \mathbf{S}^T \mathbf{U} - \mathbf{I}_\rho}{n\gamma} \right) (\mathbf{I}_\rho + n\gamma \boldsymbol{\Sigma}^{-2})^{-1} \boldsymbol{\Sigma} \mathbf{V}^T \mathbf{W}_0 \right\|_F \\ &\leq \left(1 + \frac{\eta \sigma_{\max}^2}{gn\gamma}\right) \left\| (\boldsymbol{\Sigma}^{-2} + n\gamma \mathbf{I}_\rho)^{-1} \boldsymbol{\Sigma} \mathbf{V}^T \mathbf{W}_0 \right\|_F. \end{aligned}$$

It follows from Assumption 2.1 that

$$\left(1 - \frac{\eta \sigma_{\max}^2}{n\gamma}\right)^2 \boldsymbol{\Sigma}^{-4} \preceq \left(\boldsymbol{\Sigma}^{-2} + \frac{\eta}{n\gamma} \mathbf{I}_\rho \right)^2 \preceq \left(1 + \frac{\eta \sigma_{\max}^2}{n\gamma}\right)^2 \boldsymbol{\Sigma}^{-4}.$$

Moreover,

$$\boldsymbol{\Sigma}^{-2} (\mathbf{I}_\rho + n\gamma \boldsymbol{\Sigma}^{-2})^{-1/2} \boldsymbol{\Delta}_i (\mathbf{I}_\rho + n\gamma \boldsymbol{\Sigma}^{-2})^{-1/2} \boldsymbol{\Sigma}^{-2} \preceq \frac{\eta}{1-\eta} \boldsymbol{\Sigma}^{-2} (\mathbf{I}_\rho + n\gamma \boldsymbol{\Sigma}^{-2})^{-1} \boldsymbol{\Sigma}^{-2}$$

It follows that

$$\begin{aligned}
B &\leq \left(1 + \frac{\eta\sigma_{\max}^2}{n\gamma}\right) \cdot \frac{1}{g} \sum_{i=1}^g \left\| \Sigma^{-2} (\mathbf{I}_\rho + n\gamma\Sigma^{-2})^{-1/2} \Delta_i (\mathbf{I}_\rho + n\gamma\Sigma^{-2})^{-1/2} \Sigma^{-2} \Sigma^3 \mathbf{V}^T \mathbf{W}_0 \right\|_F \\
&\leq \frac{\eta}{1-\eta} \left(1 + \frac{\eta\sigma_{\max}^2}{n\gamma}\right) \cdot \left\| (\Sigma^2 + n\gamma\mathbf{I}_\rho)^{-1} \Sigma \mathbf{V}^T \mathbf{W}_0 \right\|_F.
\end{aligned}$$

Hence

$$\begin{aligned}
\text{bias}(\mathbf{W}^h) &\leq \gamma\sqrt{n}(A + B) \\
&\leq \left[\frac{1}{1-\eta} + \left(\frac{\eta}{g} + \frac{\eta^2}{1-\eta} \right) \frac{\sigma_{\max}^2}{n\gamma} \right] \gamma\sqrt{n} \left\| (\Sigma^2 + n\gamma\mathbf{I}_\rho)^{-1} \Sigma \mathbf{V}^T \mathbf{W}_0 \right\|_F \\
&= \left[\frac{1}{1-\eta} + \left(\frac{\eta}{g} + \frac{\eta^2}{1-\eta} \right) \frac{\sigma_{\max}^2}{n\gamma} \right] \text{bias}(\mathbf{W}^*).
\end{aligned}$$

Here the equality follows from Theorem 4. ■

References

Haim Avron, Kenneth L. Clarkson, and David P. Woodruff. Sharper bounds for regression and low-rank approximation with regularization. *arXiv preprint arXiv:1611.03225*, 2016. 7

Leo Breiman. Bagging predictors. *Machine Learning*, 24(2):123–140, 1996. 5, 14

Leo Breiman. Pasting small votes for classification in large databases and on-line. *Machine Learning*, 36(1-2):85–103, 1999. 5

Moses Charikar, Kevin Chen, and Martin Farach-Colton. Finding frequent items in data streams. *Theoretical Computer Science*, 312(1):3–15, 2004. 9

Kenneth L. Clarkson and David P. Woodruff. Low rank approximation and regression in input sparsity time. In *Annual ACM Symposium on theory of computing (STOC)*, 2013. 2, 6, 9

Petros Drineas, Ravi Kannan, and Michael W. Mahoney. Fast Monte Carlo algorithms for matrices I: Approximating matrix multiplication. *SIAM Journal on Computing*, 36(1):132–157, 2006a. 24

Petros Drineas, Michael W. Mahoney, and S. Muthukrishnan. Sampling algorithms for ℓ_2 regression and applications. In *Annual ACM-SIAM Symposium on Discrete Algorithm (SODA)*, 2006b. 2, 6, 24

Petros Drineas, Michael W. Mahoney, and S. Muthukrishnan. Relative-error CUR matrix decompositions. *SIAM Journal on Matrix Analysis and Applications*, 30(2):844–881, September 2008. 30

Petros Drineas, Michael W. Mahoney, S. Muthukrishnan, and Tamás Sarlós. Faster least squares approximation. *Numerische Mathematik*, 117(2):219–249, 2011. [2](#), [6](#), [8](#), [30](#)

Petros Drineas, Malik Magdon-Ismail, Michael W. Mahoney, and David P. Woodruff. Fast approximation of matrix coherence and statistical leverage. *Journal of Machine Learning Research*, 13:3441–3472, 2012. [7](#), [8](#)

Alex Gittens. The spectral norm error of the naive Nyström extension. *arXiv preprint arXiv:1110.5305*, 2011. [30](#)

William B. Johnson and Joram Lindenstrauss. Extensions of Lipschitz mappings into a Hilbert space. *Contemporary mathematics*, 26(189-206), 1984. [8](#)

Yichao Lu, Paramveer Dhillon, Dean P Foster, and Lyle Ungar. Faster ridge regression via the subsampled randomized Hadamard transform. In *Advances in Neural Information Processing Systems (NIPS)*, 2013. [6](#), [8](#)

Ping Ma, Michael W Mahoney, and Bin Yu. A statistical perspective on algorithmic leveraging. *Journal of Machine Learning Research*, 16(1):861–911, 2015. [2](#), [7](#), [8](#), [15](#), [23](#)

Michael W. Mahoney. Randomized algorithms for matrices and data. *Foundations and Trends in Machine Learning*, 3(2):123–224, 2011. [2](#), [23](#)

Xiangrui Meng and Michael W Mahoney. Low-distortion subspace embeddings in input-sparsity time and applications to robust linear regression. In *Annual ACM Symposium on Theory of Computing (STOC)*, 2013. [2](#), [6](#), [9](#), [30](#)

John Nelson and Huy L Nguyêñ. Osnap: Faster numerical linear algebra algorithms via sparser subspace embeddings. In *IEEE Annual Symposium on Foundations of Computer Science (FOCS)*, 2013. [2](#), [6](#), [9](#), [30](#)

Mihai Patrascu and Mikkel Thorup. The power of simple tabulation-based hashing. *Journal of the ACM*, 59(3), 2012. [31](#)

Ninh Pham and Rasmus Pagh. Fast and scalable polynomial kernels via explicit feature maps. In *ACM SIGKDD International Conference on Knowledge Discovery and Data Mining (KDD)*, 2013. [9](#)

Mert Pilanci and Martin J Wainwright. Iterative Hessian sketch: Fast and accurate solution approximation for constrained least-squares. *Journal of Machine Learning Research*, pages 1–33, 2015. [2](#), [3](#), [7](#)

Garvesh Raskutti and Michael W Mahoney. A statistical perspective on randomized sketching for ordinary least-squares. *Journal of Machine Learning Research*, 17(214):1–31, 2016. [2](#), [23](#)

Gian-Andrea Thanei, Christina Heinze, and Nicolai Meinshausen. Random projections for large-scale regression. *arXiv preprint arXiv:1701.05325*, 2017. [7](#)

Joel A Tropp. Improved analysis of the subsampled randomized Hadamard transform. *Advances in Adaptive Data Analysis*, 3(01n02):115–126, 2011. 8, 30

Stephen Tu, Rebecca Roelofs, Shivaram Venkataraman, and Benjamin Recht. Large scale kernel learning using block coordinate descent. *arXiv preprint arXiv:1602.05310*, 2016. 6

Roman Vershynin. Introduction to the non-asymptotic analysis of random matrices. *arXiv preprint arXiv:1011.3027*, 2010. 31

Jialei Wang, Jason D Lee, Mehrdad Mahdavi, Mladen Kolar, and Nathan Srebro. Sketching meets random projection in the dual: A provable recovery algorithm for big and high-dimensional data. *arXiv preprint arXiv:1610.03045*, 2016a. 3, 7

Shusen Wang, Luo Luo, and Zhihua Zhang. SPSD matrix approximation vis column selection: Theories, algorithms, and extensions. *Journal of Machine Learning Research*, 17(49):1–49, 2016b. 30

Shusen Wang, Zhihua Zhang, and Tong Zhang. Towards more efficient SPSD matrix approximation and CUR matrix decomposition. *Journal of Machine Learning Research*, 17(210):1–49, 2016c. 30

Yining Wang, Adams Wei Yu, and Aarti Singh. Computationally feasible near-optimal subset selection for linear regression under measurement constraints. *arXiv preprint arXiv:1601.02068*, 2016d. 2

Kilian Weinberger, Anirban Dasgupta, John Langford, Alex Smola, and Josh Attenberg. Feature hashing for large scale multitask learning. In *International Conference on Machine Learning (ICML)*, 2009. 9

David P Woodruff. Sketching as a tool for numerical linear algebra. *Foundations and Trends® in Theoretical Computer Science*, 10(1–2):1–157, 2014. 2, 9, 30

Franco Woolfe, Edo Liberty, Vladimir Rokhlin, and Mark Tygert. A fast randomized algorithm for the approximation of matrices. *Applied and Computational Harmonic Analysis*, 25(3):335–366, 2008. 9

Jiyan Yang, Xiangrui Meng, and Michael W Mahoney. Implementing randomized matrix algorithms in parallel and distributed environments. *Proceedings of the IEEE*, 104(1):58–92, 2016. 15

Matei Zaharia, Mosharaf Chowdhury, Michael J Franklin, Scott Shenker, and Ion Stoica. Spark: Cluster computing with working sets. *HotCloud*, 10(10-10):95, 2010. 21

Yuchen Zhang, John C. Duchi, and Martin J. Wainwright. Communication-efficient algorithms for statistical optimization. *Journal of Machine Learning Research*, 14:3321–3363, 2013. 6, 7

Yuchen Zhang, John Duchi, and Martin Wainwright. Divide and conquer kernel ridge regression: a distributed algorithm with minimax optimal rates. *Journal of Machine Learning Research*, 16:3299–3340, 2015. 7